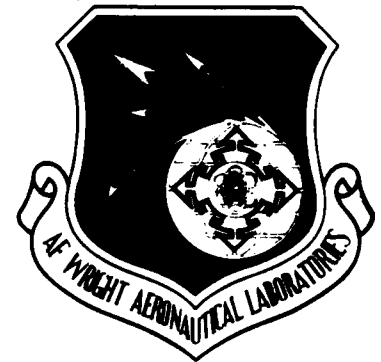ADA130786

SEMIELLIPTICAL CRACKS ALONG HOLES IN PLATES AND LUGS

A.F. Grandt, Jr., J.A. Harter,
  and D.E. Tritsch
School of Aeronautics & Astronautics
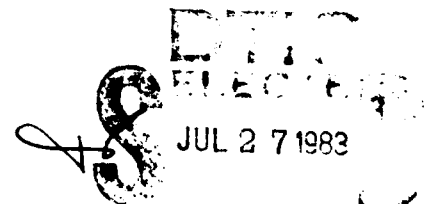Purdue University
W. Lafayette, IN 47907

May 1983

Final Report for Period 5 January 1981 - 30 November 1982

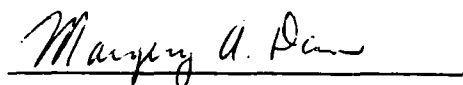DTIC FILE COPY

DTIC ELECTE
JUL 2 7 1983
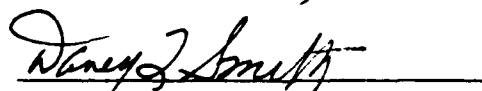
A

83 07 27 025

NOTICE

When Government drawings, specifications, or other data are used for any purpose other than in connection with a definitely related Government procurement operation, the United States Government thereby incurs no responsibility nor any obligation whatsoever; and the fact that the government may have formulated, furnished, or in any way supplied the said drawings, specifications, or other data, is not to be regarded by implication or otherwise as in any manner licensing the holder or any other person or corporation, or conveying any rights or permission to manufacture use, or sell any patented invention that may in any way be related thereto.

This report has been reviewed by the Office of Public Affairs (ASD/PA) and is releasable to the National Technical Information Service (NTIS). At NTIS, it will be available to the general public, including foreign nations.

This technical report has been reviewed and is approved for publication.

MARGERY A. DEAN

Project Engineer

DAVEY L. SMITH, Chief

Structural Integrity Branch

FOR THE COMMANDER

RALPH L. KUSTER JR., Colonel, USAF

Chief, Structures & Dynamics Division

"If your address has changed, if you wish to be removed from our mailing list, or if the addressee is no longer employed by your organization please notify AFWAL/FIBE, W-PAFB, OH 45433 to help us maintain a current mailing list."

Copies of this report should not be returned unless return is required by security considerations, contractural obligations, or notice on a specific document.

REPORT DOCUMENTATION PAGE	READ INSTRUCTIONS BEFORE COMPLETING FORM

1. REPORT NUMBER	2. GOVT ACCESSION NO.	3. RECIPIENT'S CATALOG NUMBER
AFWAL-TR-83-3043	AD-A130786	

4. TITLE (and Subtitle)	5. TYPE OF REPORT & PERIOD COVERED
SEMIELLIPTICAL CRACKS ALONG HOLES IN PLATES AND LUGS	Final Report 5 January 1981 to 30 Nov.1982
	6. PERFORMING ORG. REPORT NUMBER

7. AUTHOR(s)	8. CONTRACT OR GRANT NUMBER(s)
A.F. Grandt, Jr., J.A.Harter, and D.E. Tritsch	F33615-81-K-3206

9. PERFORMING ORGANIZATION NAME AND ADDRESS	10. PROGRAM ELEMENT, PROJECT, TASK AREA & WORK UNIT NUMBERS
School of Aeronautics & Astronautics Purdue University W. Lafayette, IN 47907	2307N116

11. CONTROLLING OFFICE NAME AND ADDRESS	12. REPORT DATE
Air Force Wright Aeronautical Laboratories Flight Dynamics Laboratory, AFWAL/FIBE Wright-Patterson AFB, Ohio 45433	May 1983
	13. NUMBER OF PAGES
	146

14. MONITORING AGENCY NAME & ADDRESS(if different from Controlling Office)	15. SECURITY CLASS. (of this report)
	Unclassified
	15a. DECLASSIFICATION/DOWNGRADING SCHEDULE

16. DISTRIBUTION STATEMENT (of this Report)

Approved for public release; distribution unlimited

17. DISTRIBUTION STATEMENT (of the abstract entered in Block 20, if different from Report)

18. SUPPLEMENTARY NOTES

19. KEY WORDS (Continue on reverse side if necessary and identify by block number)

Surface Cracks, Fastener Holes, Attachment Lugs, Fracture Mechanics, Fatigue

20. ABSTRACT (Continue on reverse side if necessary and identify by block number)

This report summarizes a basic research effort directed at characterizing the growth of semielliptical surface cracks embedded along the bore of a hole in a large plate or an attachment lug. Fatigue cracks are grown in transparent polymer test specimens which allow in situ observation of the crack plane. Crack growth was recorded by time lapse photography. Subsequent measurement of the crack photographs gave crack size and shape changes as a function of elapsed cycles.

A multidegree of freedom fracture mechanics model was developed to predict the growth of embedded surface and corner cracks located at open holes in plates loaded in remote tension. Crack growth predictions gave excellent agreement for the embedded surface crack plate results obtained under the current effort and also gave good results for corner cracked hole tests conducted under an earlier program.

Crack shape changes were examined in detail. Digitized measurements of crack profiles are presented for embedded surface crack and corner crack hole experiments. The transition of part-through cracks at holes into uniform through-the-thickness flaws is also discussed in detail. Fatigue crack growth rate changes are correlated with stress intensity factor solutions for the transitioning crack geometry.

FOREWORD

iii

TABLE OF CONTENTS

LIST OF ILLUSTRATIONS

LIST OF ILLUSTRATIONS (continued)

LIST OF ILLUSTRATIONS (continued)

LIST OF TABLES

SECTION I

INTRODUCTION

It is well known that cracks which occur at fastener holes or attachment lugs are common sources of component failure in aircraft structures. Reference 1 presents a 1971 review of significant USAF aircraft structural failures which revealed that bolt and rivet holes comprised over one third of the failure origins considered. In both the lug and fastener hole geometries, high stresses are generated next to the edge of the hole by load transfer through the fastener or pin. These high stress levels can quickly initiate cracks at local imperfections along the bore of the hole. Subsequent loading may then cause further flaw growth and ultimate failure due to the combined action of fatigue and corrosion.

The objective of this report is to summarize results of an effort directed at characterizing the growth of fatigue cracks which initiate midway along the bore of a hole in a large plate or attachment lug. The specimen geometries and crack configurations of interest are shown in Figures 1 and 2. The plate specimens contained open holes and were loaded in remote tension, while the lug specimens were loaded through a pin placed in the hole. In all cases the crack plane was located perpendicular to the loading axis.

In both specimen geometries, semielliptical surface cracks, with major and semiminor axes 2a and c, were introduced midway along the hole bore as shown in Figure 2a. These cracks were extended by fatigue and monitored as they penetrated the specimen surfaces and transitioned into

1
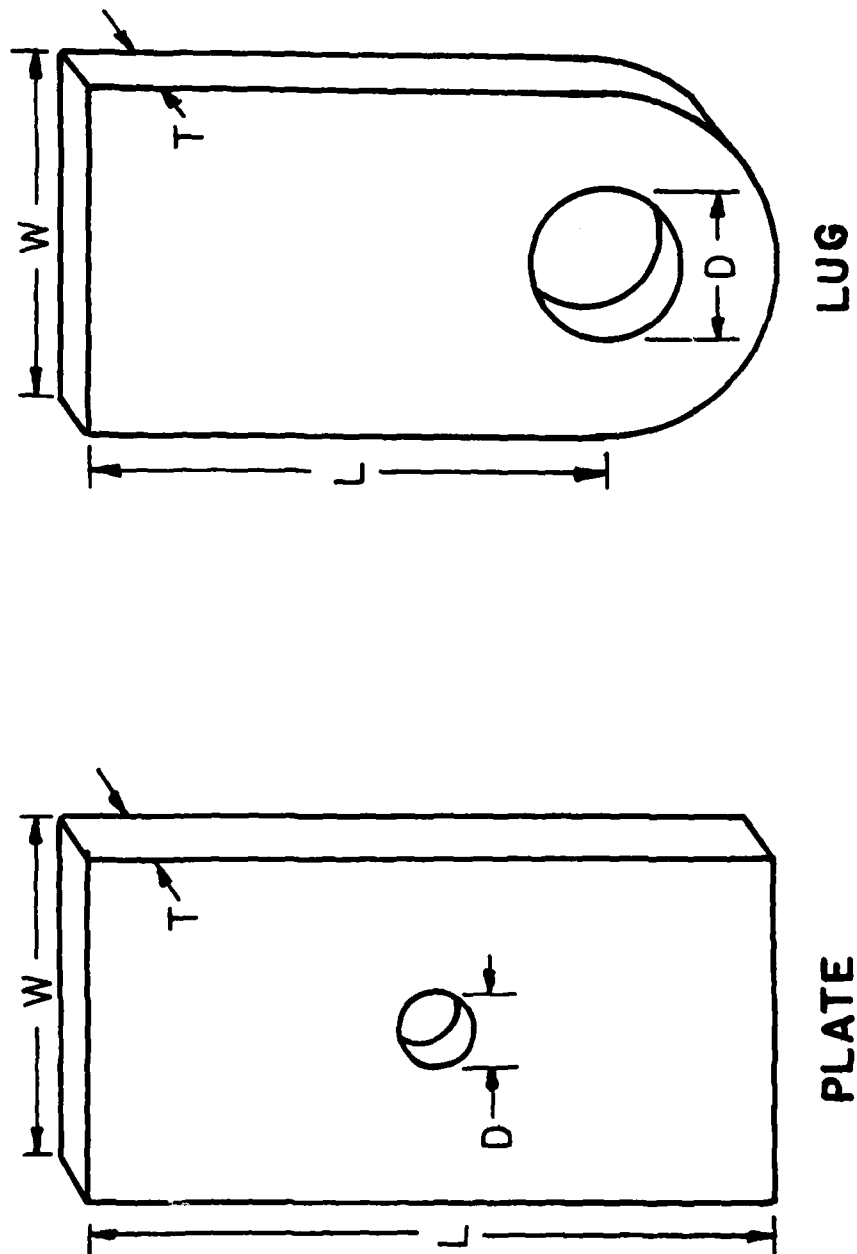
Figure 1   Lug and Plate Geometries
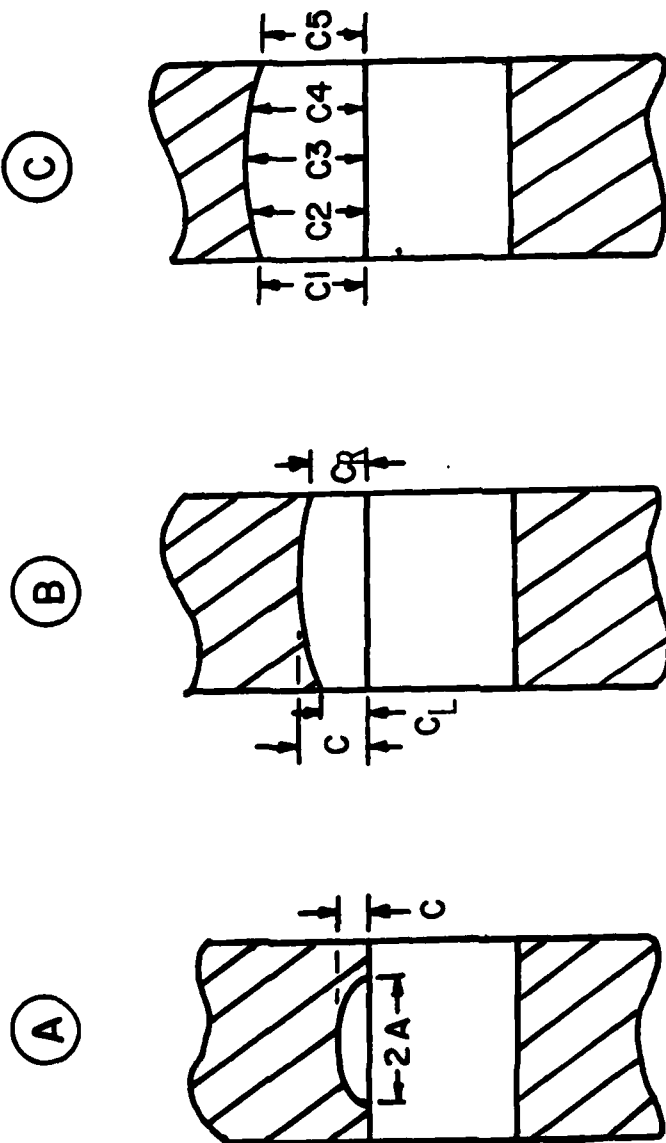
Figure 2   Definition of Measured Crack Length Dimensions
     a.   Embedded Surface Cracks Along the Bore of a Hole
     b.   Cracks that have Penetrated the Specimen Surface
     c.   Uniform Through-The-Thickness Cracks.

3

uniform through-the-thickness flaws. Immediately after the semielliptical crack penetrated the left and right specimen surfaces (see Figure 2b), the flaw shapes were characterized by the surface dimensions c_L and c_R and by the midpoint length c. Once a uniform through-the-thickness geometry was reached, the five measurements shown in Figure 2c were used to determine an average through-the-thickness crack length.

The test matrix is summarized in Table 1 along with nominal specimen dimensions. Note that three plate specimens were tested with single embedded surface cracks, while one plate contained two nonsymmetric corner cracks located at opposite sides of the hole. Nine pinloaded lug specimens were tested with single embedded surface cracks. Five of these specimens were continued as uniform through-the-thickness flaw tests. The lug specimens included four different widths (W/D = 3.0, 2.5, 2.0, and 1.5). Here W is the specimen width and D is the hole diameter. Three four-point bend edge-crack specimens were also tested to further characterize the baseline fatigue crack growth properties of the specimen material.

Since direct measurement of the internal dimensions of the semielliptical and through-the-thickness cracks would be impossible in metal specimens, the test pieces were manufactured from polymethylmethacrylate (PMMA), a transparent polymer. The transparent nature of PMMA allows internal crack dimensions to be monitored during the test, and provides a simple, but accurate means for measuring both crack shape and size changes as a function of applied loading cycles.

Being a fairly brittle material, flaw growth in PMMA may be described by many of the same linear elastic fracture mechanics techniques employed

4

for conventional structural alloys. In particular, both fracture and fatigue crack growth rates can be characterized in terms of the stress intensity factor K. The following section describes the experimental procedure and material characterization tests, while the experimental results and corresponding fracture mechanics analyses are described in later sections.

Table 1 Test Matrix

Geometry	Load	T[1]	W[1]	D[1]	D/T	W/D	Test Number Embedded Cracks	Test Number Thru-Cracks
Plate	Remote	0.7	8.0	0.75	1.0	10.67	T1, T2, T3	
Plate[2]	Remote	0.7	8.0	0.75	1.0	10.67	U1	
lug	pin	0.7	6.75	2.25	3.0	3.0	PT4, PT5	PT4, PT5
lug	pin	0.7	5.625	2.25	3.0	2.5	PT6, PT7	
lug	pin	0.7	4.50	2.25	3.0	2.0	PT8, PT14	PT8, PT9
lug	pin	0.7	3.375	2.25	3.0	1.5	PT10, PT11,PT13	
Baseline crack growth rate tests[3]								BT1, BT2, BT3
Total Tests								20

Comments:

1. Nominal specimen dimensions given in inches. See Fig. 1 for dimensions.

2. Two nonsymmetric corner cracks located at opposite sides of hole.

3. Four-point bend edge crack specimens.

6

SECTION II

EXPERIMENTAL PROCEDURE

The transparent property of PMMA was used in the present experiments
to make direct measurements of the embedded surface cracks. The methods
used to characterize the test material and to measure the cracks in the
PMMA plate and lug specimens are described in this section. Additional
details may be found in Reference 2.

1. Material Characterization

All specimens were cut from a single sheet of PMMA and were located
so that the crack plane had the same orientation with respect to sheet
reference axes. The PMMA sheet had supplied specimens for previous pro-
grams (3-6) and was fairly well characterized. The 0.2 per cent tensile
yield strength was previously found to be 7000 psi and the fracture tough-
ness K_{IC} was 990 ± 60 psi-in$^{1/2}$.

Baseline fatigue crack growth rate tests were conducted with edge-
cracked beams loaded in four-point bending as shown in Figure 3. The cy-
clic load was applied at a frequency of $2H_z$ with $0 < R \leq 0.05$ (R = minimum/
maximum load). The crack plane was illuminated with a fibre optics light
source and photographed through the transparent end of the specimen at
periodic cyclic intervals. A Nikon F3 camera, 135 mm lens, and bellows
were used to photograph the cracks. A typical baseline test photograph
is shown in Figure 4.

The crack photographs were measured by projecting the 35 mm black
and white negatives onto a screen. Measuring the projected images to the
nearest millimeter resulted in an accuracy of 0.001 in. for the actual
crack lengths. Since the crack front is curved, a five point average was
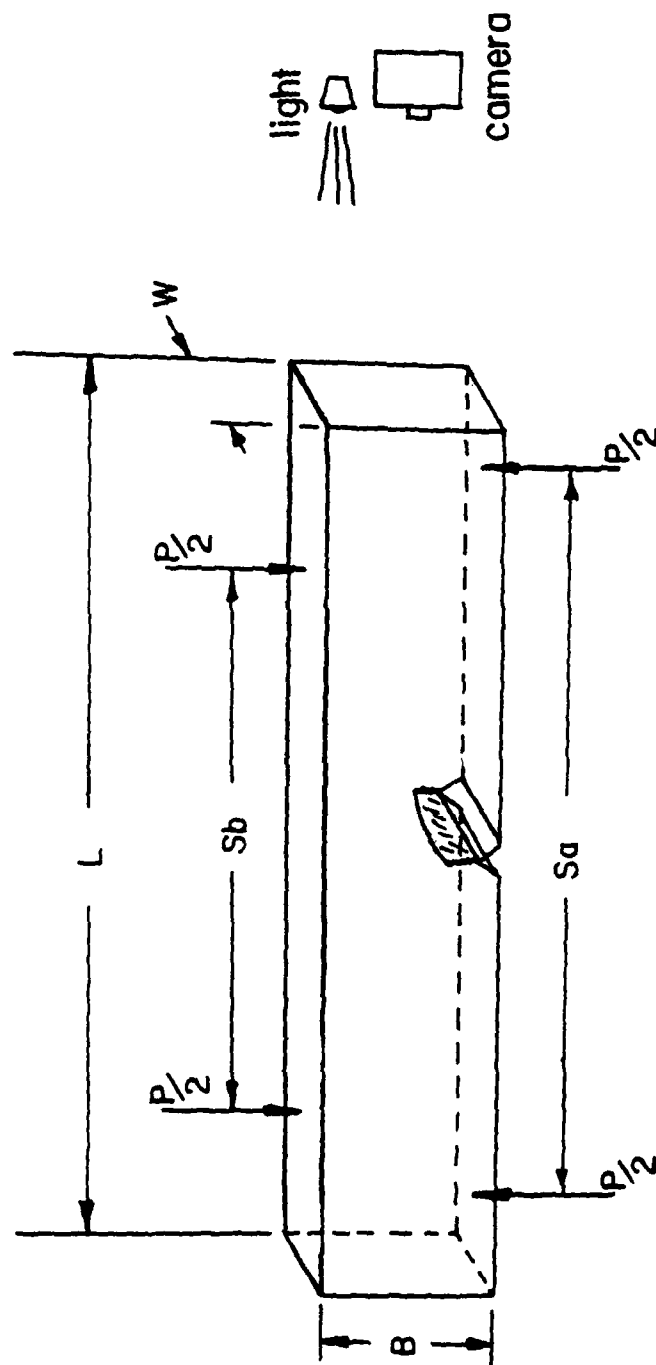
Figure 3   Schematic of the Four-Point Bend Test Showing
Specimen Dimensions

8
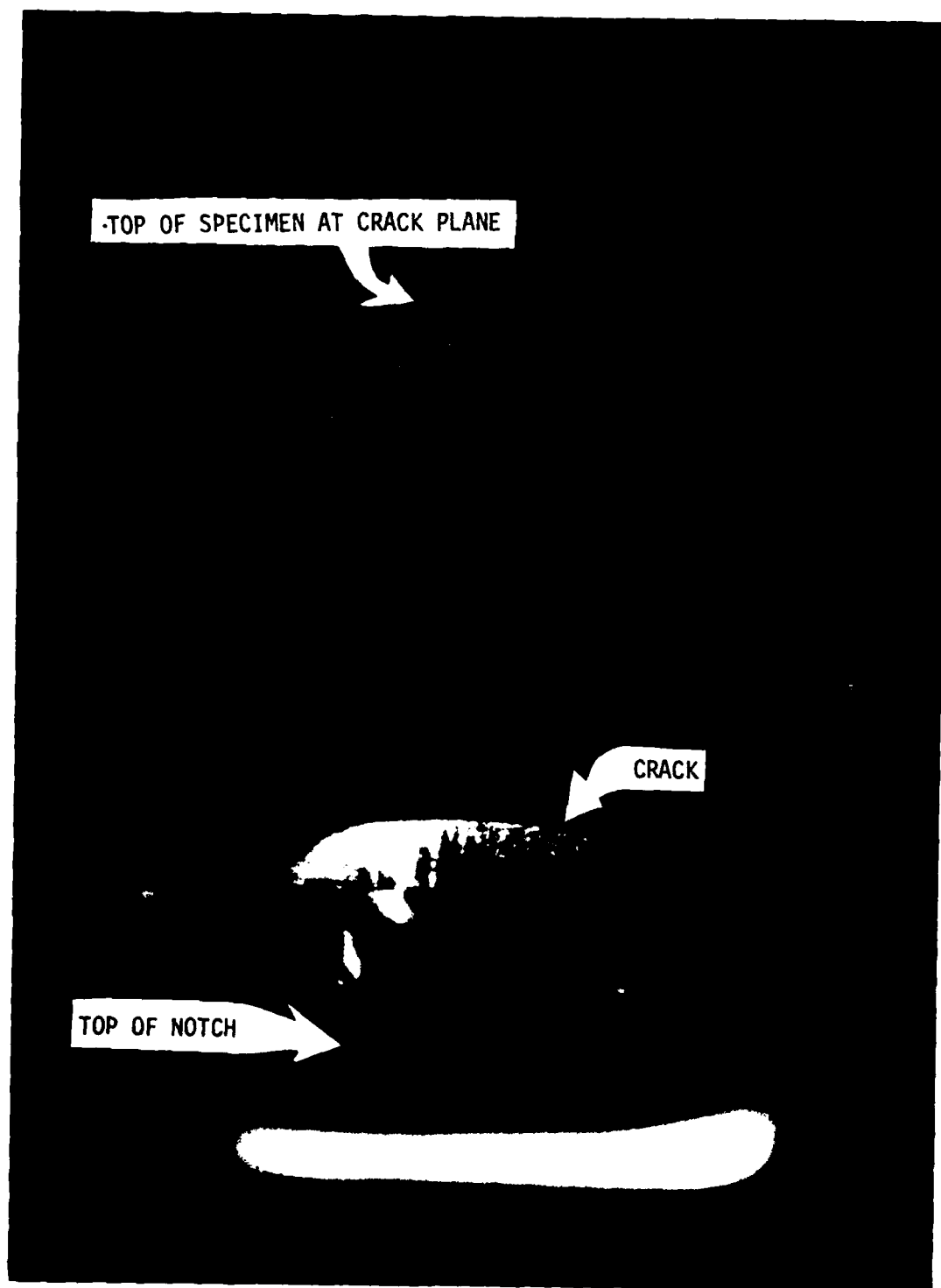
Figure 4   Photograph of a Through-The-Thickness Edge Crack
in a Four-Point Bend Baseline Specimen

9

used as the crack length (see Figure 2c). ASTM guidelines [7] recommend that cyclic crack growth increments be on the order of 0.01 in. for this level of precision. This criterion was used as much as possible when choosing cyclic intervals between photographs. The crack length data for the tests are shown graphically in Figure 5. Fatigue crack growth rates (da/dN) were determined by a five-point polynomial method [8] for differentiating the experimental data.

The baseline da/dN versus cyclic stress intensity factor data are compared in Figure 6 with a band representing data reported in Reference 4 for the same sheet of material. (The Reference 4 data were obtained at a cyclic frequency of 1 Hz.) Note that the crack growth rate is described quite well over the range shown by the simple power law

$$\frac{da}{dN} = C \, \Delta K^m \qquad \qquad (1)$$

Here C and m are the empirical constants given on Figure 6. Stress intensity factors were computed for the four-point bend geometry by the appropriate expression given in Reference 9.

2. Plate and Lug Specimen Preparation

Steel grips were bonded and bolted to the plate and lug specimens as shown in Figures 7 and 8. A mirror placed over the specimen ends allowed direct observation of the crack plane. Preparation of the plate and lug specimens included five steps: machining, annealing, surface preparation, bonding, and crack initiation.

a. Machining

The plate and lug specimens described in Figure 1 were machined to proper dimensions from the same 0.7 in. thick PMMA sheet used for
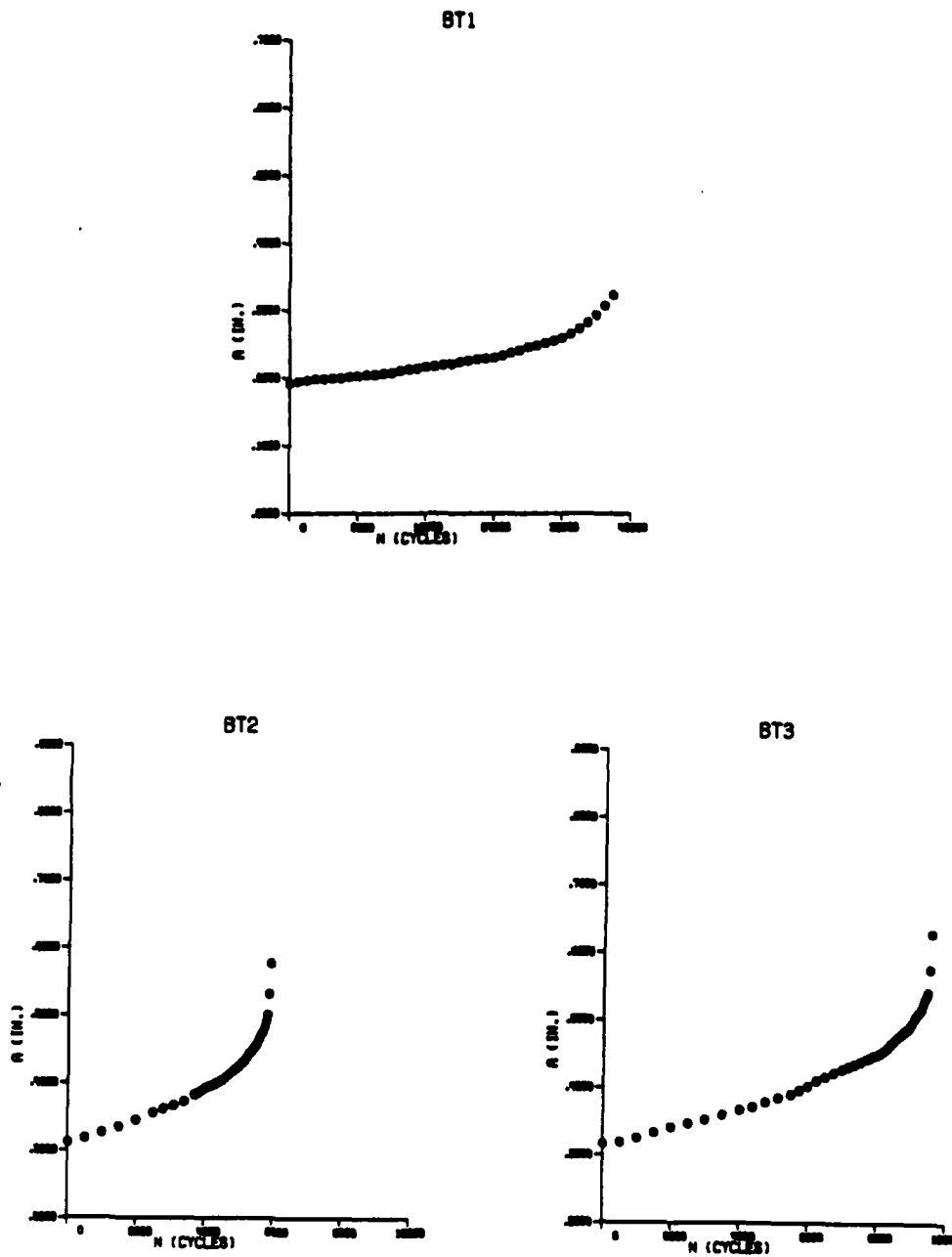
Figure 5   Fatigue Crack Growth Curves for Four-Point
            Bend Baseline Tests BT1, BT2, and BT3.

$$DA/DN = C(\Delta K)^m, \quad C = 1.0701789 \times 10^{-31}$$
$$m = 9.2141356$$

Units of C are for da/dN in IN./CYCLE
and ΔK in PSI$\sqrt{IN}$.
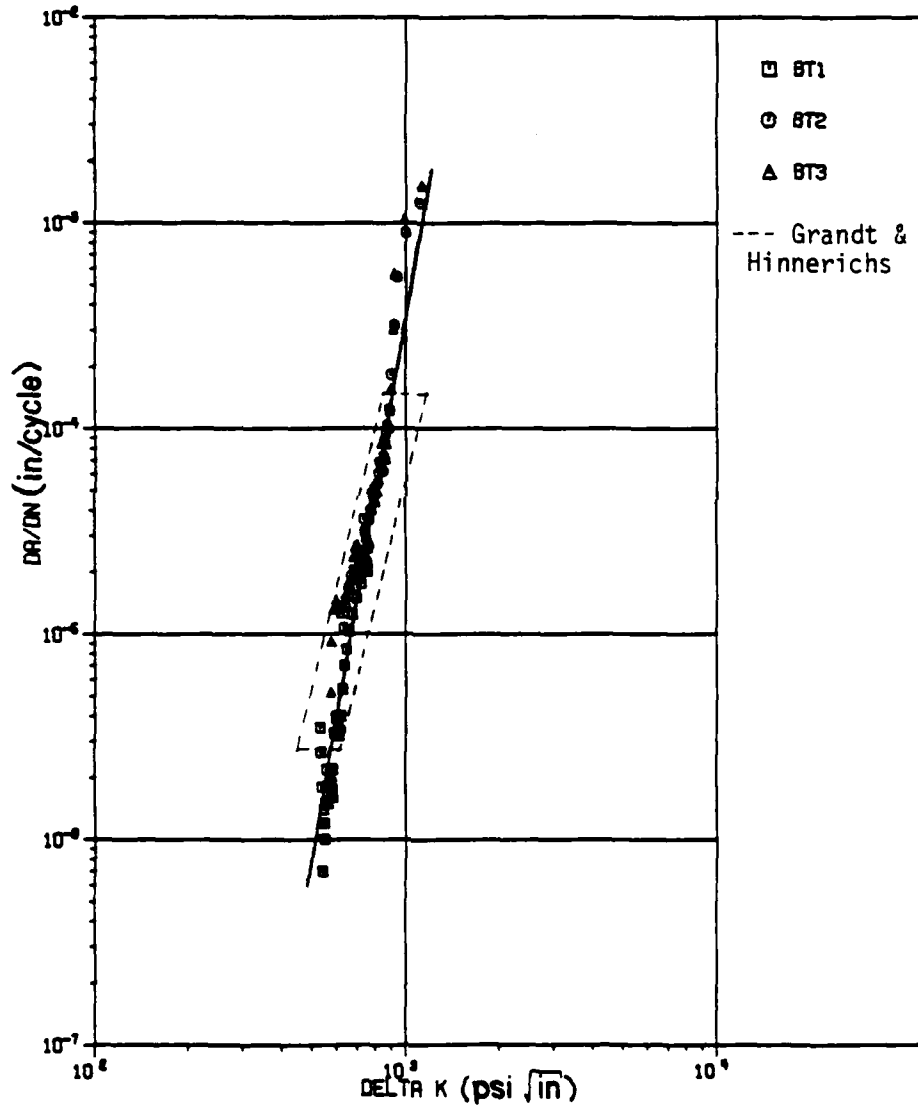
Figure 6   Baseline da/dN vs. ΔK data for PMMA
Test Material

12
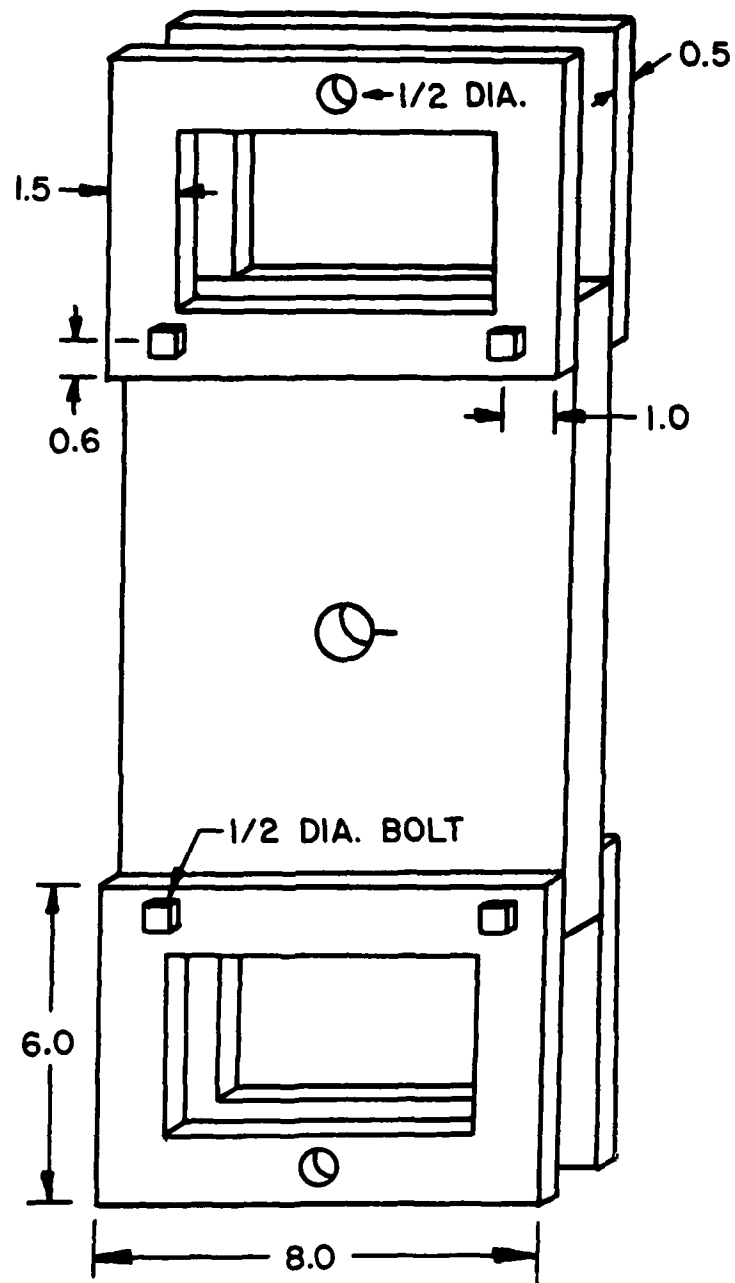
Figure 7   Schematic View of a Plate Specimen Fastened
to the Test Grips (All Dimensions in Inches)

13
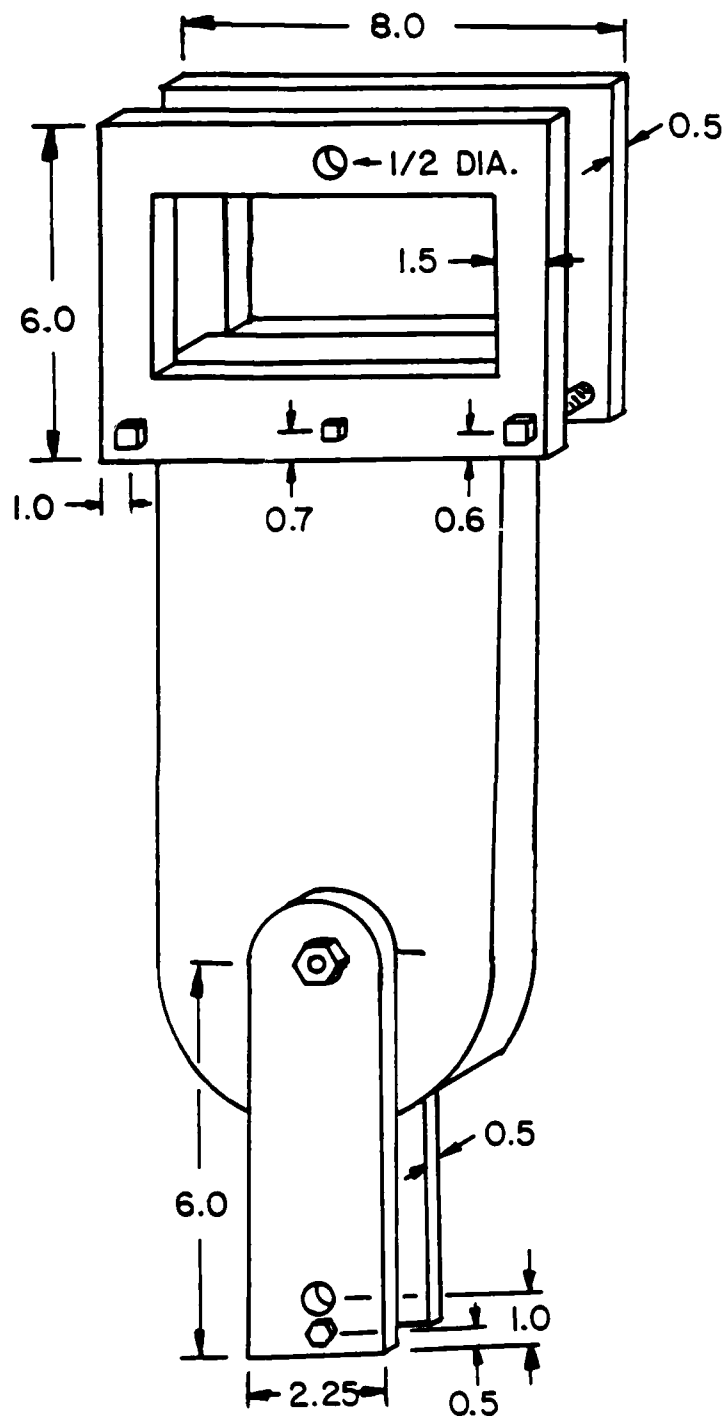
Figure 8   Schematic View of Pin-Loaded Lug
Specimen Fastened to the Test Grips
(All Dimensions in Inches).

the baseline specimens. As mentioned earlier, all of the specimens were cut so that the cracks would grow in the same direction relative to the sheet.

b. Annealing

Each specimen was annealed in an oven at 101°C (214°F) for 24 hours to relieve any residual stresses that may have been present after machining. The specimens were cooled to 50°C (122°F) at a rate of 2°C per hour (3.6°F per hour). Then the heat was turned off and the specimens were allowed to cool to room temperature (21°C = 70°F) with the oven door closed. Total cooling time was approximately 40 hours.

c. Surface Preparation

The PMMA material was covered with protective paper that needed to be removed prior to bonding to the metal grips. Since the material used here was several years old, the paper was difficult to remove. A flat wood file proved to be the most efficient way to remove the paper. The bonding areas were then sanded with 120 weight sandpaper for good bond adhesion between the specimens and loading grips.

The viewing end of each specimen serves as a lens and must be clear and flat in order to view the cracks without distortion. The end was sandwiched flush between two flat pieces of scrap material and clamped in place. A sanding block was used to sand the surface to a uniform texture with the following order of sandpaper: 120, 220, 440, and 600 weight. The final step was to polish the end to transparency with one micron aluminum oxide powder on a moist cloth.

d. Bonding

All bonding surfaces were wiped clean with alcohol. Thermoset 103 adhesive was used with a resin/hardener ratio of 2/1 which provides a tensile shear strength of 3,100 psi [10]. The grip/specimen alignment was provided by a gluing rig. Bonding pressure was applied by a 25 pound lead weight, and silica grease was used to prevent bond adhesion at the viewing surface or grip/gluing rig interface. Using holes in the steel grips as guides, holes were drilled through the PMMA specimens and used to bolt the grips to the test specimens (in addition to the bonding).

e. Crack Initiation Methods

Before any of the specimens could be tested, an initial embedded flaw had to be introduced. The plate specimens had a hole diameter of 0.75 in. which gave little working room for starting a crack. A pointed soldering iron was used to make an indentation in the center of the hole normal to the loading direction. This stress concentration caused a crack to start at that point. The hole diameter of the lug specimens was large enough to allow the use of a X-acto knife for crack initiation. The knife was positioned in the hole and impacted with a small hammer to cause a precrack to propagate in front of the blade. Late in the testing, it was found that this method occasionally caused some crack retardation due to crack tip blunting, and in some cases caused cracks to grow out of plane. A hot X-acto knife was used to initiate cracks in lug tests PT5 and PT11.

All of the precracks were further extended with cyclic loads approximately 40-50% larger than the final test load. A frequency of

16

3 Hertz was used for this precracking. Although PMMA is brittle, and shows little fatigue crack retardation [3], care was taken to reduce the loading slowly during precracking to avoid any retardation at the final test loads. The initial crack lengths along the hole were precracked to approximately 50% of the specimen thickness. All of the final crack growth testing was conducted at the same cyclic frequency of 2 hertz used for the baseline testing in order to avoid possible rate effects in the polymer test material. The same R ratio (0 < R ≤ 0.05) was used for these tests as for the baseline tests.

It should be noted that an attempt at making small initial flaws was made with the lug specimens. This was accomplished by drilling a smaller two inch diameter hole in the lugs. The lugs were then precracked, and the hole was bored to its final size (2.25 inch) leaving a small initial flaw. Since the small flaws (<0.5 T) did not yield fast enough crack growth rates at the test loads, and the procedure was fairly time consuming, this method was abandoned. However, it was used on lug tests PT4 and PT6.

3. Fatigue Crack Growth Testing

A 10 kip programmable MTS machine was used to load the specimens. The grips were pinned to the load cell and the hydraulic piston through eyebolts. A movable arm was designed and used as a mount for the camera and bellows. The cracks were viewed through a front surface mirror set at approximately 45 degrees in the upper grips. A double gooseneck fiber optics (cold) light source was used to illuminate the cracks. The cold light source avoided heating the test specimens. The testing arrangement is illustrated in Figure 9 for one of the plate specimens.

17
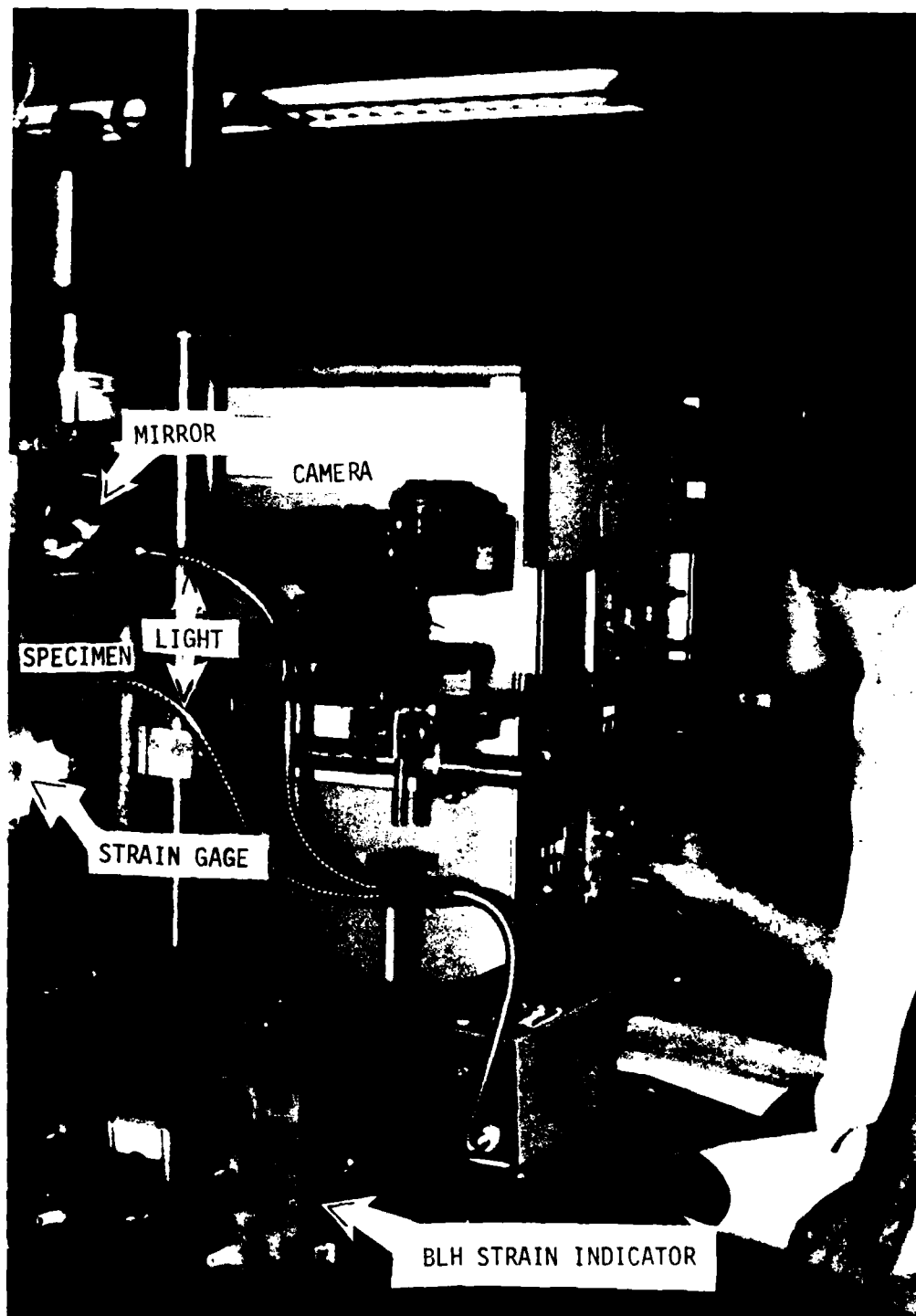
Figure 9a   Photograph of Testing Apparatus Showing Plate Specimen
             Mounted in Fatigue Machine, Viewing Mirror, Camera,
             Light Source, and Strain Indicator.

13
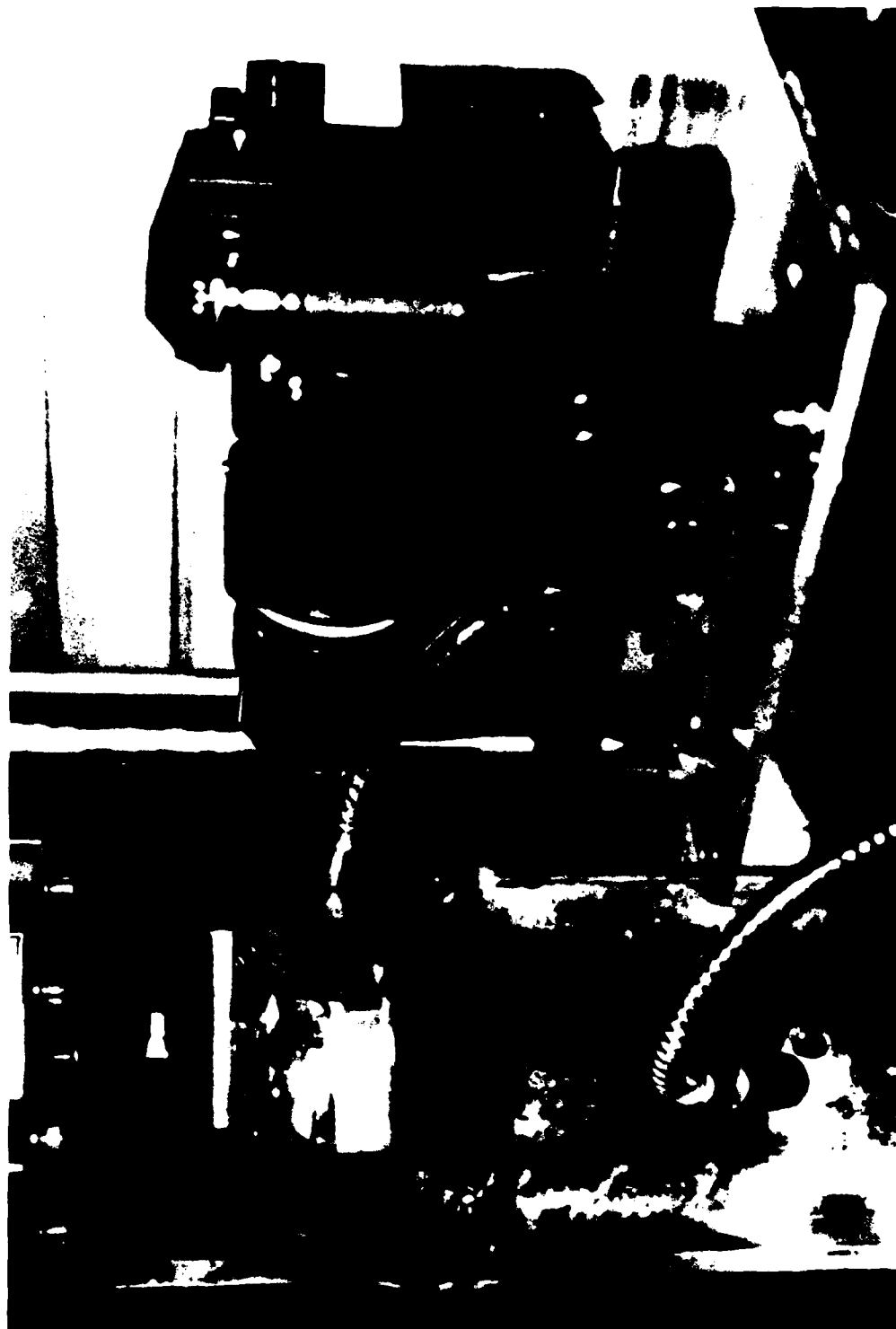
Figure 9b   Closeup View of Test Apparatus Showing Camera and Viewing Mirror for Plate Specimen

19

Although the specimens were pinned at both ends, out of plane bending may have existed if the specimens were not loaded through their axis of symmetry. All of the plate specimens were fitted with strain gages on each side at the crack plane. These gages monitorea strain differences through the thickness of the material. Washers were used to align the specimens to minimize bending. Strain differences greater than five percent could be detected visually. Two early practice lug tests were also mounted with strain gages, and showed similar results. Lug tests PT4, PT6, and PT8 were positioned visually. All of the other lug tests were aligned by using a dial indicator to sense horizontal motion below the crack plane.

4. Crack Measurements

Several factors are involved in viewing the cracks in the plate and lug specimens. First, the viewing surface must be clear and flat since it is a lens. Also, the light has to shine nearly parallel to the camera so that the crack reflection may be observed. One of the biggest problems that was encountered was the effect of specimen length on crack observation. It was very difficult to see both sides of the lug specimens if the distance from the lens to the crack plane was greater than 8 inches. The shortest specimens that still gave uniform stress at the crack plane were determined to be those with an unbonded length/width (L/W) of unity. This was determined from stress intensity factor solutions for similar geometries that gave "infinite length" stress intensity factors [9]. Therefore, all of the lug specimens had unbonded L/W's of one. The unbonded plate lengths were 11 inches. The bond length in all cases was 1.5 inches, so that the total length to the crack plane war 7 inches for the plate specimens.

Crack growth was again recorded by time lapse photography for the plate and lug tests. A typical set of photographs for one of the plate tests is shown in Figure 10. Here the flaw plane is oriented so that the hole bore is vertical and the crack is growing toward the right from the right edge of the hole. Note that the transparent specimen acts as a prism and the crack image is reflected at the specimen walls. The initial surface crack grows along the hole bore and penetrates one of the plate surfaces at approximately 46,300 cycles. Penetration through the opposite surface follows shortly after, and the crack continues to grow into a through-the-thickness geometry. (Detailed measurements are reported later.)

The crack photographs were measured as before. The negatives were projected to a scale so that 0.001 inch in actual size could be resolved. Scaling of the photographs was based on known reference dimensions in two perpendicular directions. The hole diameter and plate thickness provided convenient reference distances. Slight scribe marks along the front and back surfaces in the crack plane were sometimes used to highlight the plate thickness in the photographs.

Since the embedded flaws eventually transition to become through-the-thickness cracks, the crack shapes were divided into three categories: embedded, intermediate, and transition crack lengths. The embedded case implies that the crack is completely inside the material along the bore of the hole (see Figure 2a). The intermediate case occurs when one side of the crack has penetrated the surface of the material while the other side is still embedded. This is a result of unsymmetrical initial flaws, material inhomogeneity, and the existence of some out of plane bending. When both sides of the crack have penetrated the surface, as shown in
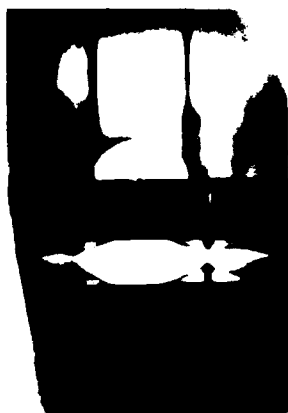
N = 46,310

N = 47,550

N = 52,050

N = 44,750

N = 46,500

N = 51,600

N = 37,500
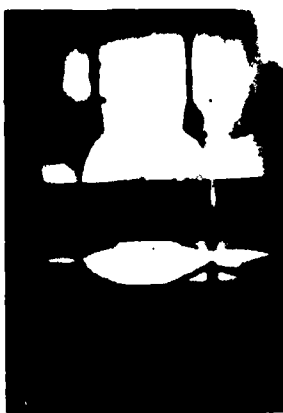
N = 46,430

N = 50,650

Figure 10   Sample Set of Photographs Taken During Plate Test T2

22

Figure 2b, transition is achieved. In the embedded case, the hole bore crack dimension 2a, and the maximum length of the crack radiating from the hole (dimension c) were measured as a function of elapsed load cycles. Crack lengths along each side of the specimen (c_L and c_R), as well as the maximum penetration c, were measured after transition. In the intermediate case, after surface penetration by one crack tip, but not both, the hole dimension 2a was also recorded. The crack growth results are summarized in the following section.

SECTION III

EXPERIMENTAL RESULTS

The results of the experiments conducted here may be divided into three categories: plate tests, lug embedded crack tests, and lug through-crack tests. All of the plate specimens were loaded in remote tension, and the cracks grew from the open holes. There were four different lug sizes, all of which were pin loaded. The data for each test are given here in graphical format and are presented in tabular form in Reference 11. The actual specimen dimensions and applied cyclic force for each test are summarized in Table 2.

1. Plate Test Results

All of the actual crack lengths were calculated by scaling the photograph measurements using known dimensions as discussed in Section II. These crack lengths were plotted versus elapsed load cycles before and after both sides of the crack had penetrated the specimen thickness. Before either side of the crack penetrated the plate thickness, crack dimensions a and c were measured and plotted (see Figure 2). After one side of the crack had "popped" through a plate surface, a new plot was prepared to describe the transition and growth of the through-the-thickness flaw. This second plot presents the dimensions c_L, c_R, and c for the through-crack, and for reference, also includes the last 5 measurements of the embedded flaw prior to free surface penetration.

The crack growth data for plate specimens T1, T2, T3 and U1 are shown in Figures 11-14. Note the crack growth behavior following penetration of the specimen thickness by the embedded cracks in Specimens T1, T2, and T3 (Figures 11b, 12b and 13b). Here the new crack dimensions created at the

Table 2   Specimen Dimensions and Applied Loads

Specimen Number	W (inch)	T (inch)	D (inch)	Applied Load P(lbs) Minimum	Applied Load P(lbs) Maximum
Surface Cracked Plate Specimens					
T1	7.975	0.699	0.750	10	3400
T2	7.970	0.720	0.750	25	3400
T3	7.960	0.700	0.750	50	3400
U1	8.000	0.699	0.750	30	3400
Surface Cracked Lug Specimens					
PT4	6.750	0.712	2.250	10	1100
PT5	6.750	0.715	2.250	50	1200
PT6	5.625	0.711	2.250	10	1100
PT7	5.625	0.714	2.250	10	1000
PT8	4.500	0.714	2.250	5	750
PT14	4.500	0.714	2.250	20	900
PT10	3.375	0.724	2.250	5	500
PT11	3.375	0.711	2.250	5	500
PT13	3.375	0.750	2.250	0	800
Through-Cracked Lug Specimens					
PT4	6.750	0.712	2.250	10	1100
PT5	6.750	0.715	2.250	50	1000
PT8	4.500	0.714	2.250	5	550
PT9	4.500	0.724	2.250	5	550
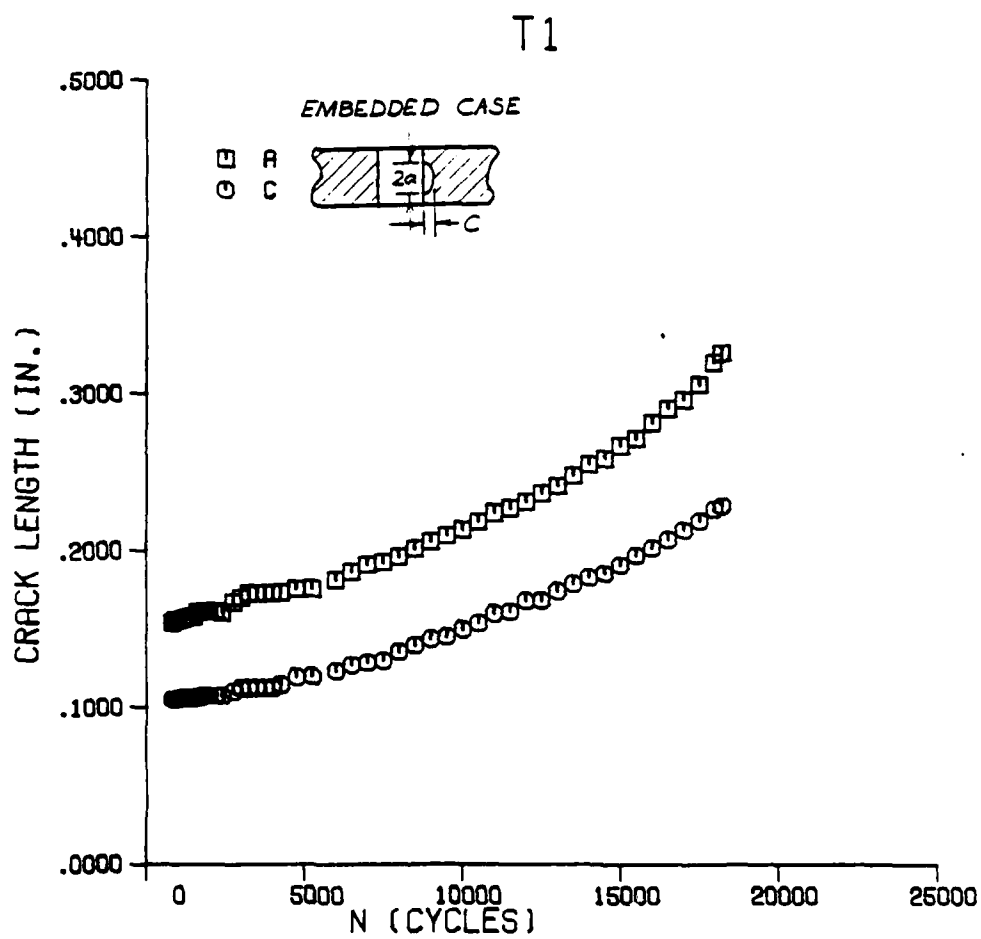
Figure 11a   Fatigue Crack Growth Data for Plate Specimen
              T1 Prior to Crack Transition
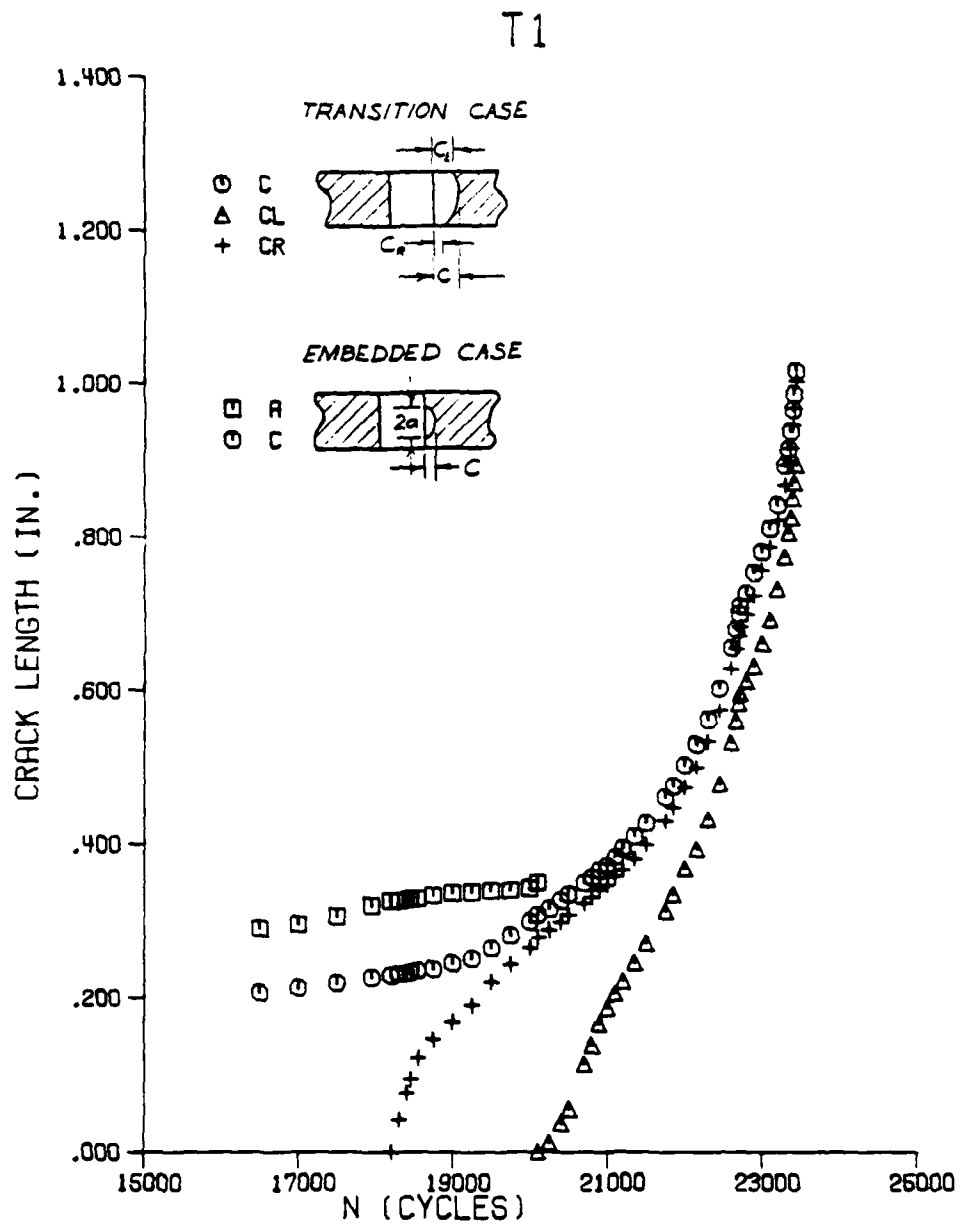
Figure 11b   Fatigue Crack Growth Data for Plate Specimen
             T1 During Transition Period

28
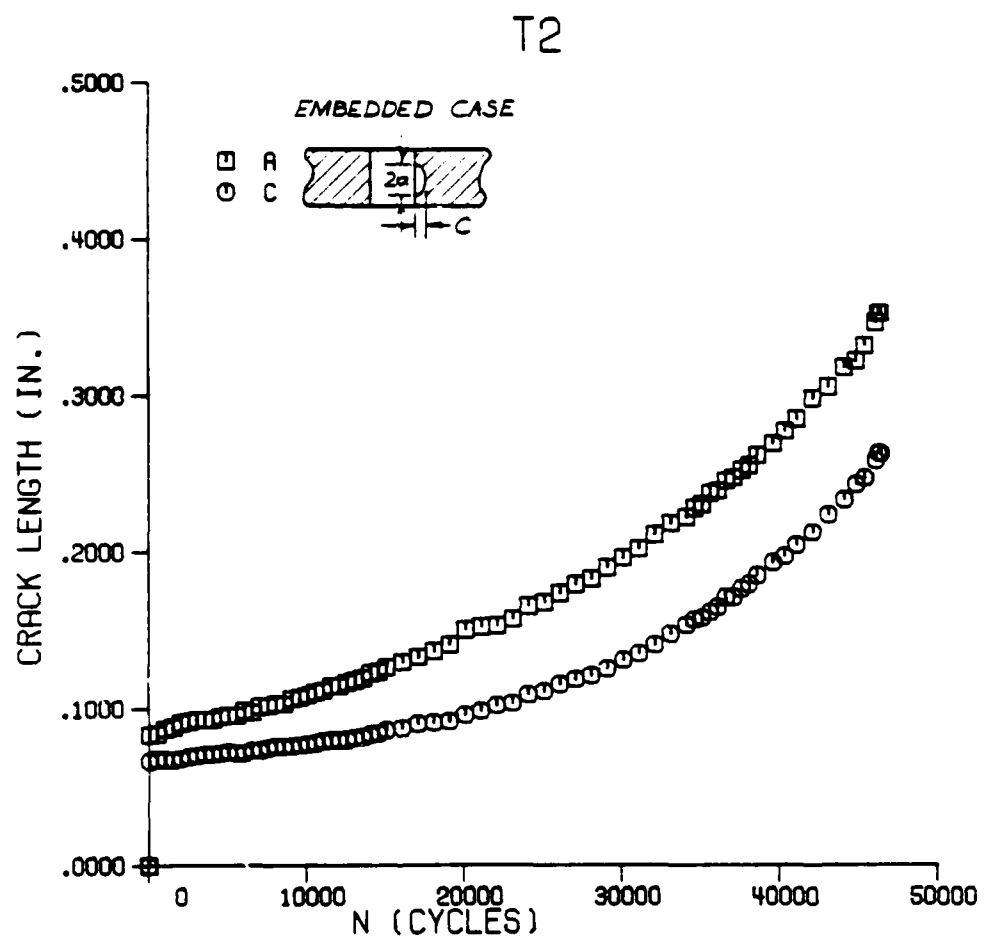
Figure 12a   Fatigue Crack Growth Data for Plate Specimen
T2 Prior to Crack Transition
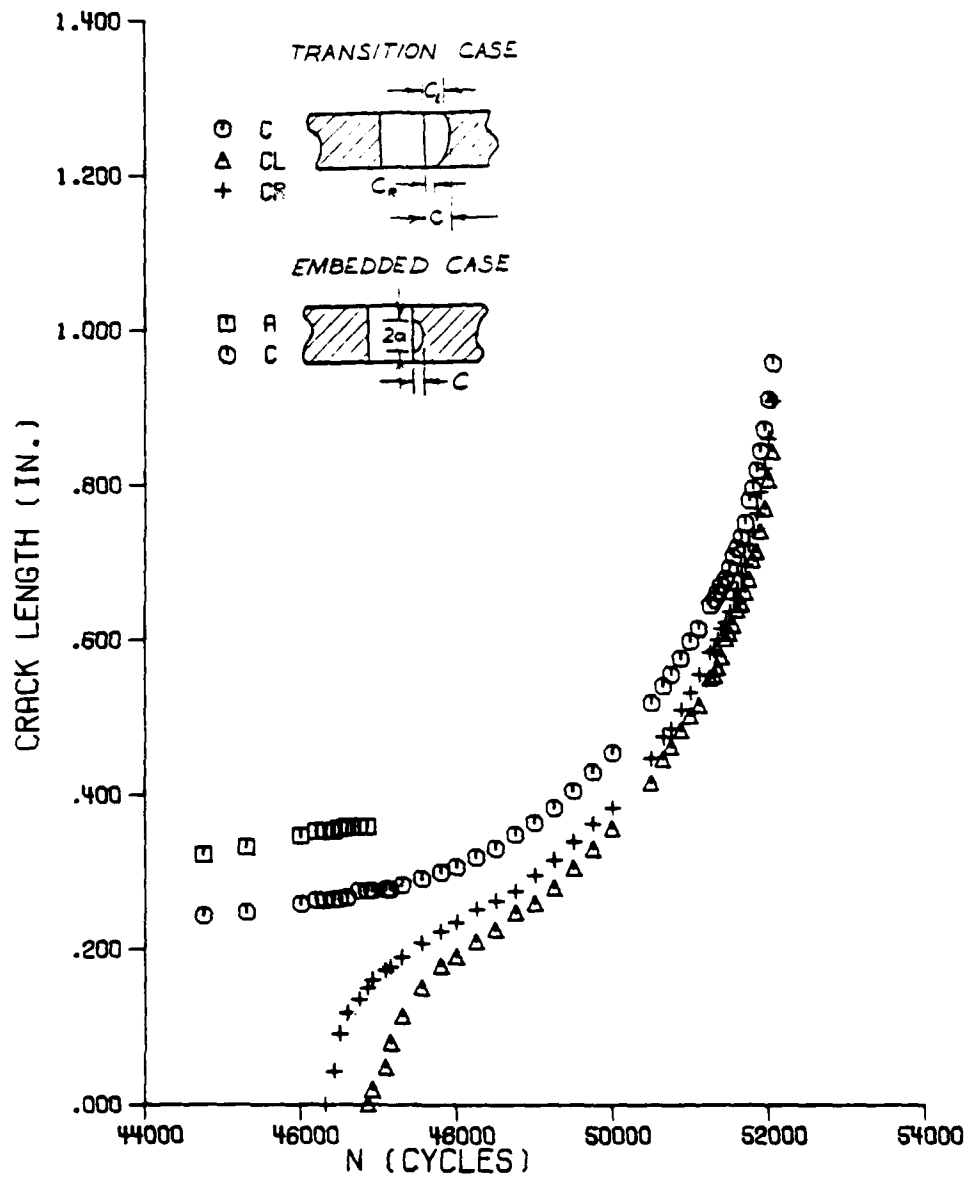
Figure 12b   Fatigue Crack Growth Data for Plate Specimen
T2 During Transition Period
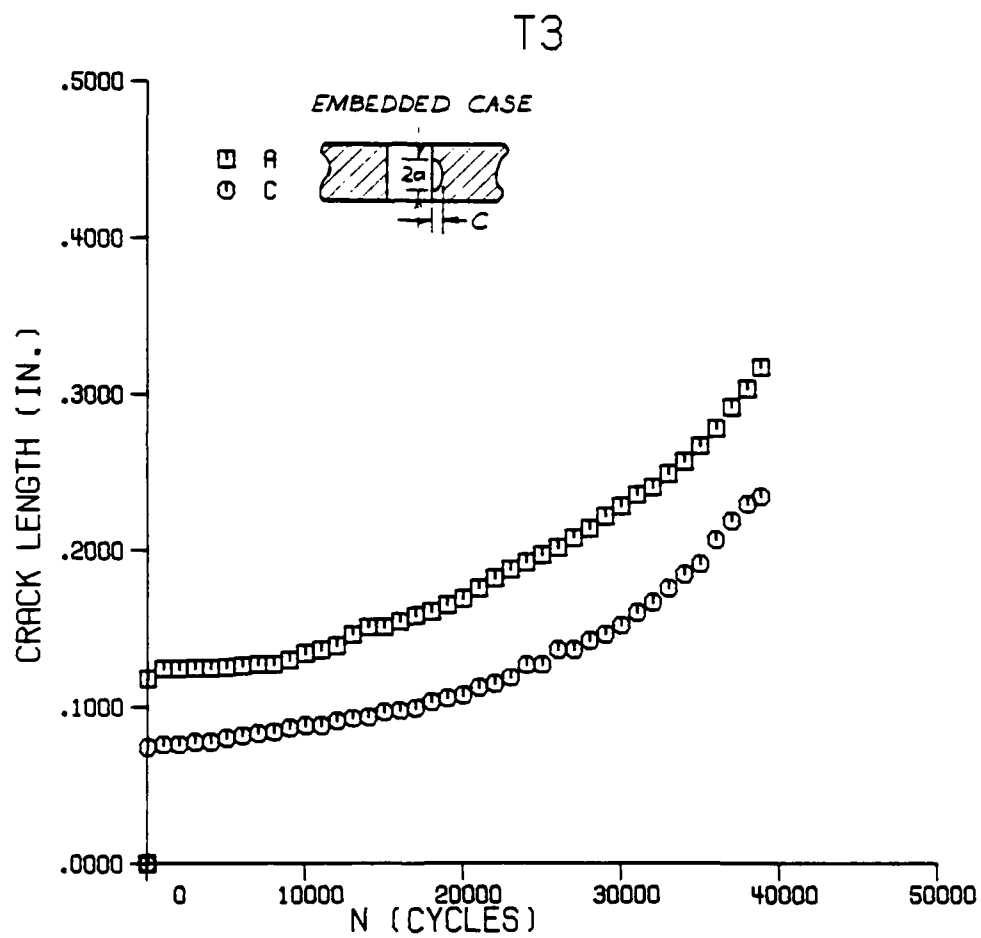
Figure 13a   Fatigue Crack Growth Data for Plate Specimen
T3 Prior to Crack Transition

T3
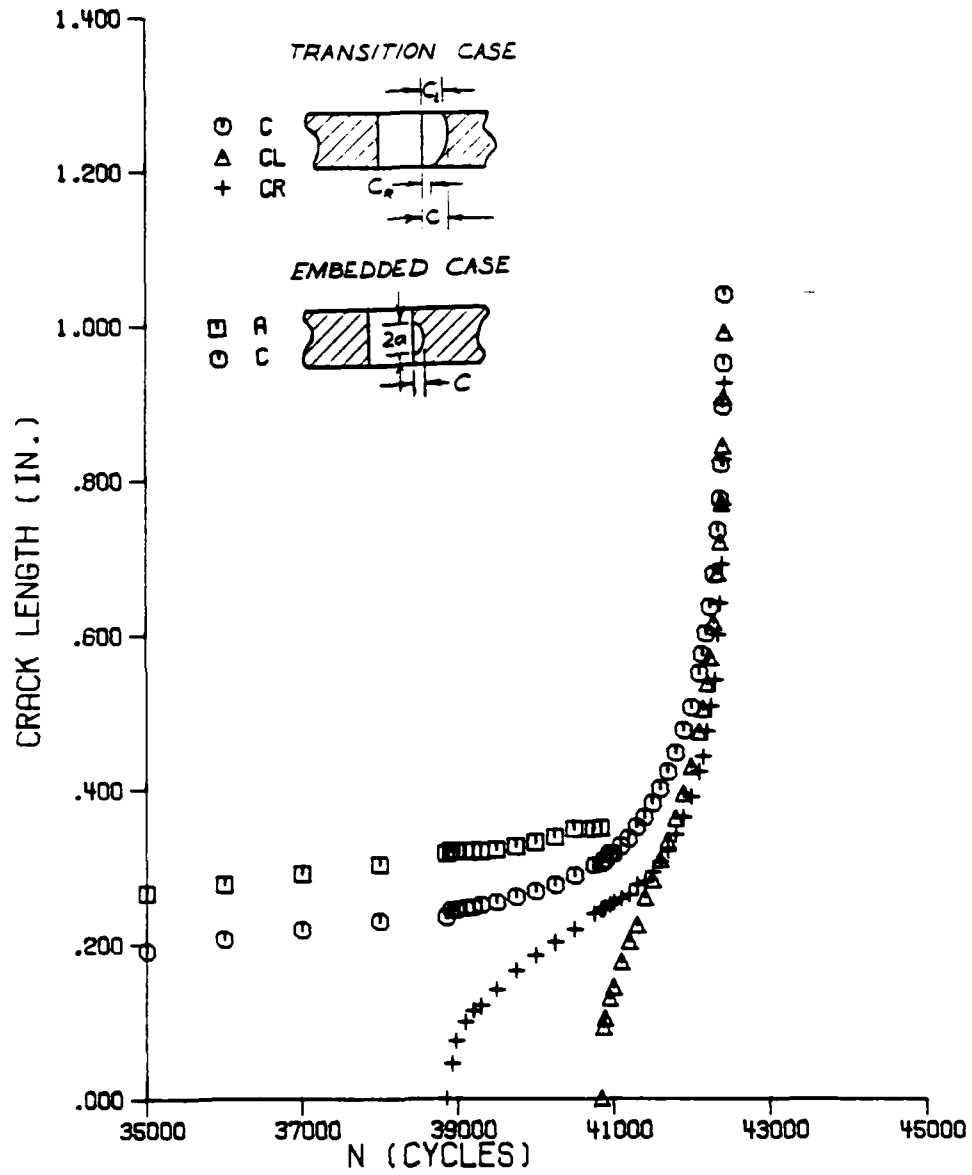
Figure 13b   Fatigue Crack Growth Data for Plate Specimen
             T3 During Transition Period

U1

EMBEDDED CASE   TRANSITION CASE
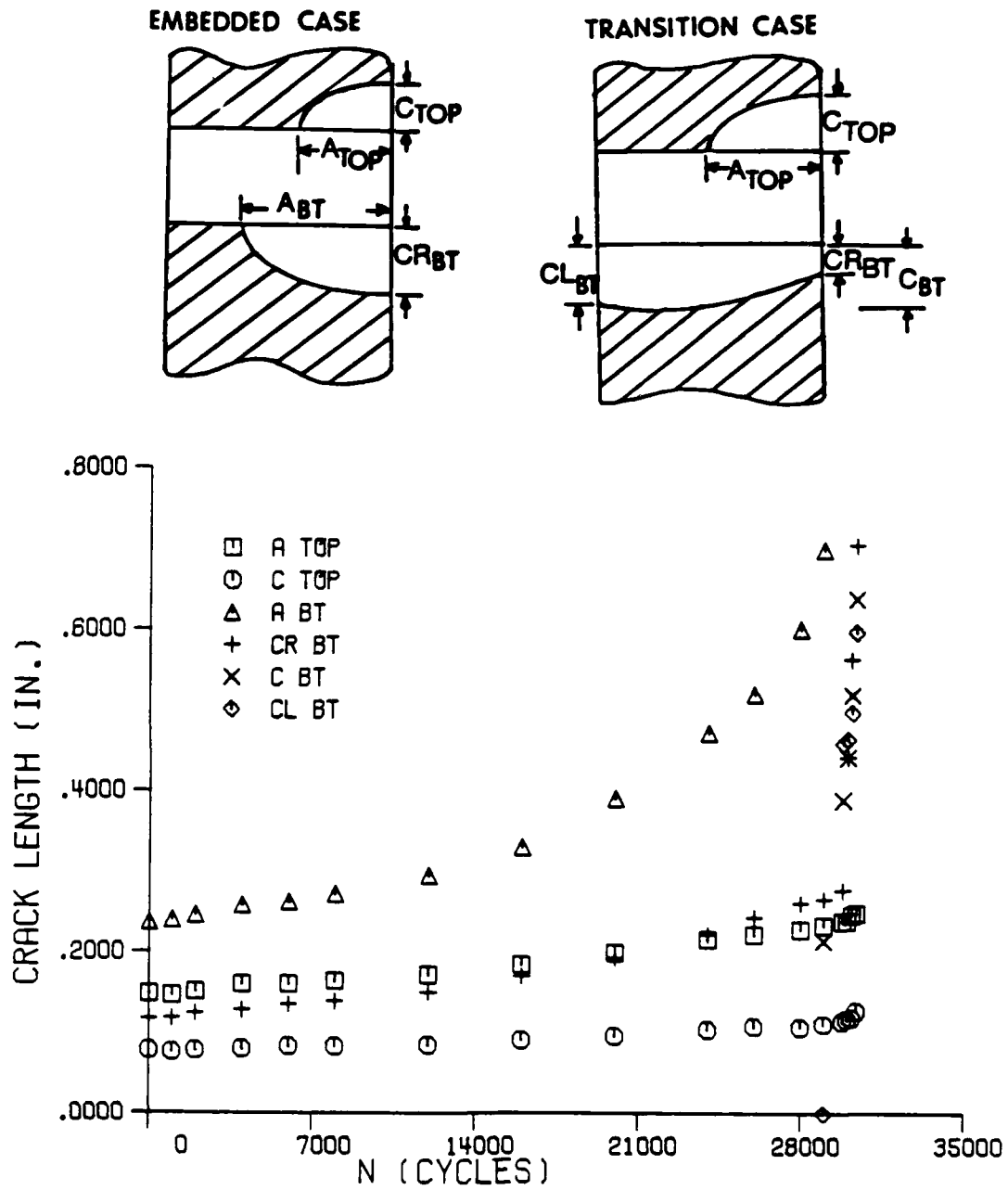
Figure 14   Fatigue Crack Growth Data for Nonsymmetric Double
             Corner Crack Plate Specimen U1

plate surfaces (c_L and c_R) initially grow very rapidly, but then slow down as a uniform through-the-thickness geometry is reached. These dimensions then increase rapidly again prior to final fracture. This transition behavior is correlated with corresponding stress intensity factor analyses, and is discussed in greater detail in a separate paper [12].

A composite plot of crack aspect ratio a/c versus flaw size 2a/T is given in Figure 15 for the three embedded plate tests. Note that all three tests yielded similar crack shapes prior to penetration through the plate surfaces. The natural aspect ratio for the fatigue cracks generally fall in the range 1.3 < a/2c < 1.6.

The nonsymmetric corner crack results presented in Figure 14 are the only data obtained for that geometry. This experiment was preliminary in nature and was conducted mainly to determine suitability of the experimental approach for the nonsymmetric flaw configuration. As indicated, two corner cracks, intentionally precracked to different initial sizes, were located at opposite sides of the hole. As expected, final fracture was controlled by the larger of the two cracks. In this particular test, relatively few measurements were obtained during the transition phase, which occured quite rapialy and led almost immediately to specimen fracture.

2. Lug Embedded Crack Results

The PMMA lug specimens were gripped at one end and loaded through a steel pin placed in the large hole in the other end as shown in Figure 8. The degree-of-fit between the lugs and the pin used to transfer load to the lugs was such that the pin could be removed by hand when no load was applied. Although there were no specified tolerances for the lug/pin fit, all of the lugs were machined and fit by the same technician.

34
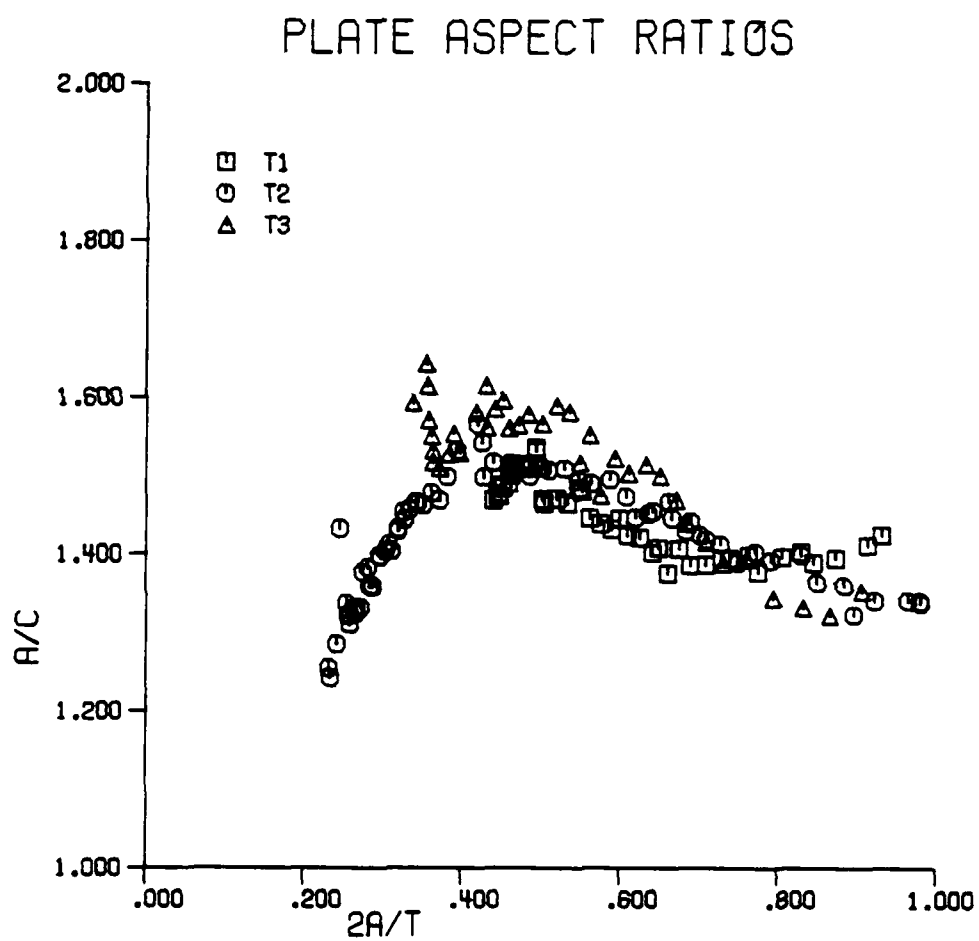
Figure 15   Natural Crack Shape a/c as Function of Crack Size
            2a/T for Open Hole Plate Tests

The actual crack lengths for the embedded flaw lug specimens were plotted in the same manner as the plate specimens and are presented in Figures 16 through Figure 24. It should be noted that several of the lug tests were slightly different from the others in terms of the collected data. The embedded crack in specimen PT10 (Figure 22) grew slightly out of plane (approximately 15°) so that the crack lengths measured in the 2a direction are projections of the actual length. A corner crack also existed at the opposite side of the hole in this specimen but did not grow during the test. The other exceptions were lug specimens PT14, PT11, and PT13 (Figures 21, 23, and 24), where fracture occurred before both sides of the crack penetrated the lug thickness. Since the latter specimens contained the smallest wall thicknesses (W/D = 1.5 and 2.0), the embedded cracks had a proportionately larger size upon penetrating the specimen thickness, and fracture occurred sooner.

Note again in Figures 16 through 23 that the transition crack dimensions c_L and c_R initially grow quite rapidly after penetrating the wall thickness, slow down as the middepth crack dimension c is approached, and then speed up again prior to final fracture. This behavior is similar to that seen in the plate specimens, and occurred both for nearly symmetric flaws (when $c_R \simeq c_L$) and for significantly skewed crack shapes.

The embedded crack aspect ratio a/c for the different lug shapes are plotted versus flaw size 2a/T in Figures 25 to 28. Although different initial crack shapes were considered, the natural aspect ratio upon penetrating the wall thickness (2a/T = 1.0) was almost always approximately a/c = 1.5.

PT4
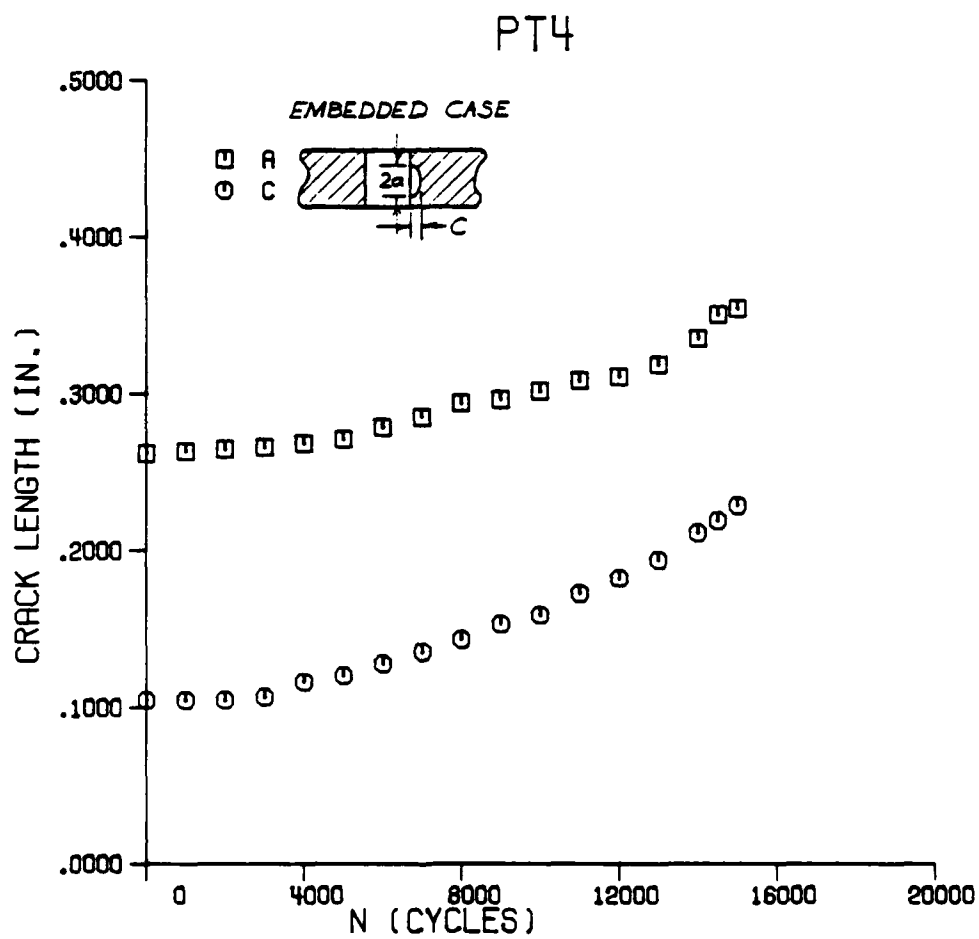
Figure 16a   Fatigue Crack Growth Data for Lug Specimen PT4
             (W/D = 3.0) Prior to Transition

37
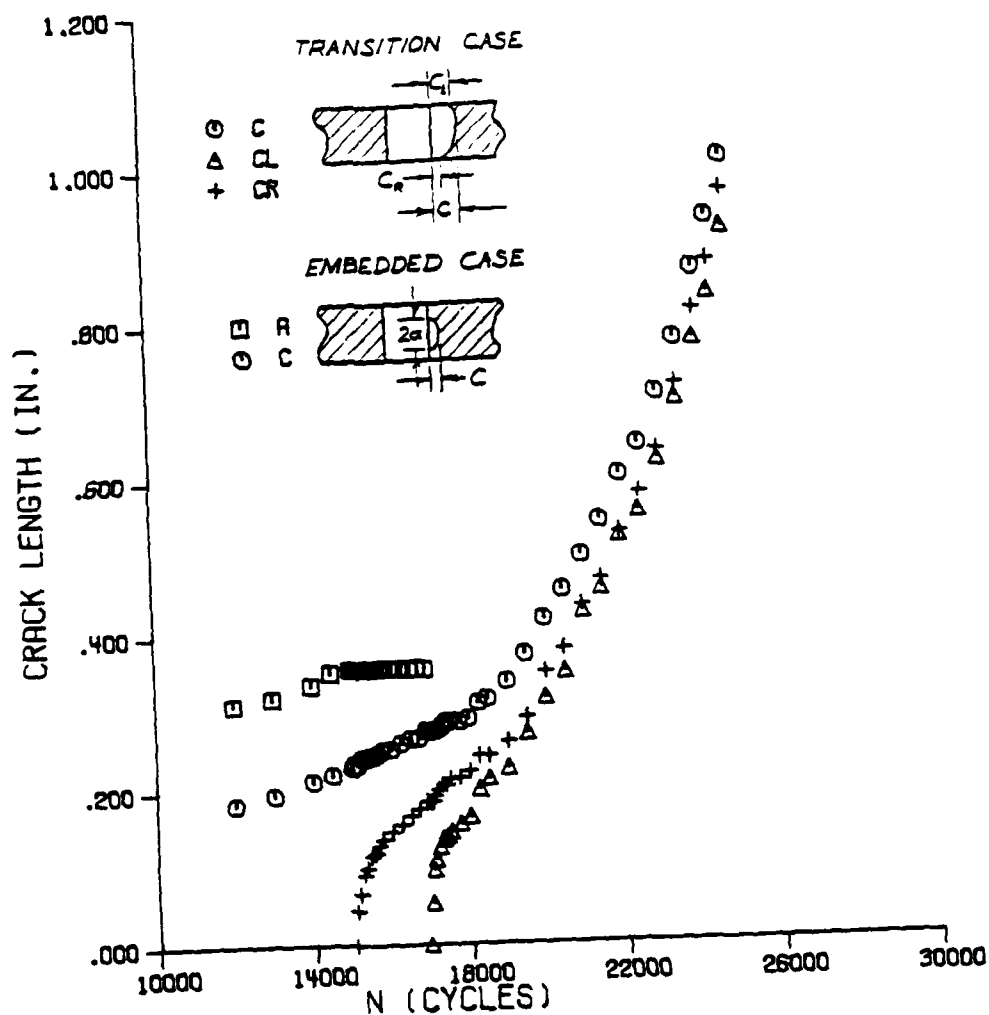
Figure 16b   Fatigue Crack Growth Data for Lug Specimen PT4
              (W/D = 3.0) During Transition Period
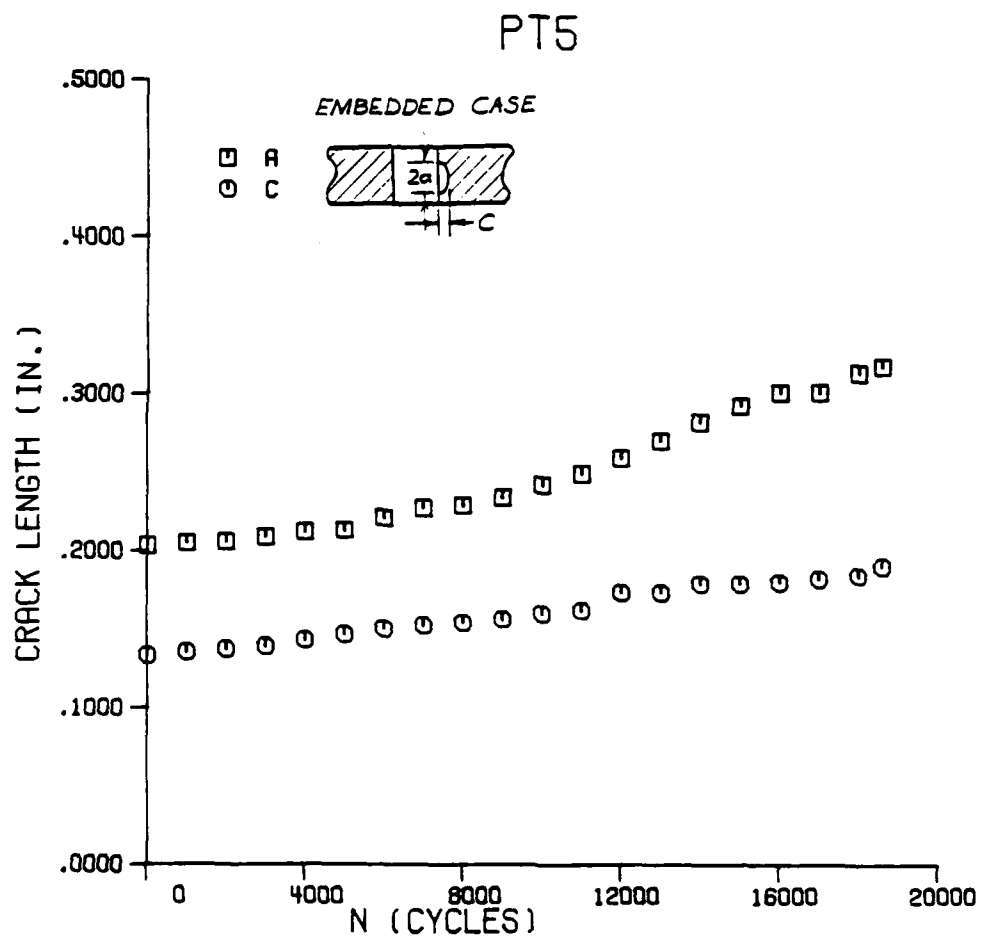
Figure 17a   Fatigue Crack Growth Data for Specimen PT5
              (W/D = 3.0) Prior to Transition

PT5
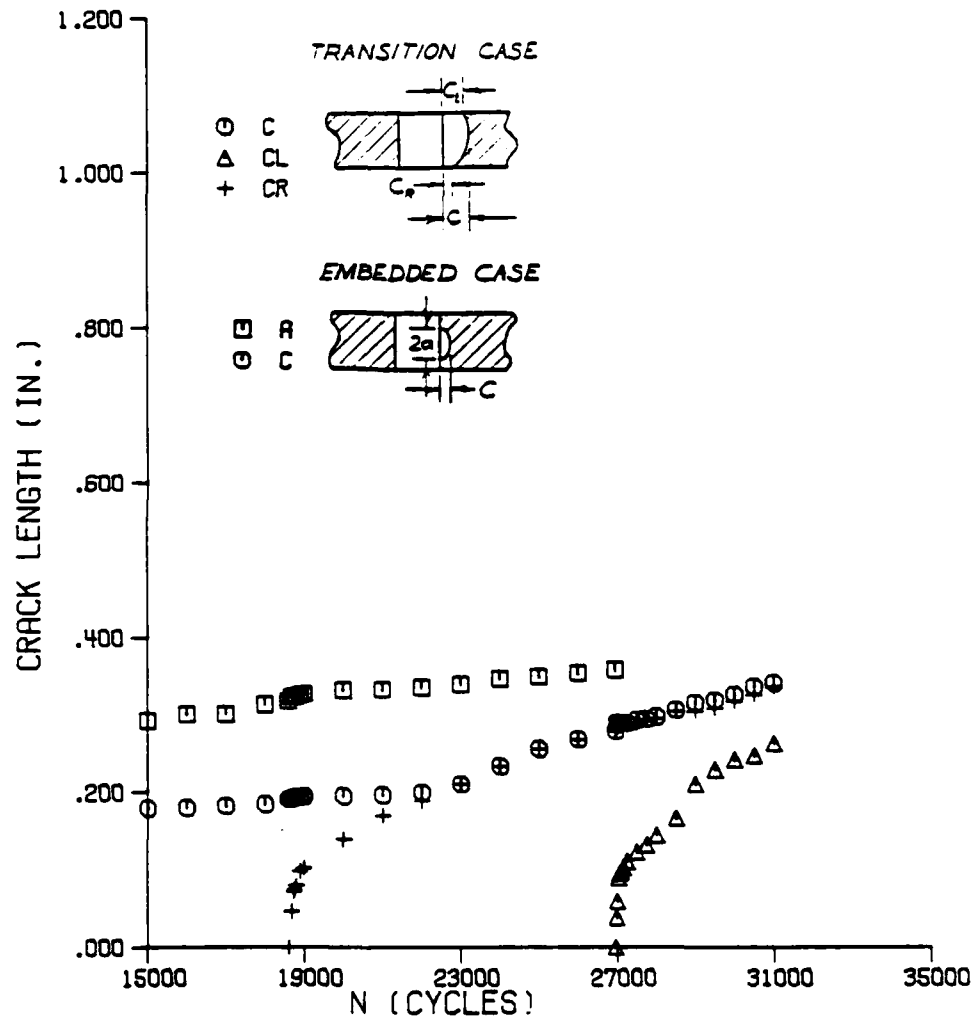
Figure 17b   Fatigue Crack Growth Data for Lug Specimen PT5
(W/D = 3.0) During Transition Period
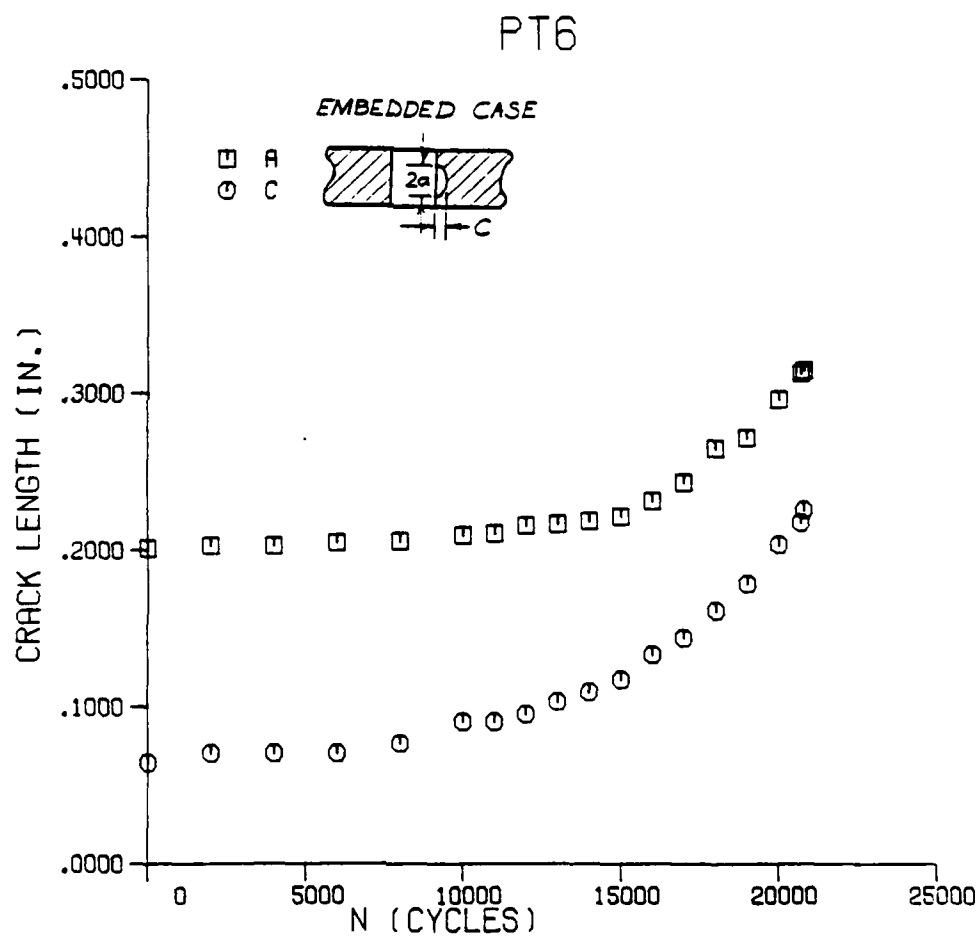
Figure 18a   Fatigue Crack Growth Data for Lub Specimen PT6
(W/D = 2.5) Prior to Transition
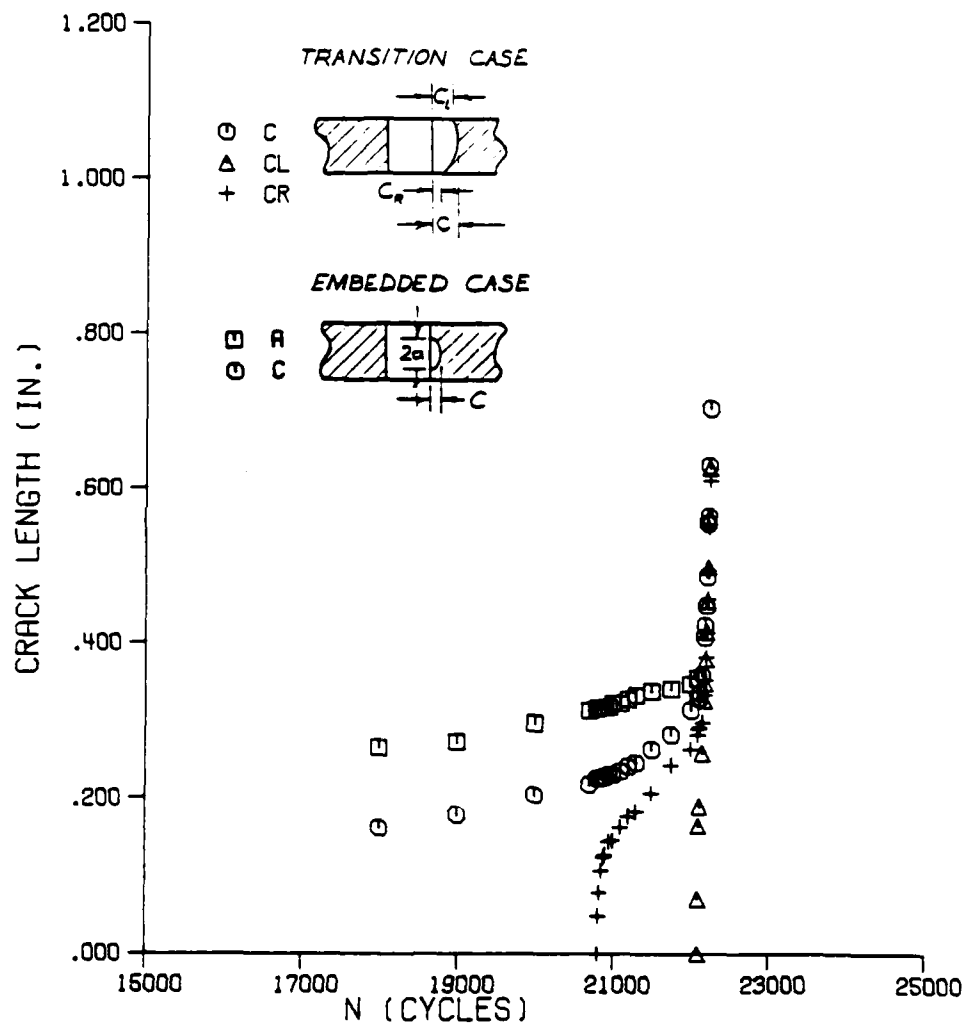
Figure 18b   Fatigue Crack Growth Data for Lug Specimen
PT6 (W/D = 2.5) During Transition Period

PT7
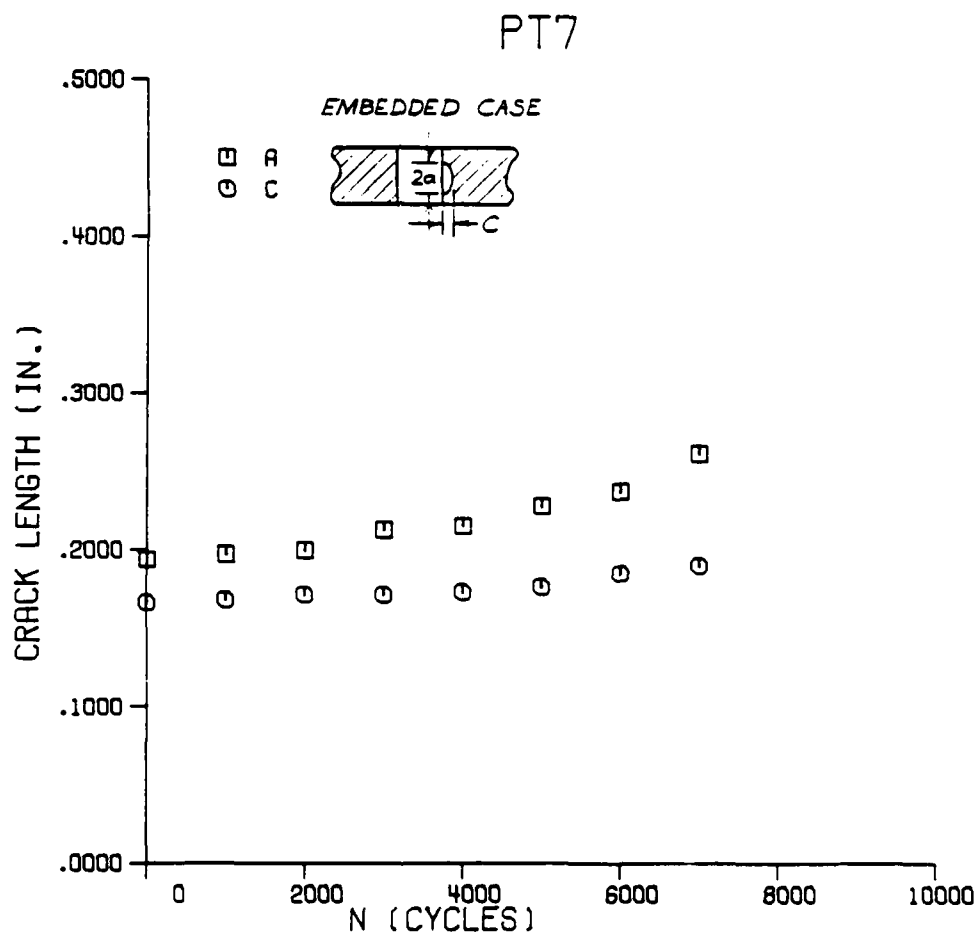
Figure 19a   Fatigue Crack Growth Data for Lug Specimen PT7
(W/D = 2.5) Prior to Transition
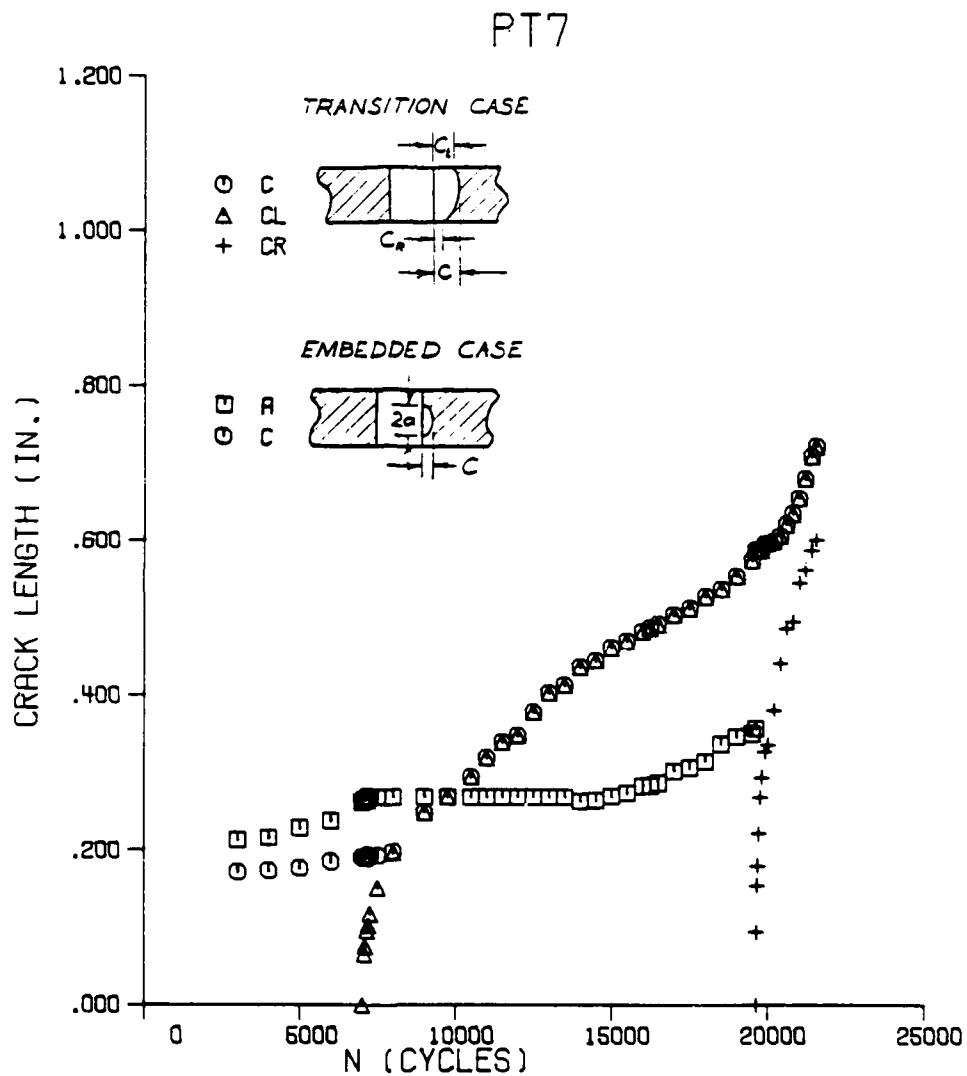
Figure 19b Fatigue Crack Growth Data for Lug Specimen
PT7 (W/D = 2.5) During Transition Period
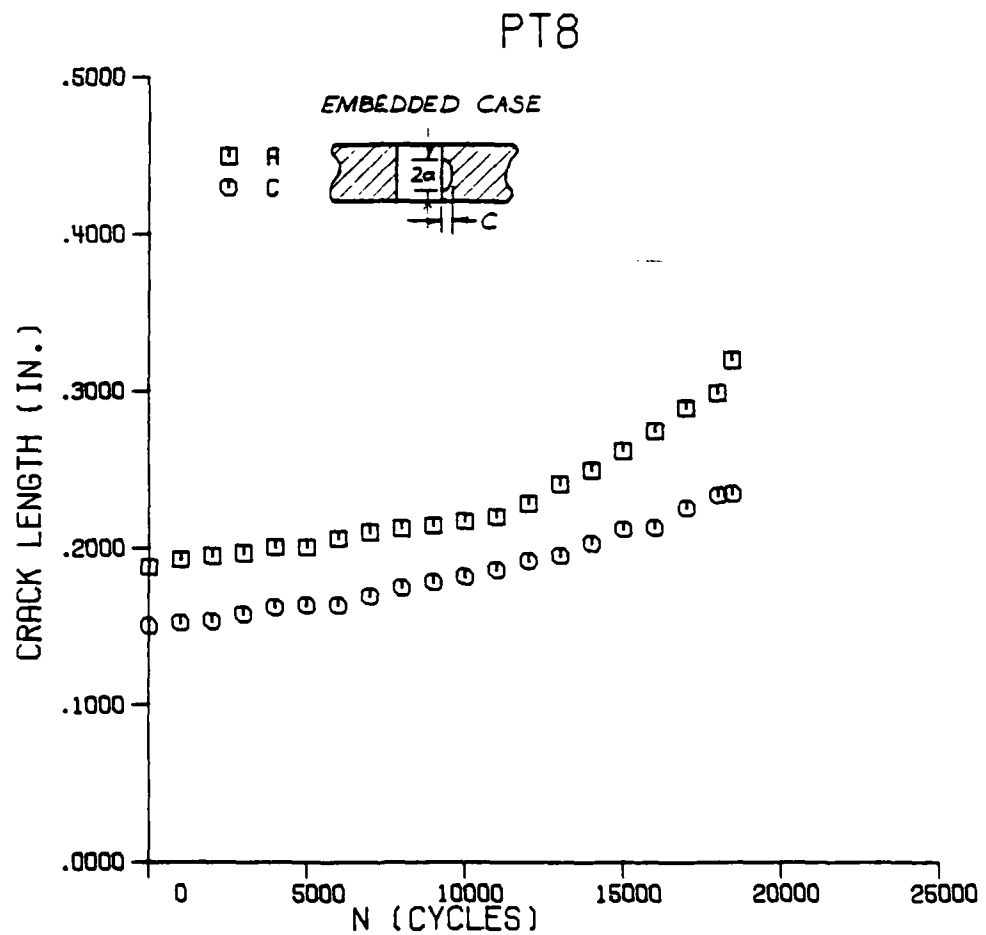
Figure 20a   Fatigue Crack Growth Data for Lug Specimen
PT8 (W/D = 2.0) Prior to Transition

PT8
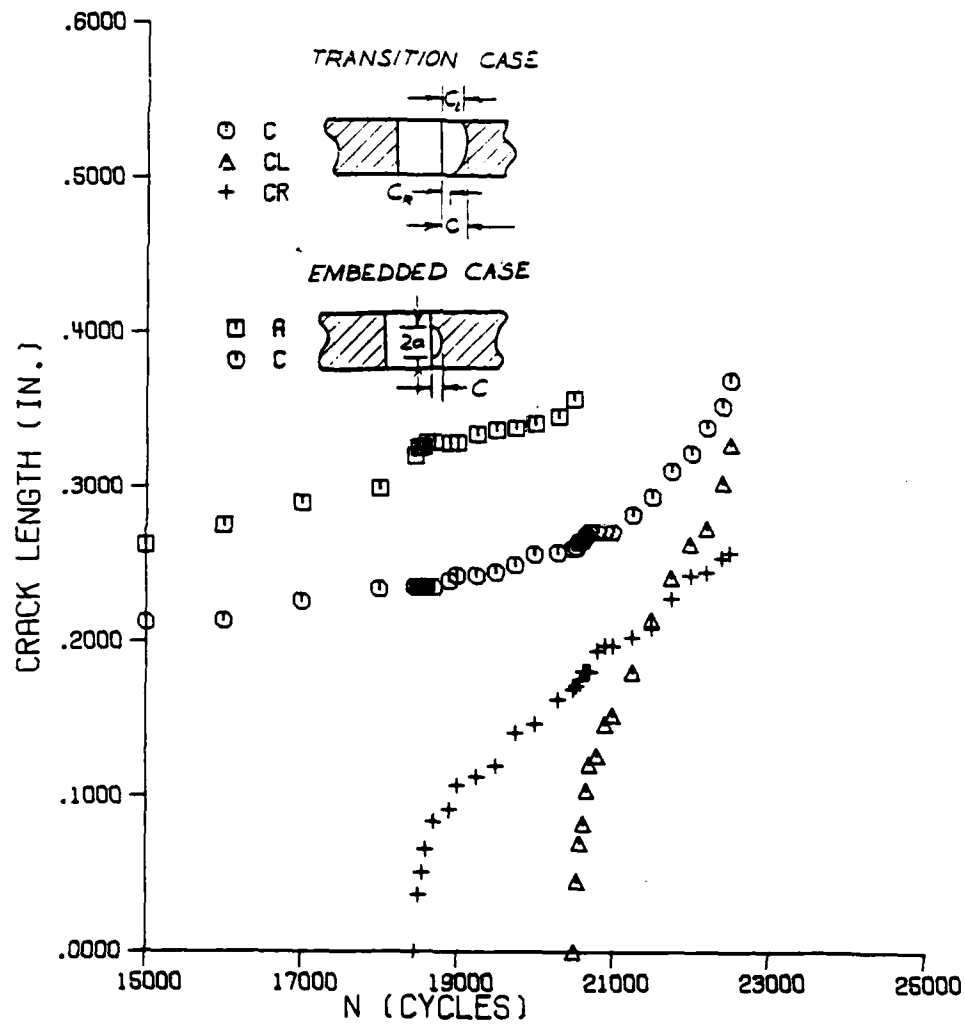
Figure 20b   Fatigue Crack Growth Data for Lug Specimen
             PT8 (W/D = 2.0) During Transition Period

46

PT14

TRANSITION CASE
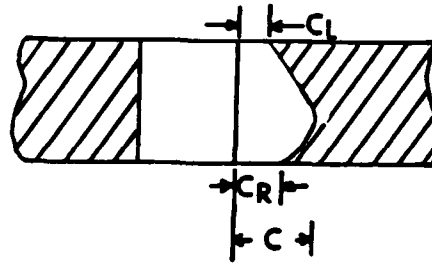
EMBEDDED CASE
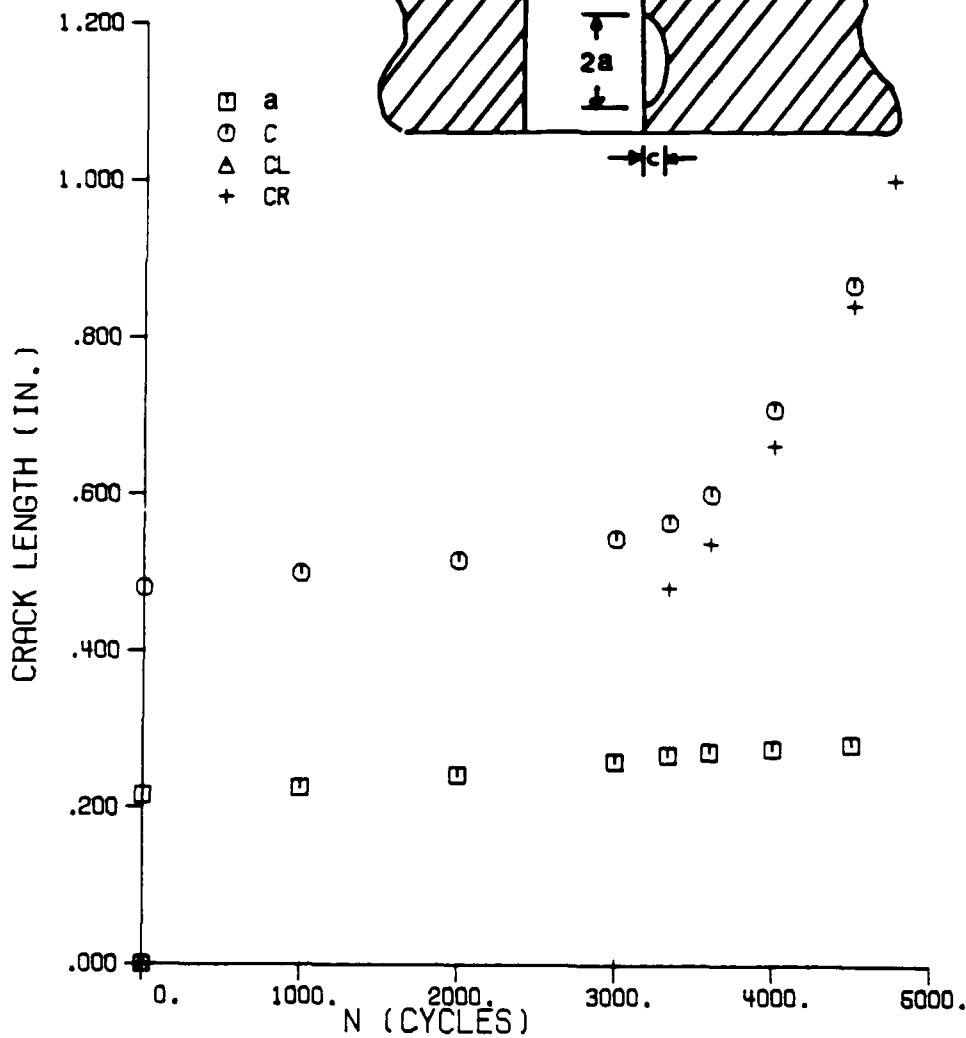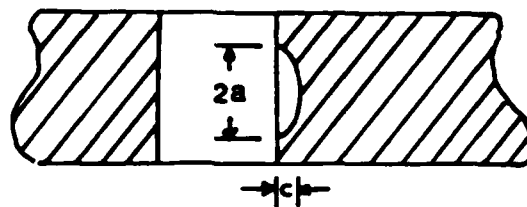
Figure 21   Fatigue Crack Growth Data for Lug Specimen PT14
(W/D = 2.0)

47
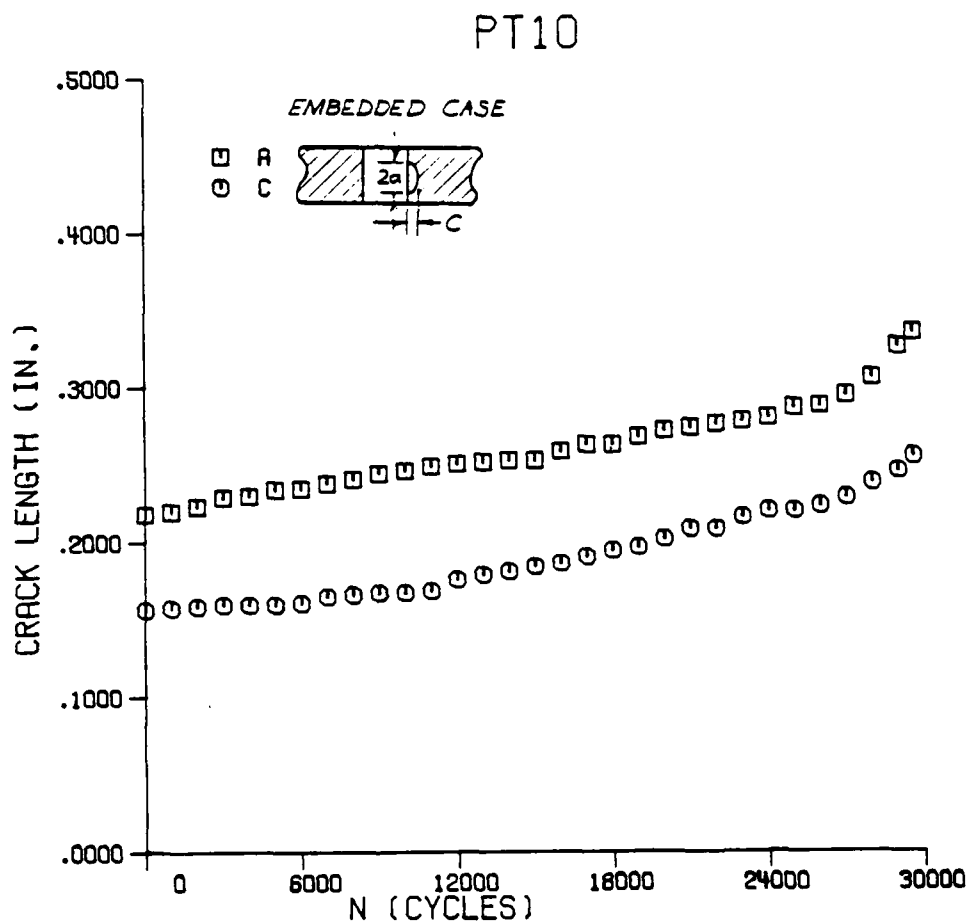
PT10

Figure 22a Fatigue Crack Growth Data for Lug Specimen PT10
(W/D = 1.5) Prior to Transition
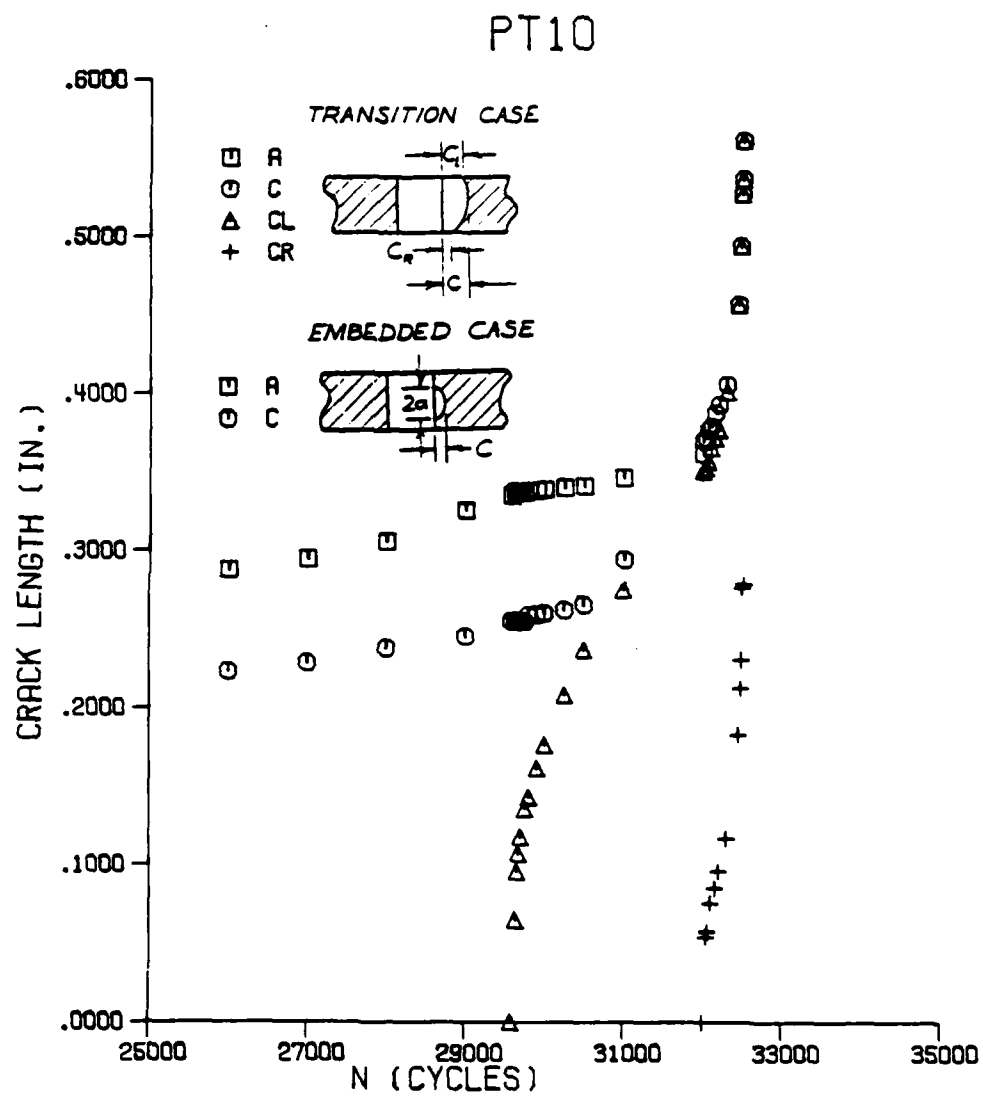
Figure 22b   Fatigue Crack Growth Data for Lug Specimen PT10
            (W/D = 1.5) During Transition Period
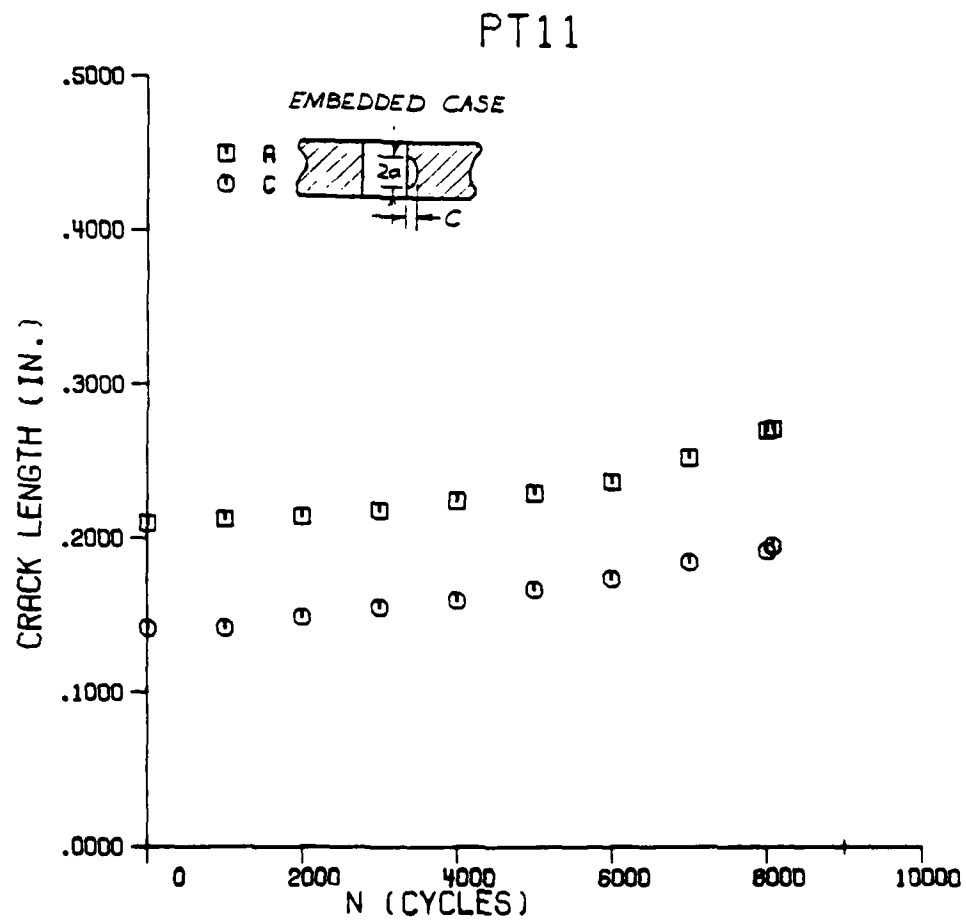
Figure 23a   Fatigue Crack Growth Data for Lug Specimen PT11
(W/D = 1.5) Prior to Transition
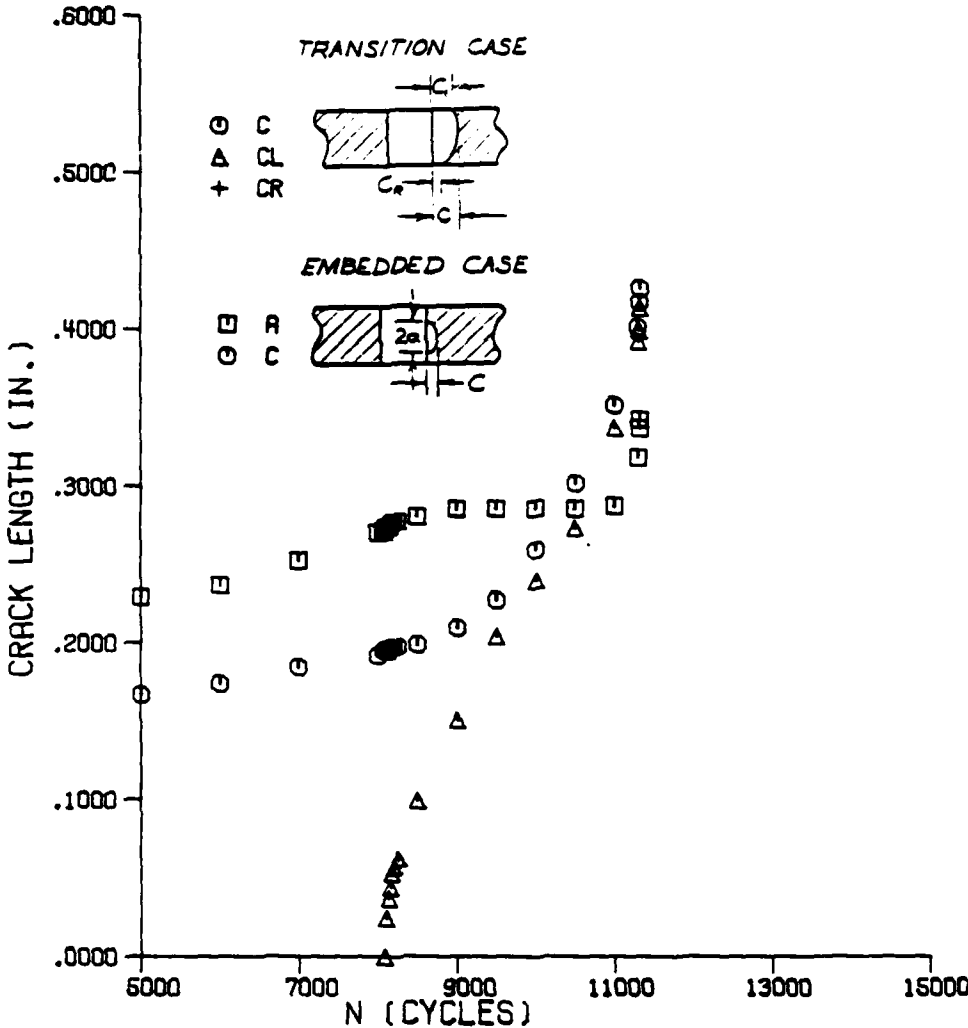
Figure 23b Fatigue Crack Growth Data for Lug Specimen
PT11 (W/D = 1.5) During Transition Period

PT13
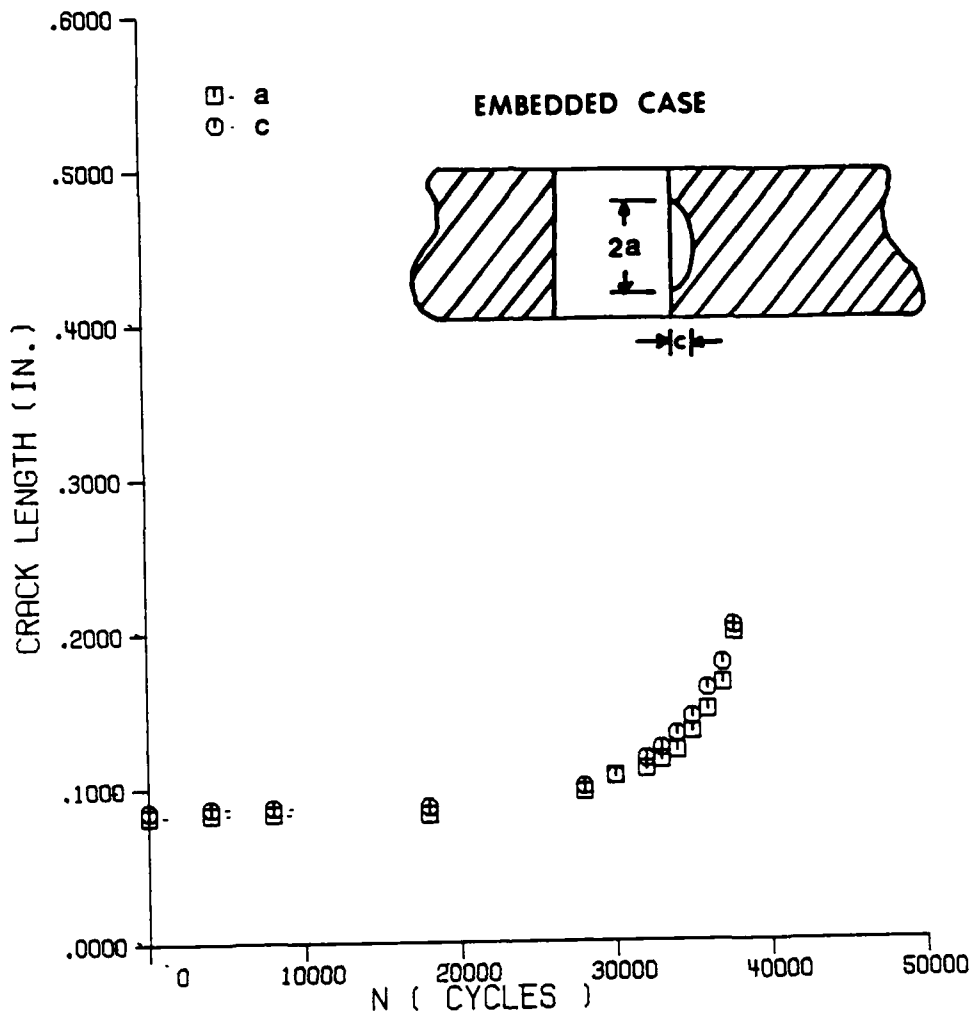
Figure 24   Fatigue Crack Growth Data for Lug Specimen
PT13 (W/D = 1.5)
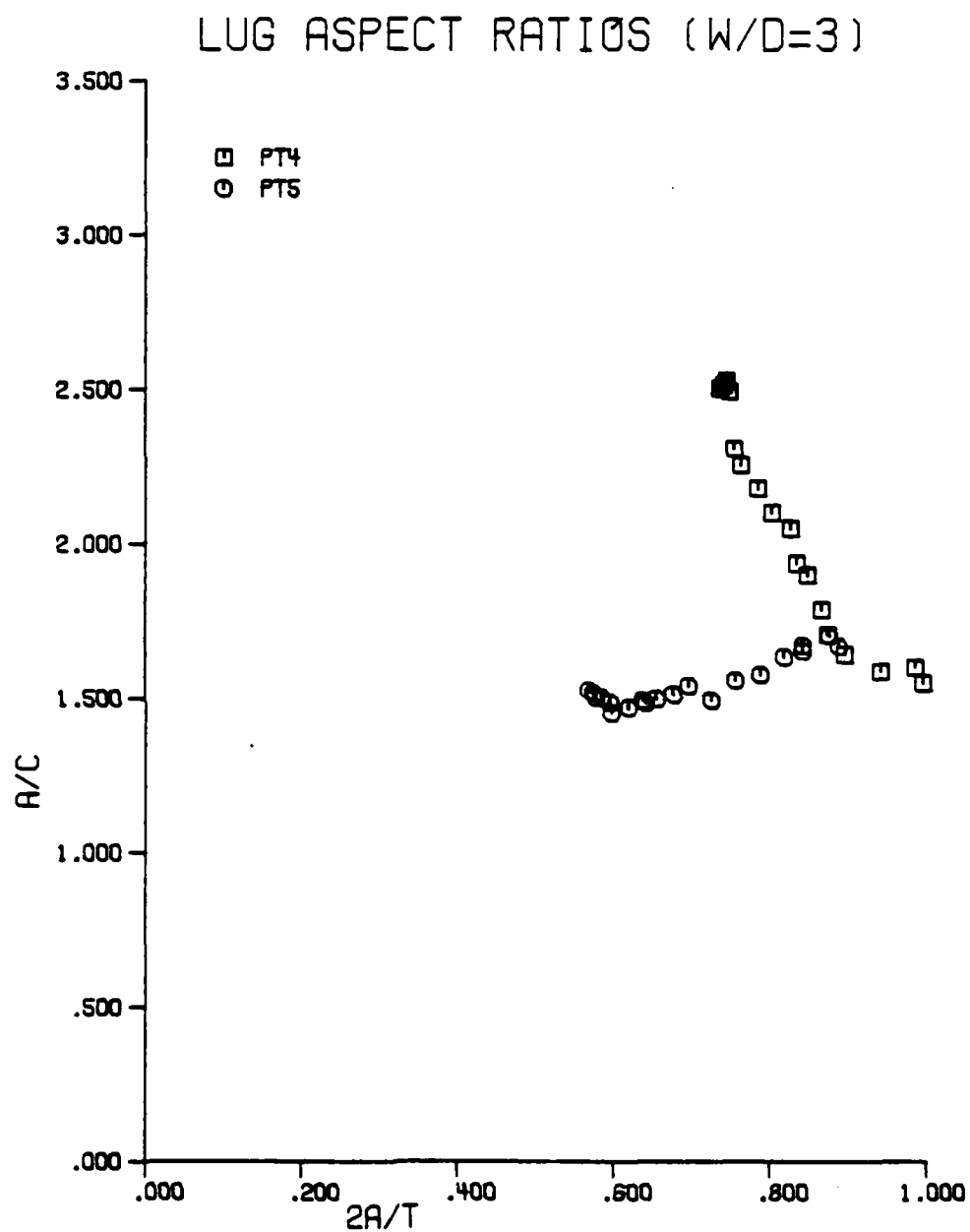
Figure 25   Crack Shape a/c Versus Crack Size 2a/T for W/D = 3.0
Pin-Loaded Lug Tests
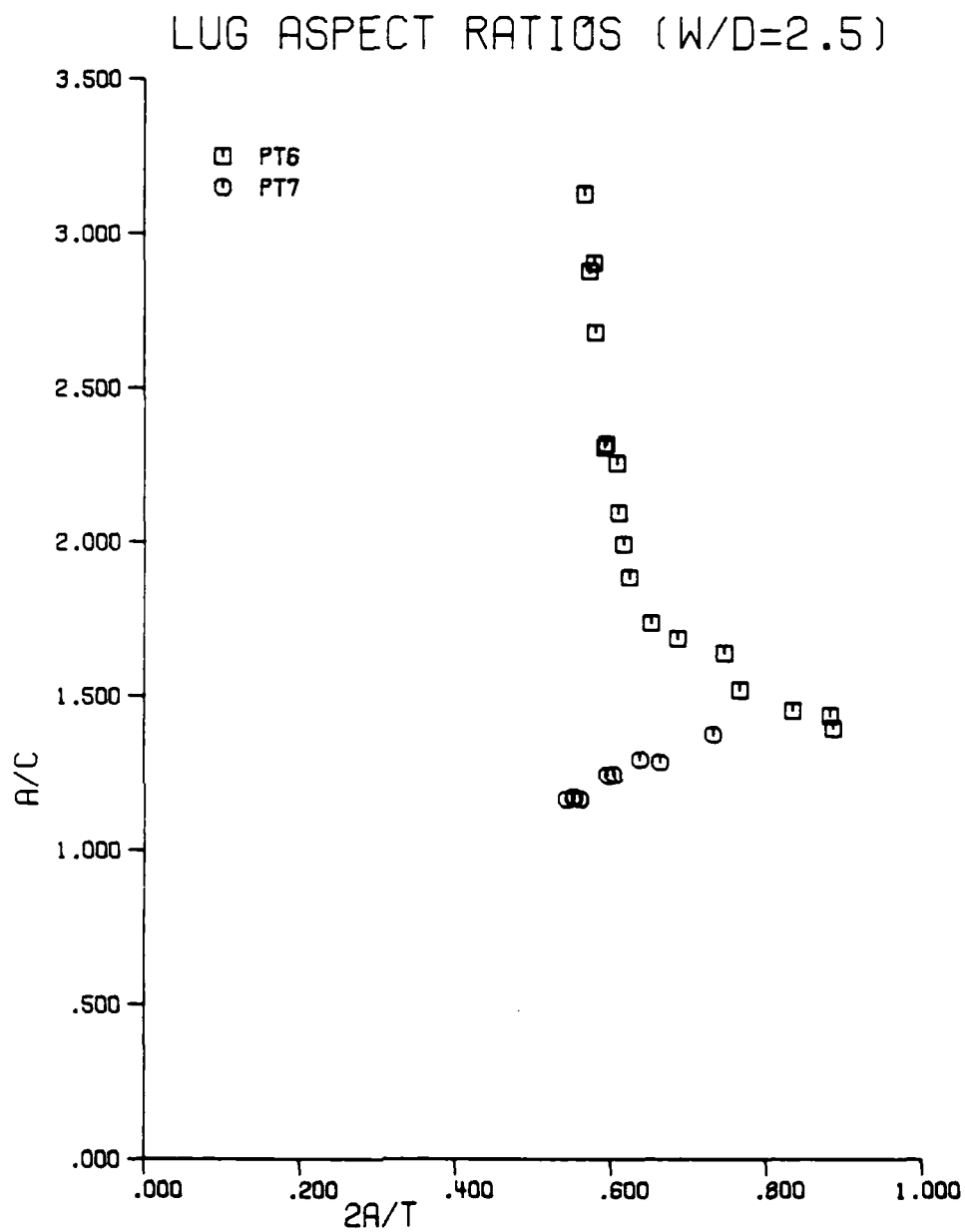
Figure 26   Crack Shape a/c Versus Crack Size 2a/T for W/D = 2.5
             Pin-Loaded Lug Tests
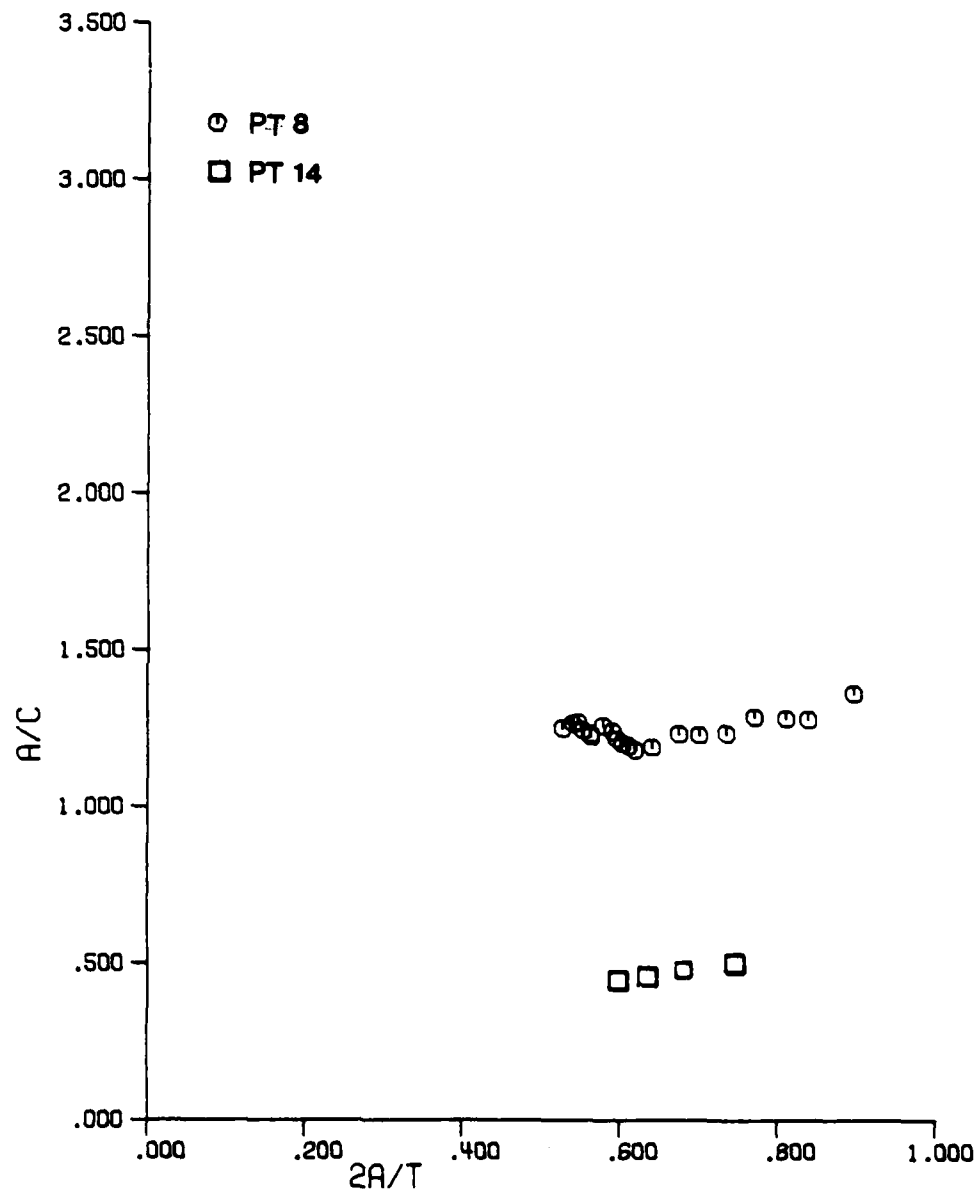
Figure 27   Crack Shape a/c Versus Crack Size 2a/T for
W/D = 2.0 Pin-Loaded Lug Tests

55
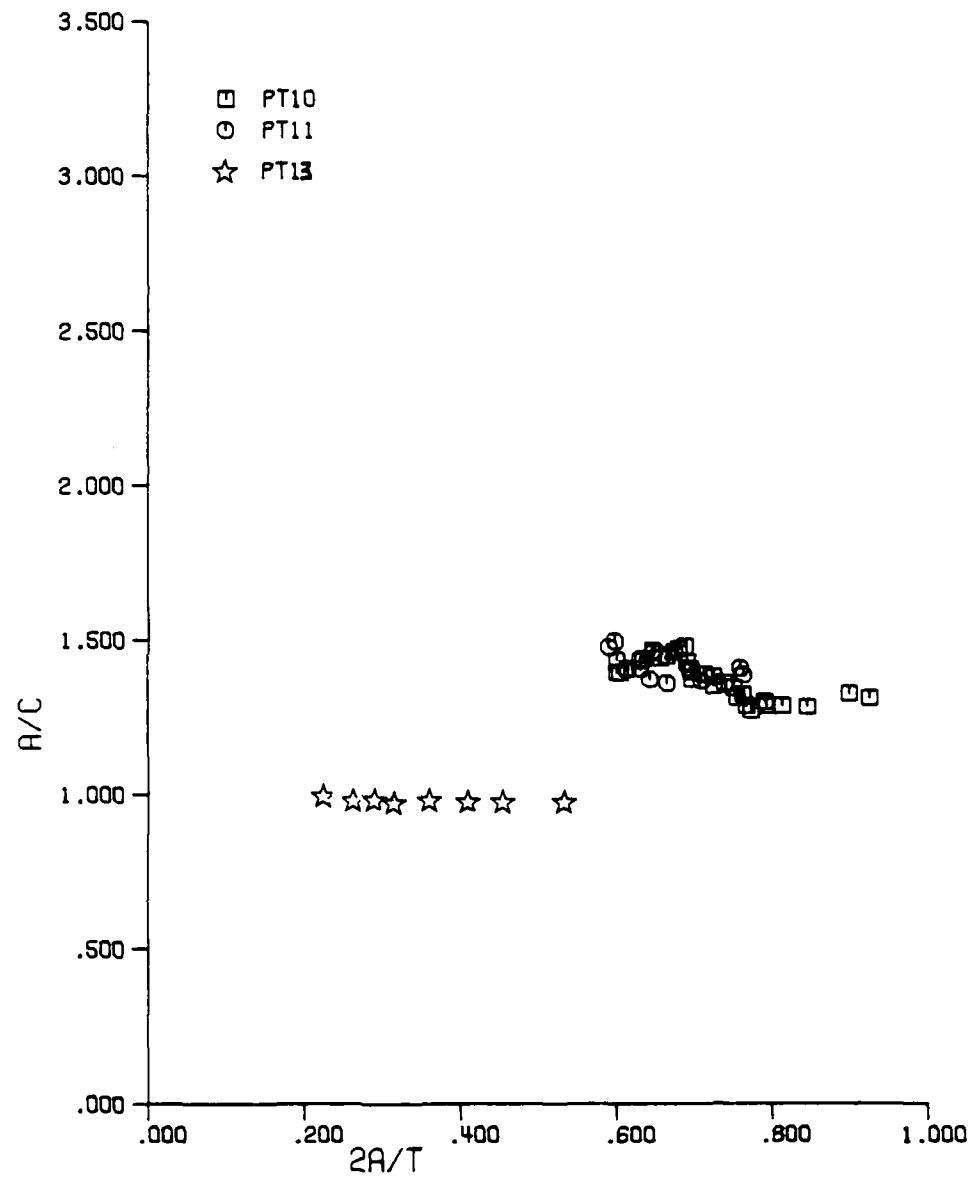
Figure 28   Crack Shape a/c Versus Crack Size 2a/T for
W/D = 1.5 Pin-Loaded Lug Tests

3. Lug Through Crack Test Results

Several of the lug through-the-thickness crack tests were continua-
tions of the embedded tests for the appropriate specimens (PT4, PT5, PT8).
After the cracks were large enough to be considered through-the-thickness
cracks, the load was lowered, if necessary, to avoid fracture, and the
fatigue tests continued. Lug specimen PT9 was saw cut to initiate a through-
the-thickness crack. All of the crack lengths were determined from the
test photographs using the five point average discussed earlier. This effec-
tive crack length was called c to be consistant with the other tests. The
crack length versus elapsed load cycle data are shown in Figure 29 for all
of the tests. (Note that the specimen PT5 data are given in two plots).

The through-cracked lug results were used to compute stress intensity
factors from the known fatigue crack growth law for the test material.
Crack growth rates were computed by a least squares sliding polynomial method
as described in Section 2 for the baseline tests. Equation 1 was then used
to compute the apparent cyclic stress intensity factor corresponding to the
crack length for that particular growth rate. These data are given in
dimensionless form in Figures 30 and 31. Here K is the cyclic stress inten-
sity factor computed by Equation 1 for the measured crack growth rate, D is
the hole diameter in the lug, R_0 is the outer lug radius ($R_0 = W/2$), R_i is
the radius of the hole ($R_i = D/2$), c is the average through-the-thickness
crack length, and σ_0 is the remote cyclic stress defined by

$$\sigma_0 = \frac{P_{max} - P_{min}}{TW} \qquad (2)$$

In equation 2, P_{max} and P_{min} are the maximum and minimum cyclic loads, T
is the lug thickness and W is the width as shown in Figure 1.
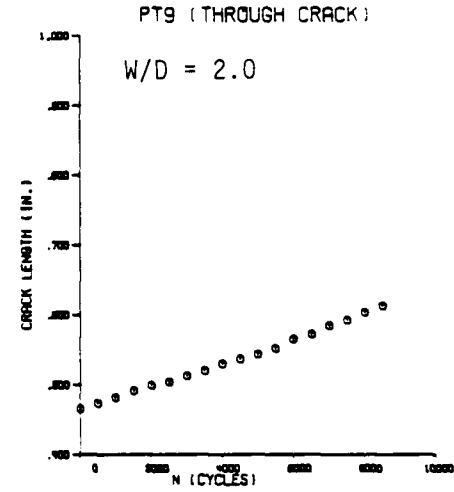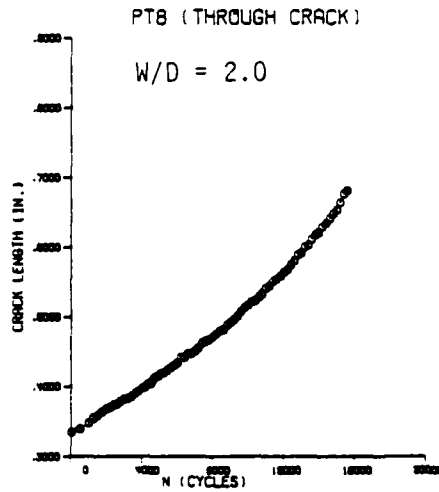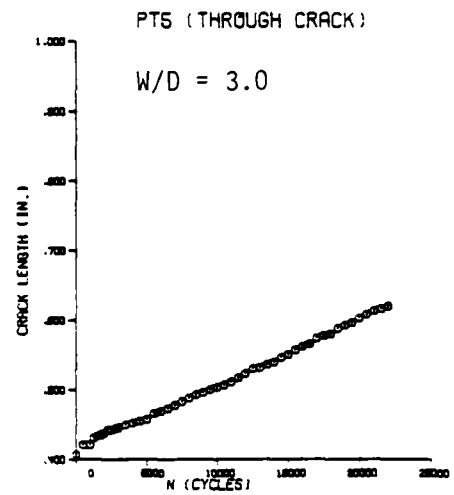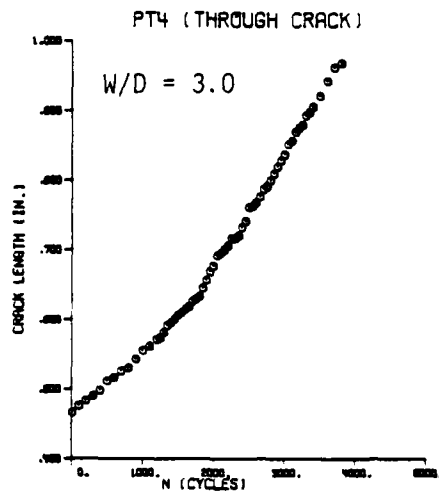
Figure 29a   Fatigue Crack Growth Data for Lug Through-Crack
Tests PT4, PT5, PT8, and PT9.

58

PT5 THRU-CRACK

W/D = 3.0
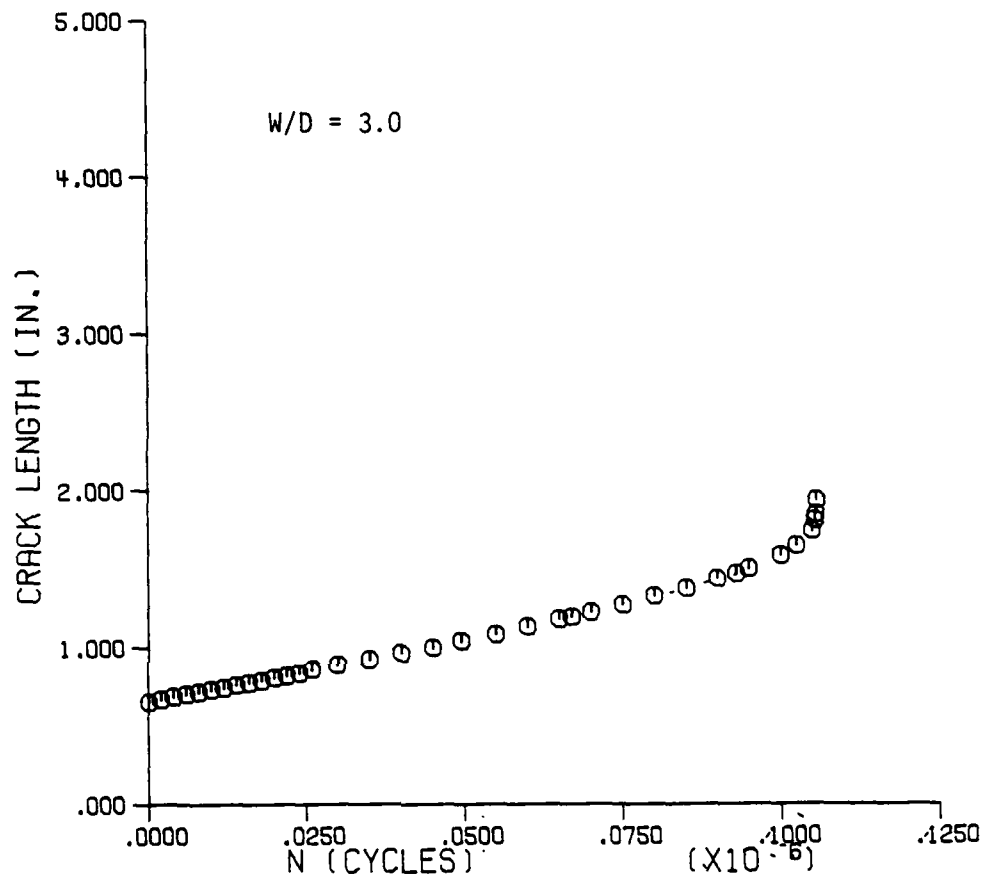
Figure 29b   Additional Fatigue Crack Growth Data for Lug
              Through-Crack Crack Test PT5

59
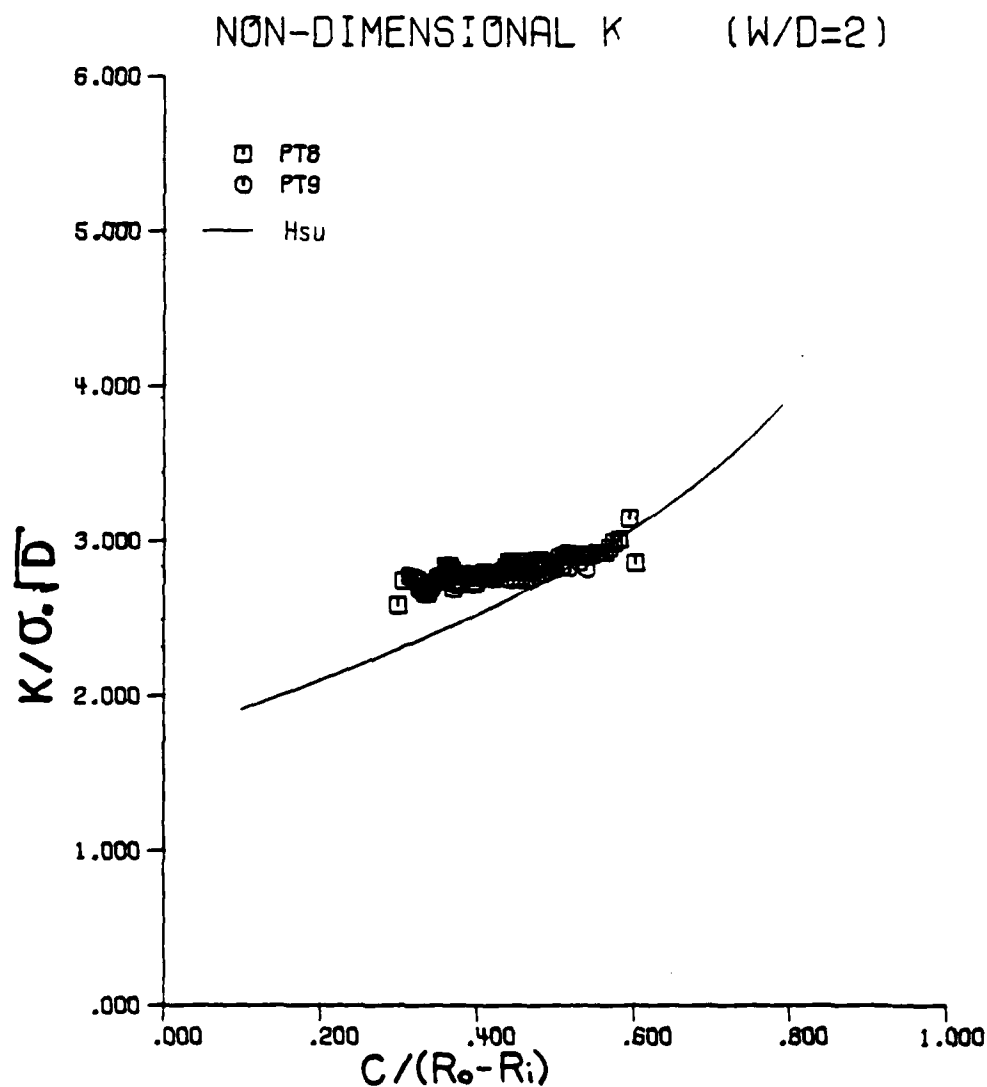
Figure 30   Comparison of Experimental Measurements of
Dimensionless Stress Intensity Factors Computed
from Fatigue Crack Growth Rates with Hsu Finite
Element Analysis (W/D = 2.0)

60
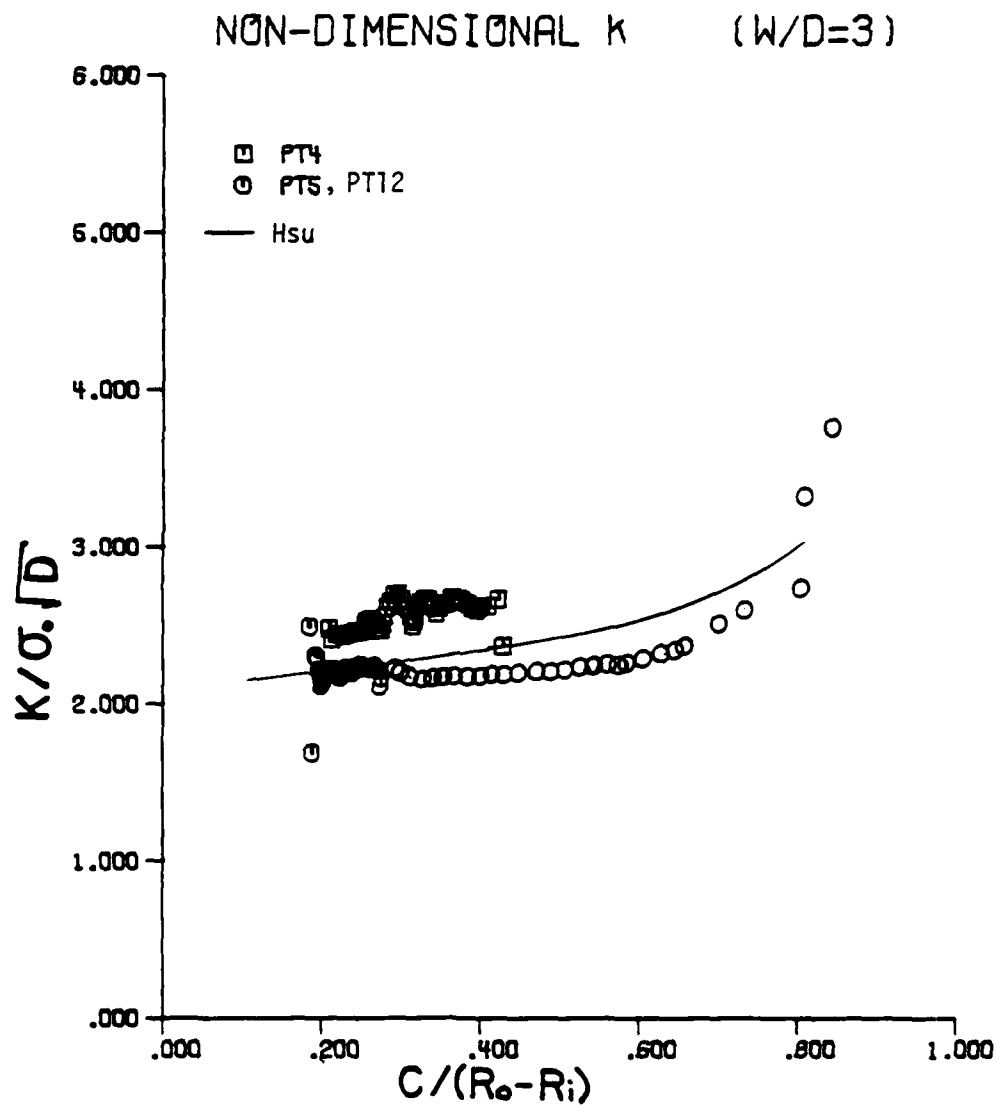
Figure 31   Comparison of Experimental Measurements of
Dimensionless Stress Intensity Factors Computed
from Fatigue Crack Growth Rates with Hsu Finite
Element Analysis (W/D = 3.0)

61

Stress intensity factors reported by Hsu [13] for these two through-cracked lug shapes are also given for comparison in Figures 30 and 31. Note that these numerical results, obtained by the finite element method, were for a steel pin in a steel lug. These solutions generally agree fairly well with the experimental measurements, which involved a steel pin in a PMMA lug.

Additional details of the method used to compute the stress intensity factors from the measured crack lengths are given in Reference 11. Stress intensity factors were also computed from the measured surface crack growth rates in the plate and embedded lug tests by a similar procedure. Those results are reported separately in Reference 11.

SECTION IV

FATIGUE CRACK GROWTH PREDICTIONS

1. Approach

The goal here is to describe an approach for predicting the
growth of surface or corner cracks located along the bore of a hole
in a wide plate. In Figure 32, the surface crack is represented by
a semiellipse whose major and minor axes are defined by the coordinates
(x_1, y_1), (x_2, y_2), and (x_3, y_3) of points 1, 2, and 3. The surface
dimension 2a (measured along the bore of the hole) and depth c are
given by

$$2a = x_3 - x_1 \tag{3}$$

$$c = y_2 \tag{4}$$

When subjected to an applied cyclic stress, crack tips 1, 2, and
3 will grow. Let the fatigue crack growth rates for crack tips 1,
2, and 3 be $\frac{d1}{dN}$, $\frac{d2}{dN}$, and $\frac{d3}{dN}$. Note that, in general, these crack growth
rates will have different values. The crack growth increments for a
specified number of cycles ΔN of loading are, however, related.
Assume, for example, that the depth c extends a small amount $\Delta 2$ during
the interval ΔN. Then, by definition, $\frac{d2}{dN} = \frac{\Delta 2}{\Delta N}$, which gives

$$\Delta N = \frac{\Delta 2}{\frac{d2}{dN}} \tag{5}$$

Now the growth $\Delta 1$ of crack tip 1 is given by

$$\Delta 1 = \frac{d1}{dN} \cdot \Delta N \tag{6}$$
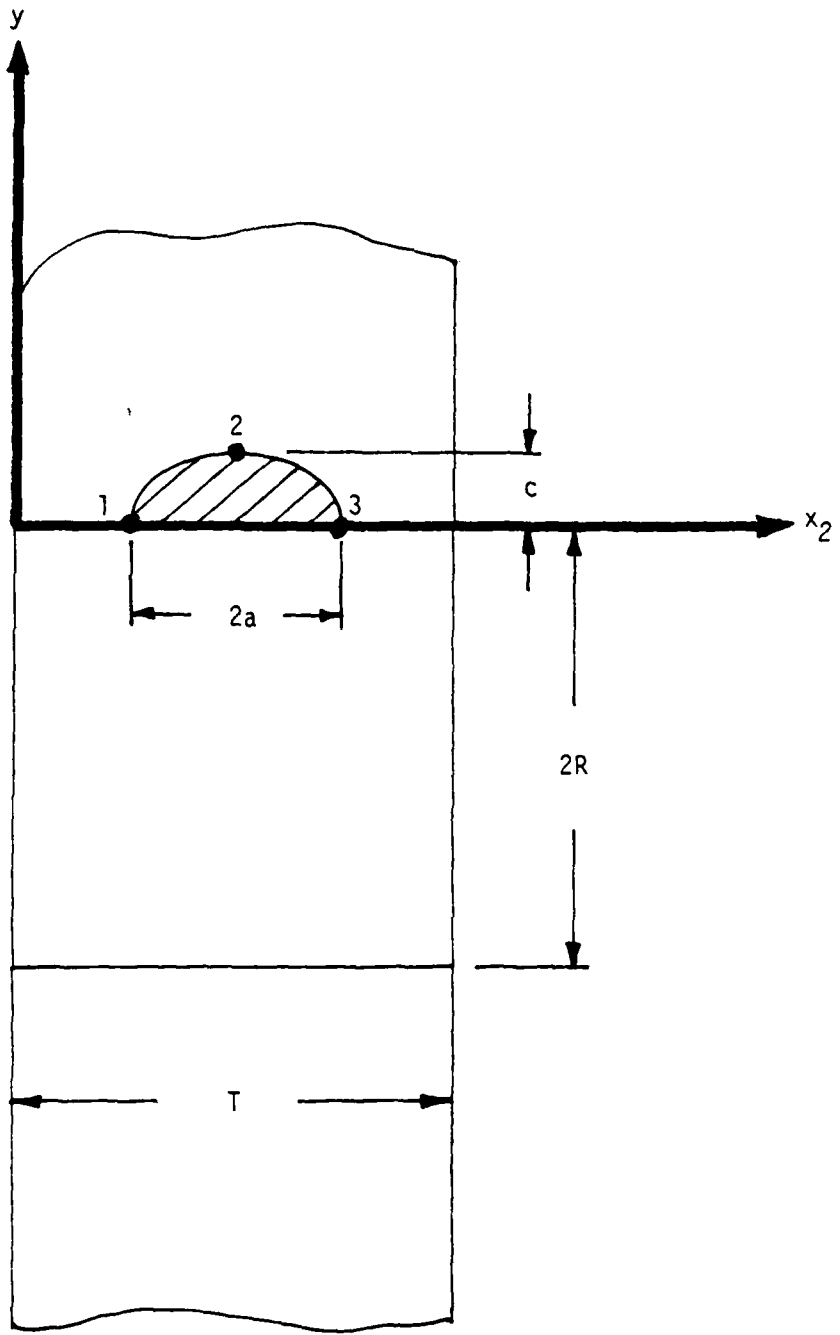
Figure 32   Coordinate System Employed to Define Embedded Surface Crack at Hole Configuration for Life Analysis Scheme

Likewise, the extensions of tips 2 and 3 are given by

$$\Delta 2 = \text{assumed small increment} \tag{7}$$

$$\Delta 3 = \frac{d3}{dN} \cdot \Delta N \tag{8}$$

Now, if the cyclic stress intensity factors ΔK_1, ΔK_2, ΔK_3 are known at crack tips 1, 2, and 3, the appropriate fatigue crack growth model (Equation 1 for the present case) can be used to compute the crack growth rates $\frac{d1}{dN}$, $\frac{d2}{dN}$, and $\frac{d3}{dN}$, which in turn give the crack growth increments $\Delta 1$ and $\Delta 3$ from Equations 6 and 8. The new positions (x_{ni}, y_{ni}) of the surface crack tips are then given by

$$x_{n1} = x_1 - \Delta 1$$

$$x_{n2} = y_2 + \Delta 2 \tag{9}$$

$$x_{n3} = x_3 + \Delta 3$$

Successive iteration of Equations 3 to 9 gives the growth of surface crack dimensions a and c as a function of elapsed cycles N.

Stress intensity factor solutions reported by Newman and Raju [14] for various surface and corner crack geometries were used here to compute ΔK_1, ΔK_2, and ΔK_3. The Newman-Raju results consist of empirical equations fit to finite element K solutions, and are readily programmed for computer use.

2. Results of Predictions

Crack growth predictions were obtained for the plate specimens by the two degree of freedom model described in the previous subsection and are presented here. Recall that individual crack tips are allowed to grow at independent rates, so that the crack shapes develop "naturally".

Predictions for plate tests T1, T2, and T3 are compared with experimental results in Figures 33 to 35. Note that these graphs are duplicates of Figures 11 to 13, except that the crack growth predictions have been added as the solid lines. Prior to penetration of a free face by the surface crack, calculations are given for both the a and c dimensions of the surface flaw (Figures 33a, 34a, and 35a). Note that, in general, the crack growth is predicted quite well. (To avoid extrapolating Equation 1 beyond its limits, the initial portions of some experiments were omitted for predictive purposes).

When the model predicted free surface penetration, it was assumed the surface crack instantly changed to a uniform through-the-thickness flaw of length c. The Bowie [15] stress intensity factor solution was then used to analyze the through-cracked hole, and the crack growth predictions continued. The results for the assumed through-crack are compared with the actual transitioning flaw shapes in Figures 33b, 34b, and 35b. Note that although the assumed through-crack grows faster than the actual flaw, the total specimen life is predicted quite well.

66
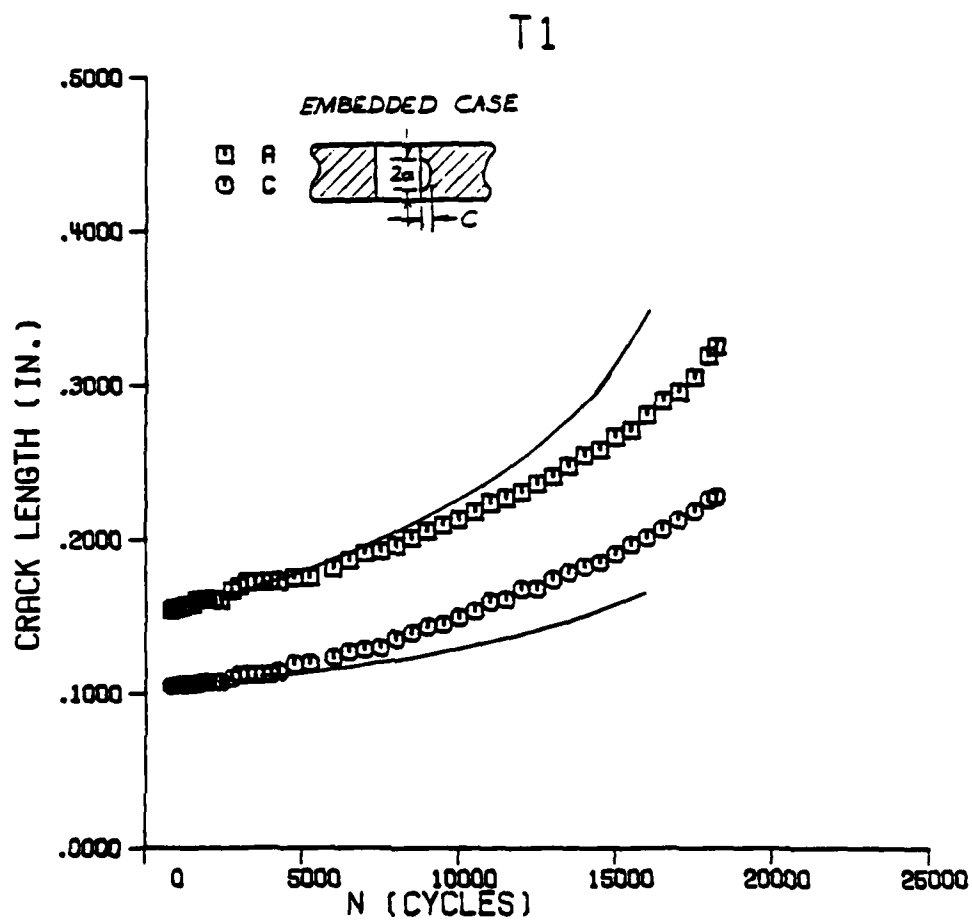
Figure 33a   Comparison of Predicted and Actual Crack Growth
Prior to Penetration for Plate Specimen T1
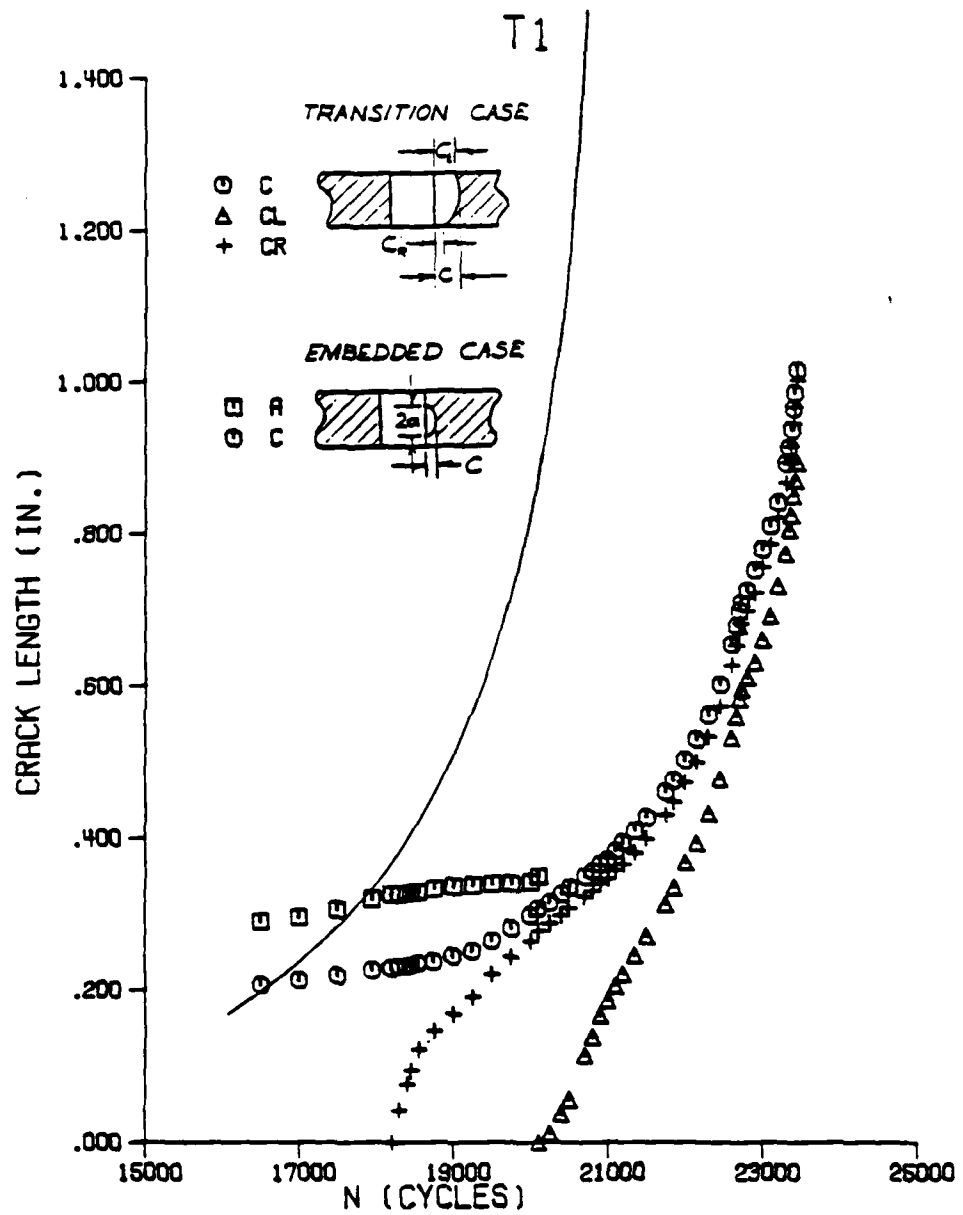
Figure 33b   Comparison of Predicted and Actual Crack
Growth During Transition Period for Plate
Specimen T1

68
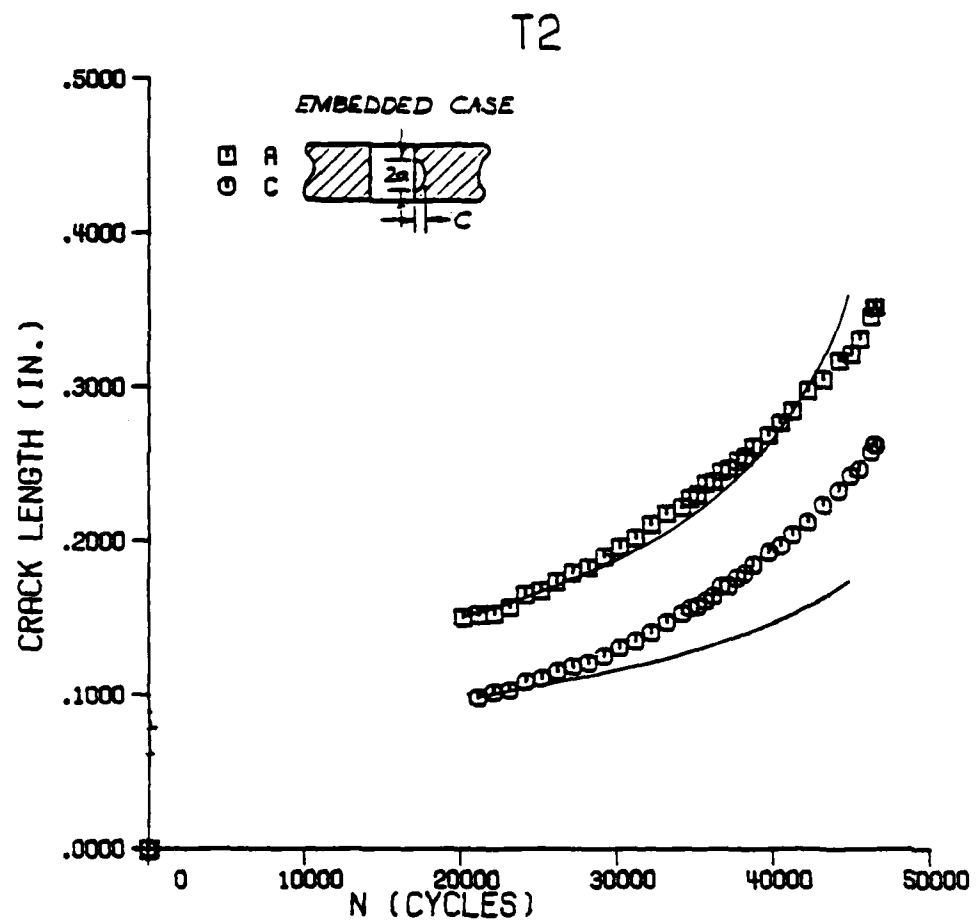
Figure 34a   Comparison of Predicted and Actual Crack Growth
Prior to Penetration for Plate Specimen T2

Figure 34b   Comparison of Predicted and Actual Crack Growth
During Transition Period for Plate Specimen T2

T3
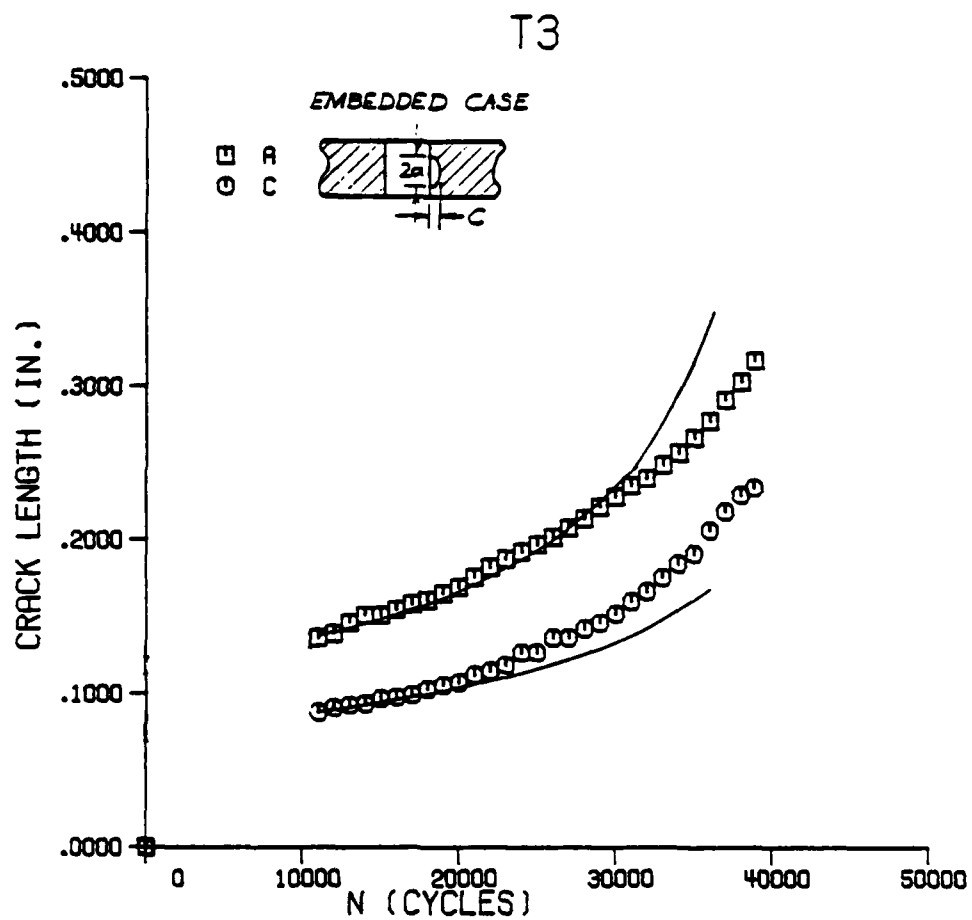
Figure 35a   Comparison of Predicted and Actual Crack Growth Prior
to Penetration for Plate Specimen T3
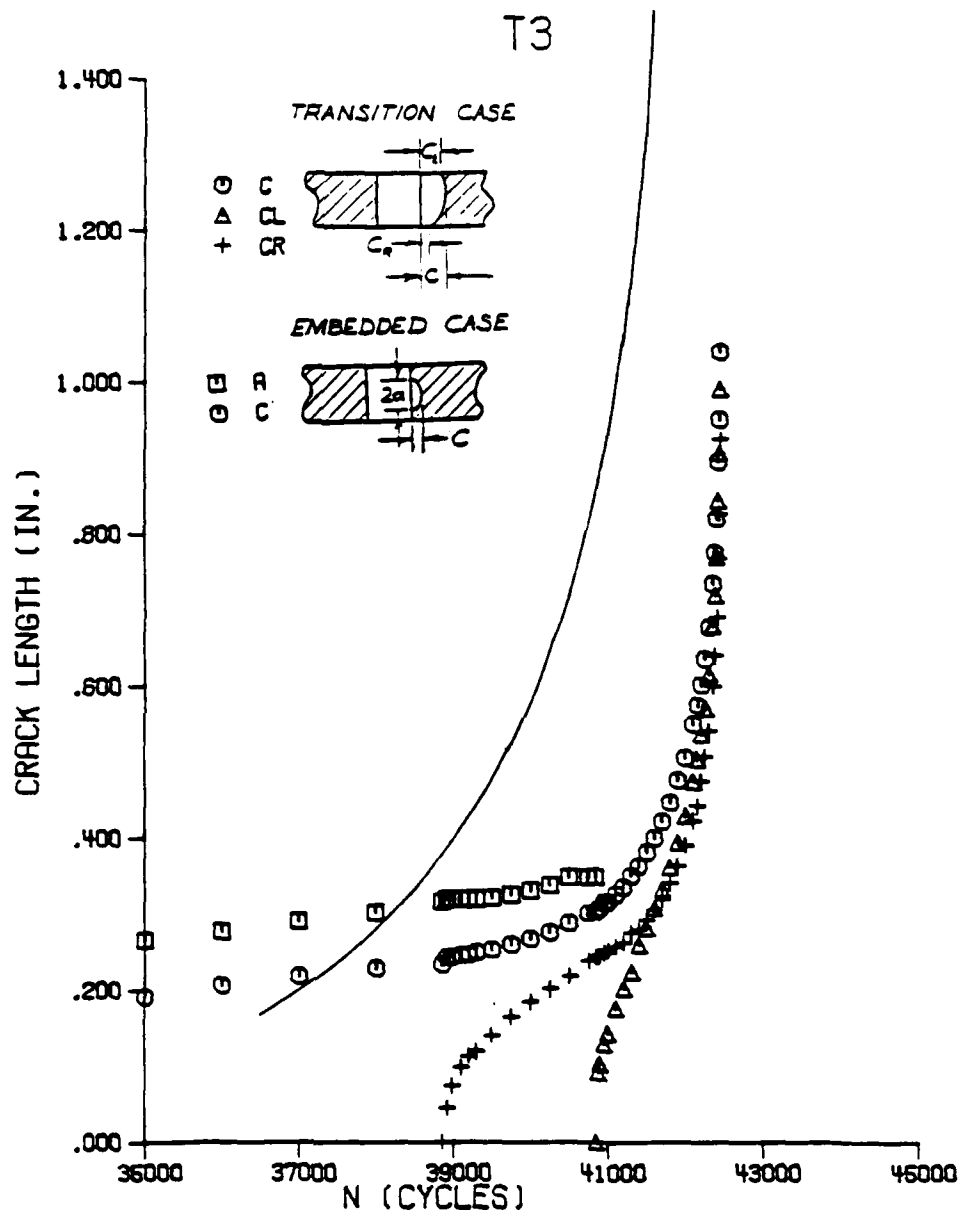
Figure 35b   Comparison of Predicted and Actual Crack Growth
During Transition Period for Plate Test T3

72

Snow [5] has presented experimental results for corner cracked hole specimens made from the same sheet of PMMA studied here. The predictive model was modified to consider the corner cracked geometry and used to predict lives for Snow's tests. Those results are given in Figures 36 to 40. As before, the open symbols represent the measured crack dimensions, while the solid lines are the predicted results.

Note that the actual crack shapes were "pinched in" at the free surface so that crack dimension c was somewhat less than length c^*, measured slightly below the surface (see sketch on Figure 36). For analysis purposes, the corner crack was assumed to be a quarter ellipse with dimensions a and c, and the additional crack growth in the specimen interior was ignored.

Note that the corner crack growth curves are predicted fairly well, although agreement is not quite as close as obtained previously for the embedded crack plate results. Nevertheless, the multi-degree of freedom crack growth model, based on the Newman-Raju empirical stress intensity factor equations, makes an adequate prediction for crack length and shape as a function of applied cycles.

An attempt was made to apply the crack growth prediction scheme to the lug results described in the last section. The difficulty lies in the fact that stress intensity factors are not available in a general form for pin-loaded surface cracks. Stress intensity factors were estimated by modifying the Newman-Raju results [14] for embedded cracks at an open hole in a wide plate. A "correction
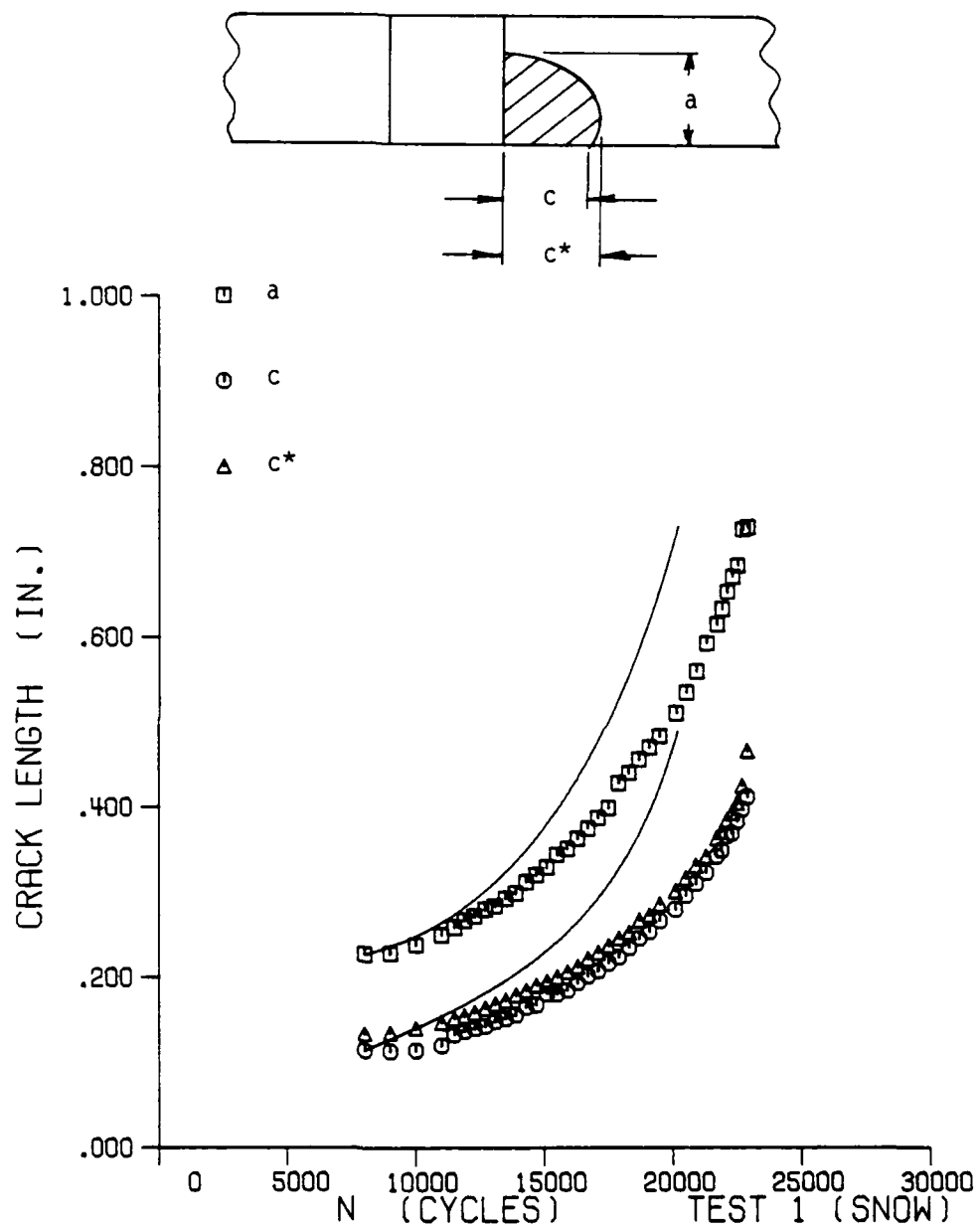
Figure 36   Comparison of Predicted and Actual Crack Growth
for Snow Corner Crack Test 1
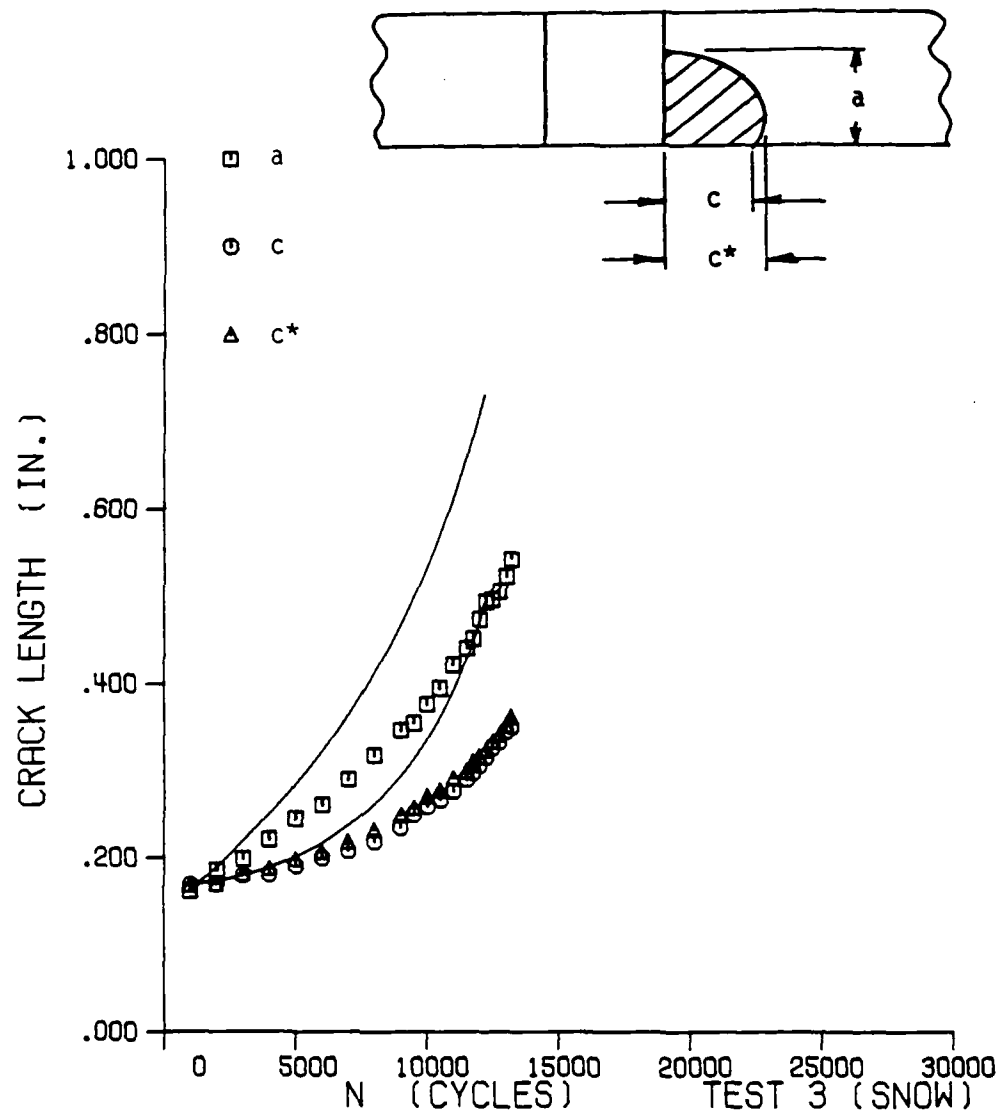
Figure 37   Comparison of Predicted and Actual Crack Growth for
Snow Corner Crack Test 3

75
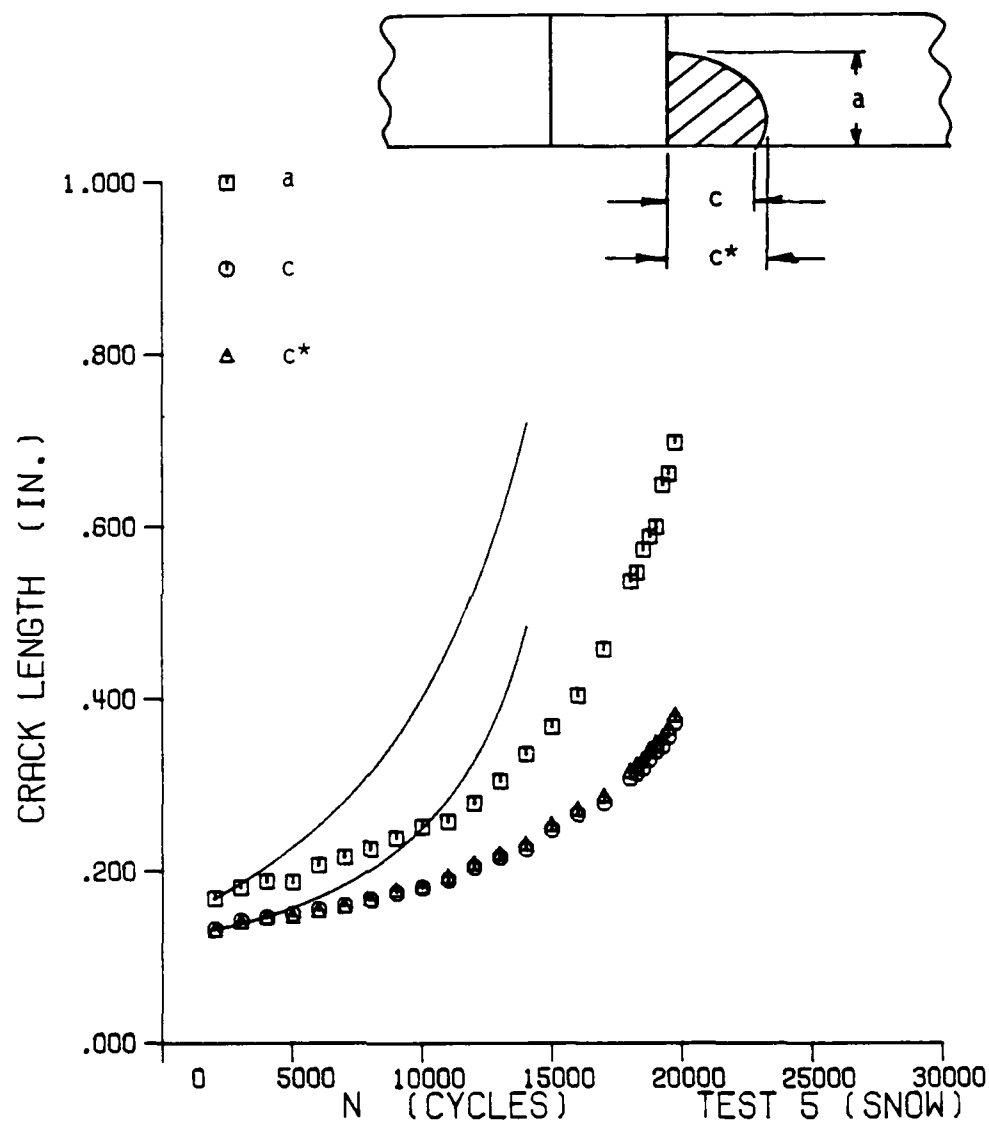
Figure 38   Comparison of Predicted and Actual Crack Growth for Snow Corner Crack Test 5
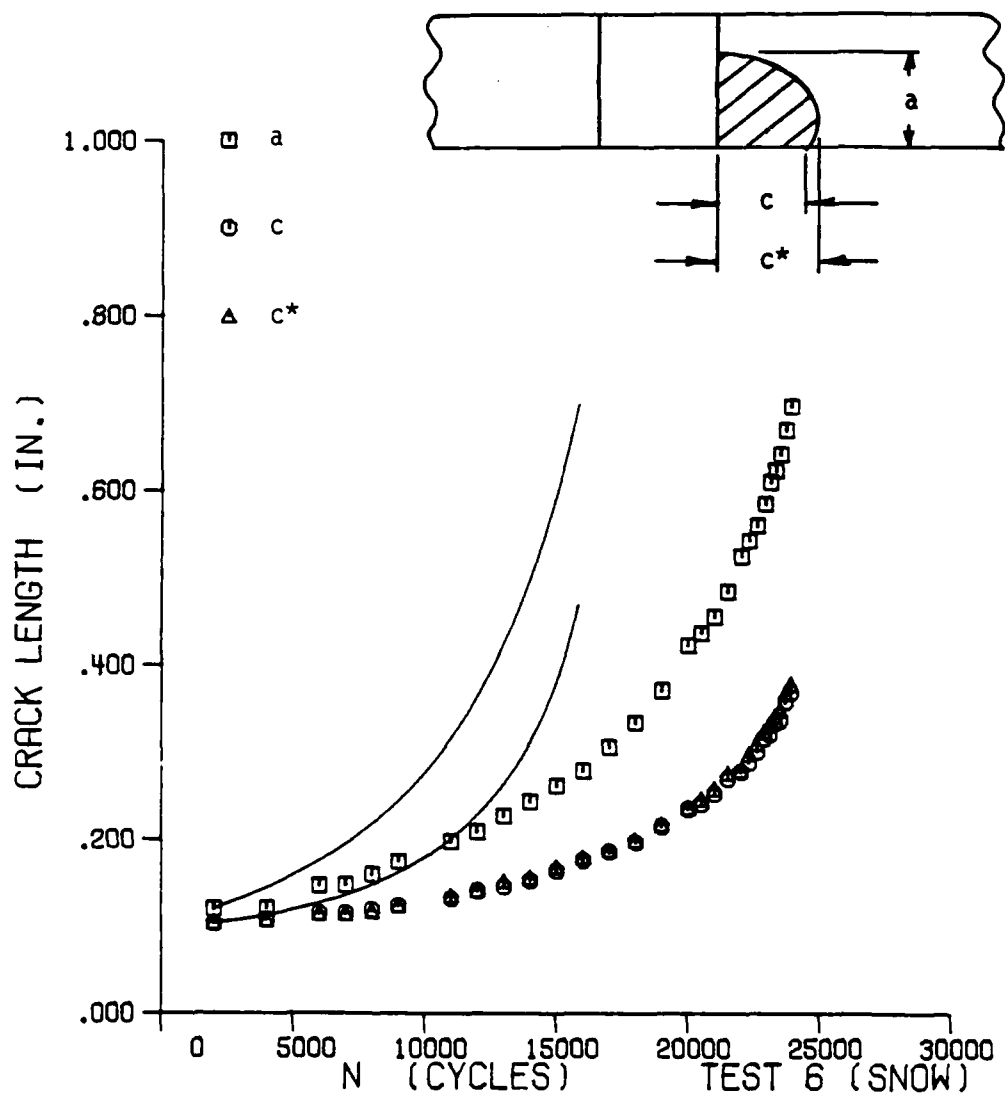
Figure 39   Comparison of Predicted and Actual Crack Growth
for Snow Corner Crack Test 6
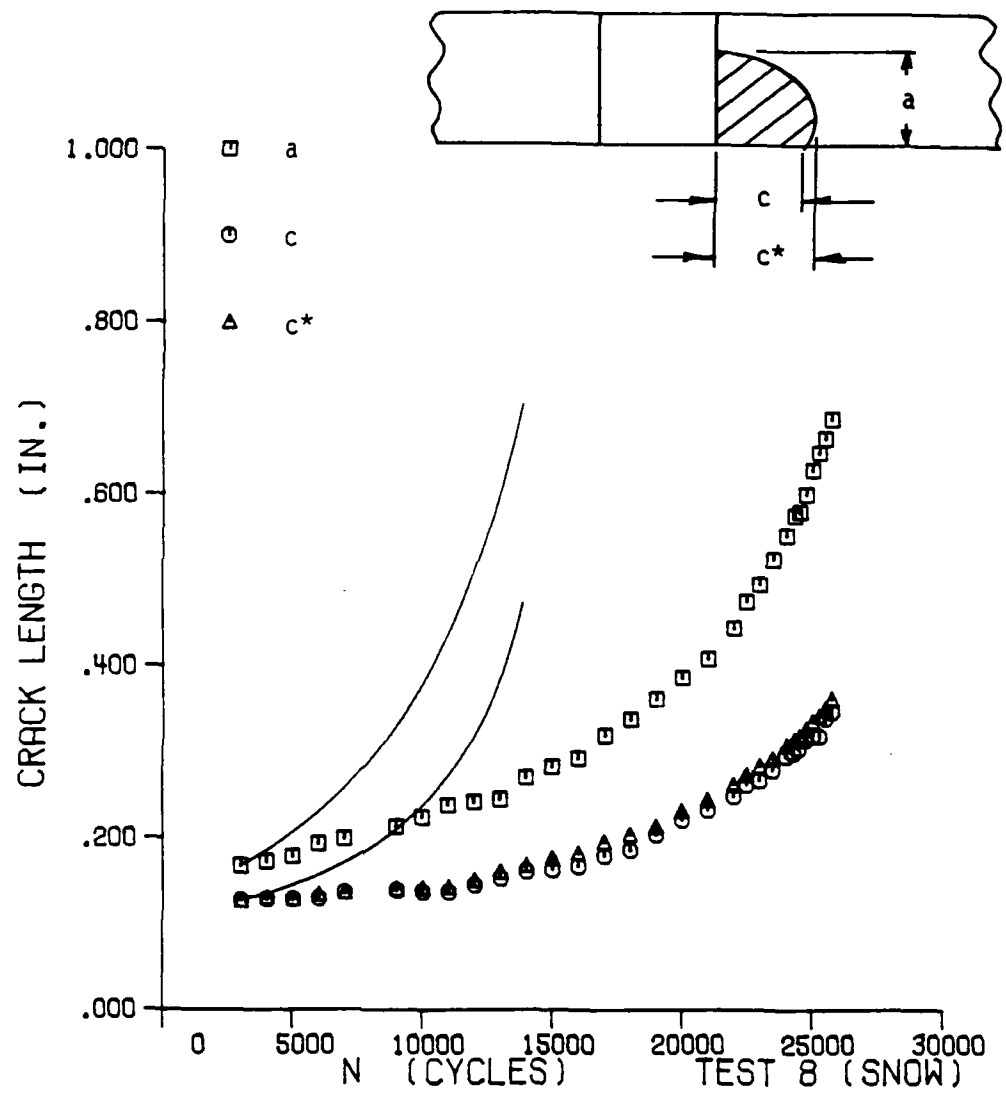
Figure 40   Comparison of Predicted and Actual Crack Growth
for Snow Corner Crack Test 8

factor" was obtained by dividing the stress intensity factor
for a through-cracked lug [13] by the Bowie result for a through-
cracked open hole [15]. It was hoped that when the Newman-Raju
surface crack result was multiplied by the "correction" factor,
one would obtain a working estimate for the surface cracked lug
stress intensity factor. Although crack growth predictions obtained
with these approximate stress intensity factors gave fairly reasonable
results in some cases, the approach was not judged successful enough
for general use.

SECTION V

DIGITIZED CRACK SHAPE MEASUREMENTS

The objective of this section is to present detailed measurements
of crack shape changes during the fatigue testing. Digitized measure-
ments of the fatigue crack profiles are given for Snow's corner crack
tests [5] and for one of the current embedded surface cracked plates
(specimen T2). It is believed that this detailed crack shape infor-
mation could be of interest to those who model surface and corner cracks
by analytical or numerical procedures.

Since the crack shapes were recorded on film as a function of elapsed
cycles, it was possible to make detailed measurements of the crack pro-
files. As shown schematically in Figures 41 and 42, tabulated results
are given here for the coordinates of points along the perimeter of
corner and embedded surface cracks located at the bore of the hole in
the PMMA plates. Digitized measurements are given for nine points along
the corner and transitioning corner cracks (Figure 41), while the co-
ordinates of ten embedded surface crack and transitioning flaw points
are presented (Figure 42).

The corner crack results were obtained by re-examining Snow's orig-
inal filmstrips on a photo interpreter/digitizer. The insturment auto-
matically punched digitized measurements of the crack profiles onto
computer cards for subsequent analysis. The data reduction system was
estimated to locate points along the crack profile to an accuray of $\pm$
0.003 inches (actual size). A different instrument was used to measure
the films for embedded crack specimen T2 tested here. In this case
a Mann digital comparator was employed, and again estimated accur-
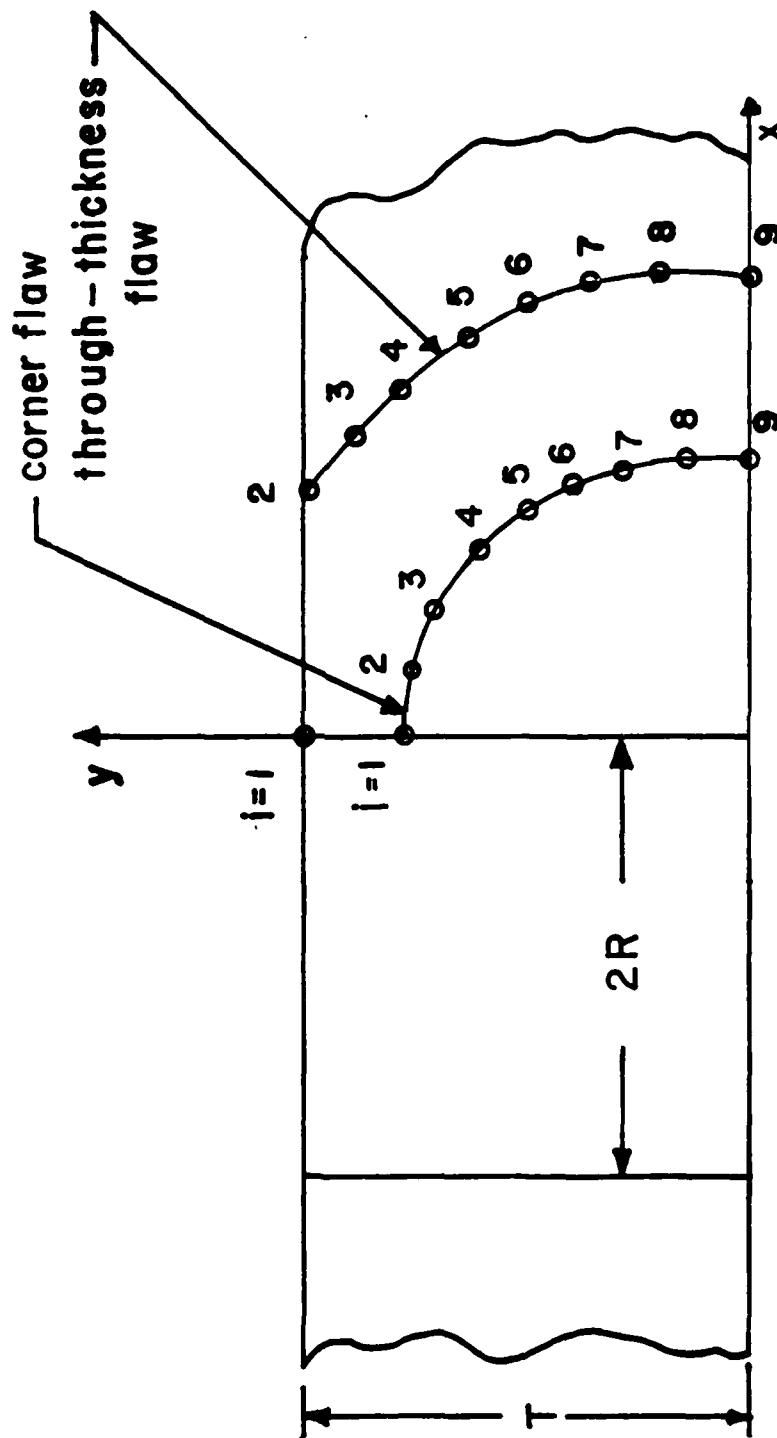
Figure 41   Schematic Representation of Corner and Through-Thickness Cracks Showing Location of Digitized Points Along Crack Front
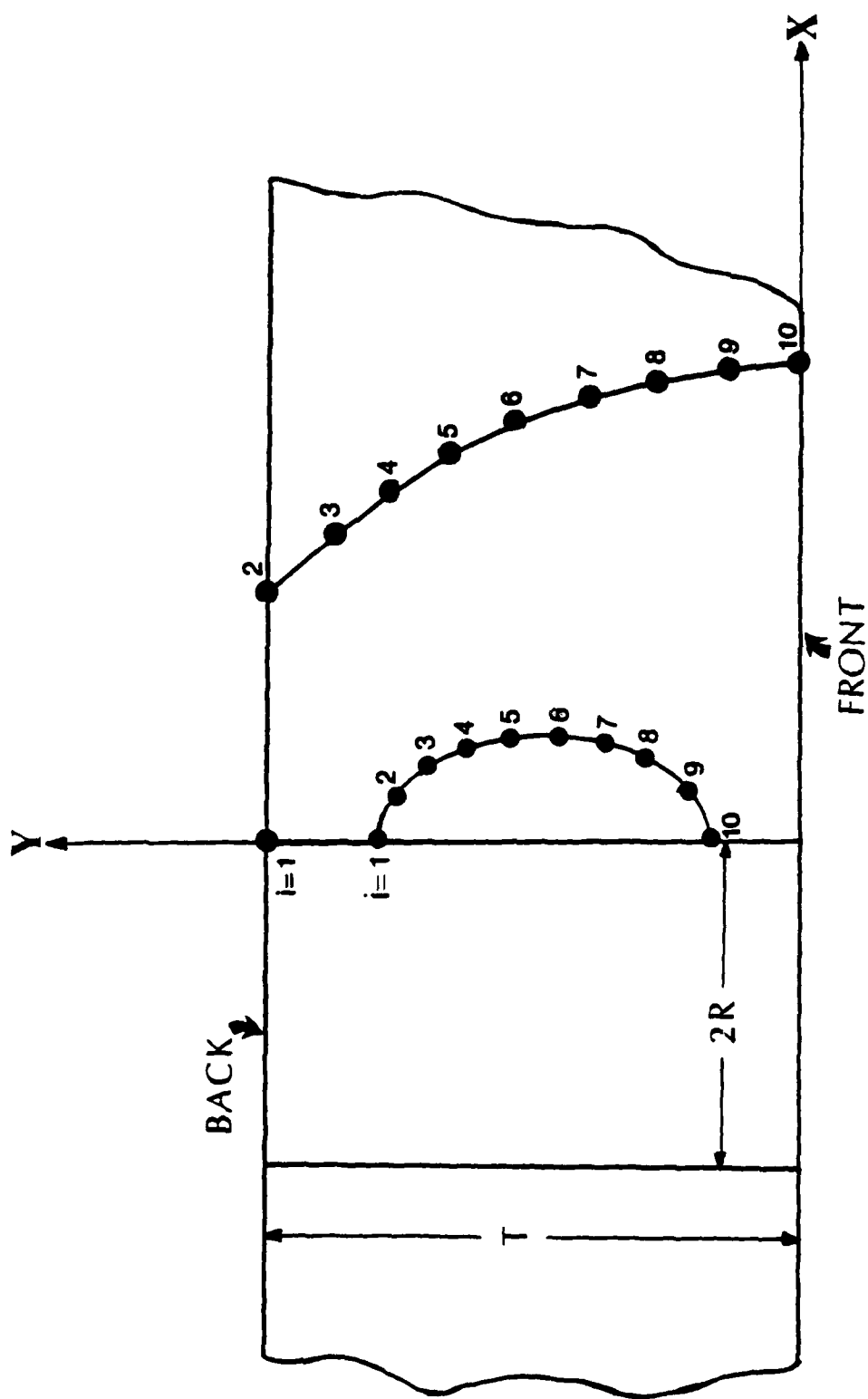
Figure 42   Schematic Representation of Embedded Surface and Through-Thickness
Cracks Showing Location of Digitized Points Along Crack Front

83

acy of $\pm$ 0.003 inches (actual size) was obtained. The latter instrument did not have the automatic data recording feature, however, and the digitized coordinates had to be recorded by hand, and then entered into the computer for analysis. Since this was a fairly time consuming procedure, only one of the embedded surface crack tests was examined in this detail.

In all cases, the photographs were scaled with respect to known distances in the x and y directions. Snow's original measurements for the a and c crack dimensions reported in Reference 5 were based on a scaling dimension in the x direction only, since he assumed that the viewing mirror was located at 45° to the crack plane, and thus gave a full view of the crack surface. Subsequent work with the loading apparatus in the present experiments indicated that the viewing mirror could sometimes give an oblique view of the crack plane. By using scaling dimensions in two perpendicular directions, it was possible to determine an angle correction and to compute the actual crack place measurement. All crack length data reported here have been corrected in this manner.

Digitized data for Snow's [5] corner crack Test 6 are given in graphical and tabular form in Figure 43 and Table 3 (this information for Test 6 is reproduced here from Reference 6). Here the remote stress varied between 18 and 630 psi, the hole diameter D = 0.739 in., the total width W = 7.950 in., and the plate thickness T = 0.698 in. Note from Figure 43 that the crack size and shapes are well documented as the corner crack grows along the bore of the hole and transitions through the thickness of the plate. Fatigue crack growth data obtained

84
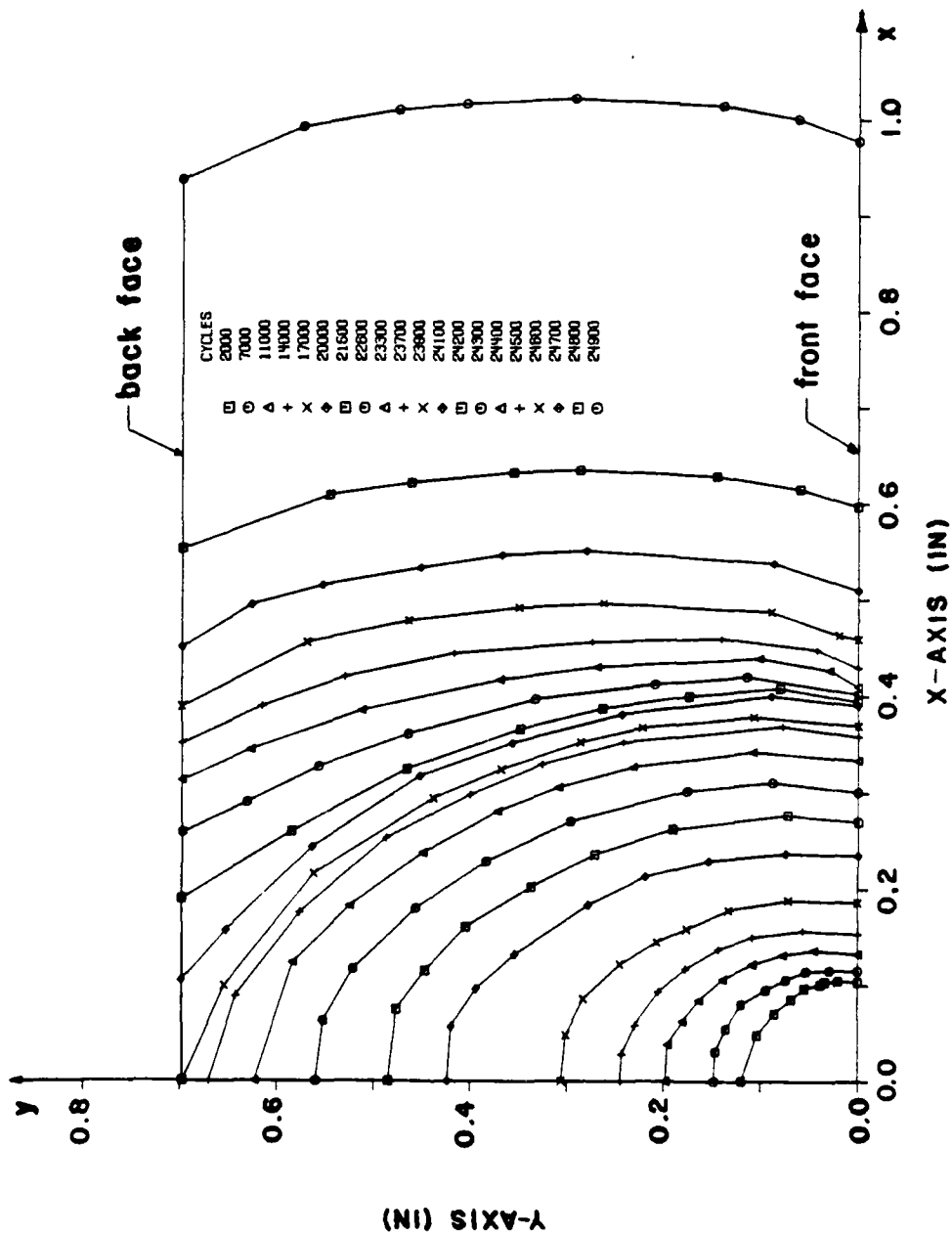
Figure 43   Digitized Fatigue Crack Profiles Showing Growth of Corner Crack into Through-The-Thickness Flaw (Snow Test 6)

85

Table 3

Digitized coordinates of points defining crack profile for Snow's Test 6 (all dimensions in inches)

cycles	x_i/y_i								
	i=1	2	3	4	5	6	7	8	9
2000	0.0 .120	.048 .104	.070 .086	.085 .068	.097 .055	.101 .038	.103 .034	.105 .020	.103 0.0
4000	0.0 .121	.028 .121	.052 .112	.079 .096	.095 .071	.102 .055	.105 .034	.108 .015	.108 0.0
6000	0.0 .147	.029 .144	.053 .131	.084 .104	.095 .089	.112 .053	.115 .031	.114 .016	.115 0.0
7000	0.0 .148	.031 .147	.055 .136	.080 .120	.095 .095	.105 .074	.114 .053	.115 .029	.115 0.0
8000	0.0 .160	.024 .158	.055 .148	.075 .135	.093 .112	.107 .086	.115 .056	.118 .032	.119 0.0
9000	0.0 .175	.033 .169	.070 .148	.098 .115	.112 .086	.120 .072	.125 .042	.124 .018	.124 0.0
11000	0.0 .198	.038 .196	.063 .181	.085 .164	.106 .139	.122 .109	.132 .077	.136 .045	.132 0.0
12000	0.0 .209	.042 .205	.066 .192	.099 .161	.125 .132	.137 .099	.143 .063	.143 .029	.141 0.0

Table 3 continued

cycles	i=1	2	3	4	5	6	7	8	9
					x_i/y_i				
13000	0.0 / .227	.053 / .216	.080 / .200	.105 / .176	.123 / .146	.134 / .125	.146 / .089	.153 / .044	.146 / 0.0
14000	0.0 / .244	.028 / .243	.058 / .230	.093 / .205	.117 / .178	.138 / .144	.150 / .109	.157 / .057	.153 / 0.0
15000	0.0 / .262	.047 / .258	.093 / .222	.118 / .195	.138 / .165	.147 / .142	.162 / .101	.169 / .042	.164 / 0.0
16000	0.0 / .279	.048 / .276	.092 / .247	.127 / .210	.149 / .176	.166 / .130	.175 / .085	.180 / .047	.176 / 0.0
17000	0.0 / .306	.048 / .301	.086 / .283	.122 / .245	.145 / .207	.159 / .177	.178 / .133	.188 / .071	.186 / 0.0
18000	0.0 / .334	.060 / .328	.097 / .297	.137 / .249	.164 / .206	.181 / .168	.194 / .117	.200 / .052	.197 / 0.0
19000	0.0 / .371	.050 / .369	.094 / .342	.134 / .298	.166 / .253	.185 / .207	.205 / .146	.218 / .068	.215 / 0.0
20000	0.0 / .423	.057 / .420	.097 / .394	.132 / .354	.184 / .278	.213 / .219	.230 / .154	.237 / .075	.235 / 0.0
20500	0.0 / .437	.058 / .435	.115 / .395	.155 / .350	.201 / .266	.229 / .195	.240 / .141	.247 / .067	.241 / 0.0

Table 3 continued

x_i/y_i

cycles	i=1	2	3	4	5	6	7	8	9
21000	0.0 / .456	.069 / .444	.124 / .409	.159 / .370	.192 / .315	.221 / .254	.244 / .188	.259 / .068	.253 / 0.0
21500	0.0 / .485	.075 / .476	.115 / .447	.161 / .405	.203 / .337	.236 / .272	.262 / .191	.277 / .072	.270 / 0.0
22000	0.0 / .525	.025 / .528	.080 / .504	.133 / .464	.187 / .400	.227 / .326	.253 / .265	.280 / .166	.278 / 0.0
22300	0.0 / .543	.114 / .503	.169 / .453	.213 / .389	.250 / .311	.275 / .236	.292 / .162	.299 / .092	.288 / 0.0
22600	0.0 / .560	.063 / .552	.117 / .521	.180 / .456	.229 / .383	.271 / .297	.302 / .176	.311 / .088	.301 / 0.0
22900	0.0 / .585	.109 / .558	.170 / .500	.214 / .443	.251 / .384	.296 / .276	.314 / .201	.324 / .106	.316 / 0.0
23100	0.0 / .610	.133 / .564	.187 / .505	.233 / .438	.288 / .327	.310 / .258	.329 / .163	.332 / .112	.321 / 0.0
23300	0.0 / .623	.124 / .583	.183 / .524	.238 / .449	.281 / .371	.305 / .309	.327 / .232	.342 / .109	.334 / 0.0
23500	0.0 / .642	.079 / .631	.176 / .555	.254 / .448	.298 / .356	.324 / .286	.340 / .217	.350 / .122	.337 / 0.0

Table 3 continued

cycles x_1/y_1

cycles	i=1	2	3	4	5	6	7	8	9
23700	0.0 / .670	.089 / .642	.176 / .576	.253 / .487	.298 / .400	.330 / .325	.352 / .242	.369 / .078	.358 / 0.0
23900	0.0 / .697	.099 / .654	.216 / .561	?94 / .438	.324 / .368	.352 / .286	.367 / .222	.379 / .107	.369 / 0.0
24100	0.0 / .698	.104 / .698	.157 / .652	.244 / .564	.317 / .452	.352 / .357	.382 / .243	.400 / .089	.390 / 0.0
24200	0.0 / .698	.189 / .698	.260 / .585	.324 / .466	.366 / .348	.387 / .263	.400 / .174	.408 / .080	.394 / 0.0
24300	0.0 / .698	.258 / .698	.290 / .630	.327 / .557	.361 / .464	.397 / .333	.413 / .209	.420 / .115	.402 / 0.0
24400	0.0 / .698	.312 / .698	.345 / .627	.385 / .512	.417 / .370	.431 / .270	.439 / .102	.427 / .027	.410 / 0.0
24500	0.0 / .698	.351 / .698	.390 / .615	.420 / .530	.445 / .417	.456 / .274	.460 / .141	.448 / .042	.429 / 0.0
24600	0.0 / .698	.389 / .698	.456 / .569	.478 / .463	.492 / .350	.496 / .263	.487 / .090	.463 / .020	.459 / 0.0
24700	0.0 / .698	.451 / .698	.495 / .626	.515 / .553	.533 / .452	.547 / .368	.551 / .281	.538 / .087	.509 / 0.0
24800	0.0 / .698	.553 / .698	.609 / .545	.622 / .462	.633 / .356	.635 / .287	.629 / .146	.615 / .060	.597 / 0.0

Table 3 continued

cycles	i=1	2	3	4	5	6	7	8	9
					x_i/y_i				
24900	0.0	.938	.994	1.011	1.018	1.023	1.015	1.001	.978
	.698	.698	.574	.475	.405	.293	.140	.063	0.0

from the same sheet of PMMA at the 1Hz cyclic frequency employed by Snow are given in Figure 44. Similar tabular and graphical data are given in the Appendix for Snow corner crack Tests 1, 3, 5, 8, and 9. As indicated previously, these measurements were all taken from Snow's original filmstrips and have been corrected for misalignment of the viewing mirror.

Digitized crack profiles for embedded surface crack Test T2 are given in Table 4 and in Figure 45. Note that only selected crack profiles are detailed here. Additional measurements of the a and c dimensions (obtained by independent measurement with the film strip projector method described in Section II) were given earlier in Figures 12a and 12b. Again note that the crack shape changes are characterized quite well by the digitized profiles shown in Figure 45.

Additional discussion of the behavior of the Snow corner crack test 6 and the present embedded flaw Test T2 are given in [12]. In particular, Figures 6 and 8 in [12] present stress intensity factors obtained by the three-dimensional finite element-alternating method for particular crack shapes. The stress intensity factor changes are correlated with fatigue crack growth rate behavior at the ends of the crack tips.

NO. OF POINTS = 226

$DA/DN = 0.694918E-22(DELTA K)^{6.095445}$

⊙ COMPACT SPECIMEN
+ 3-PT BEND SPECIMEN
✕ 4-PT BEND SPECIMEN
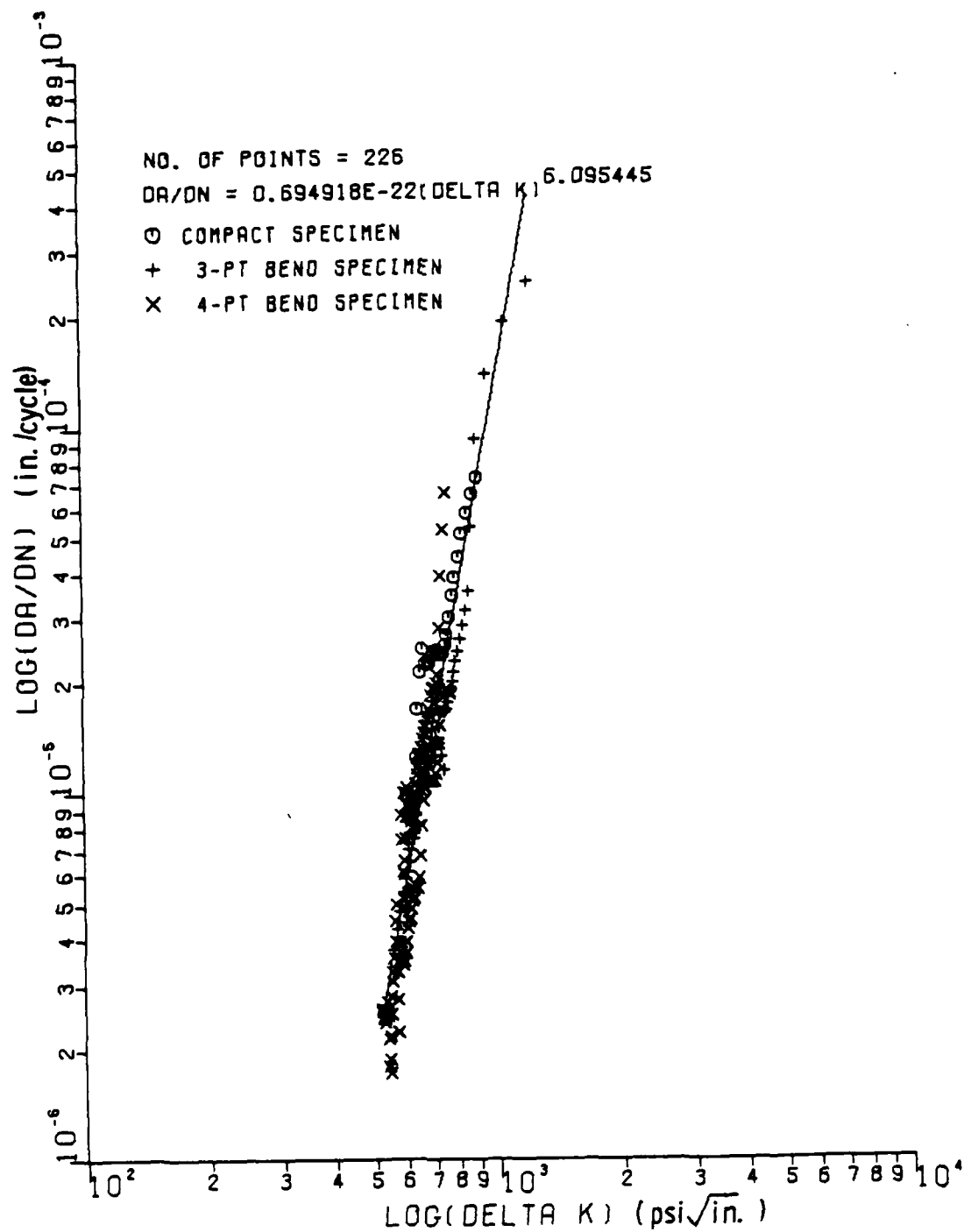
Figure 44　Baseline Fatigue Crack Growth Data for PMMA
Specimen Material Tested at 1 Hz
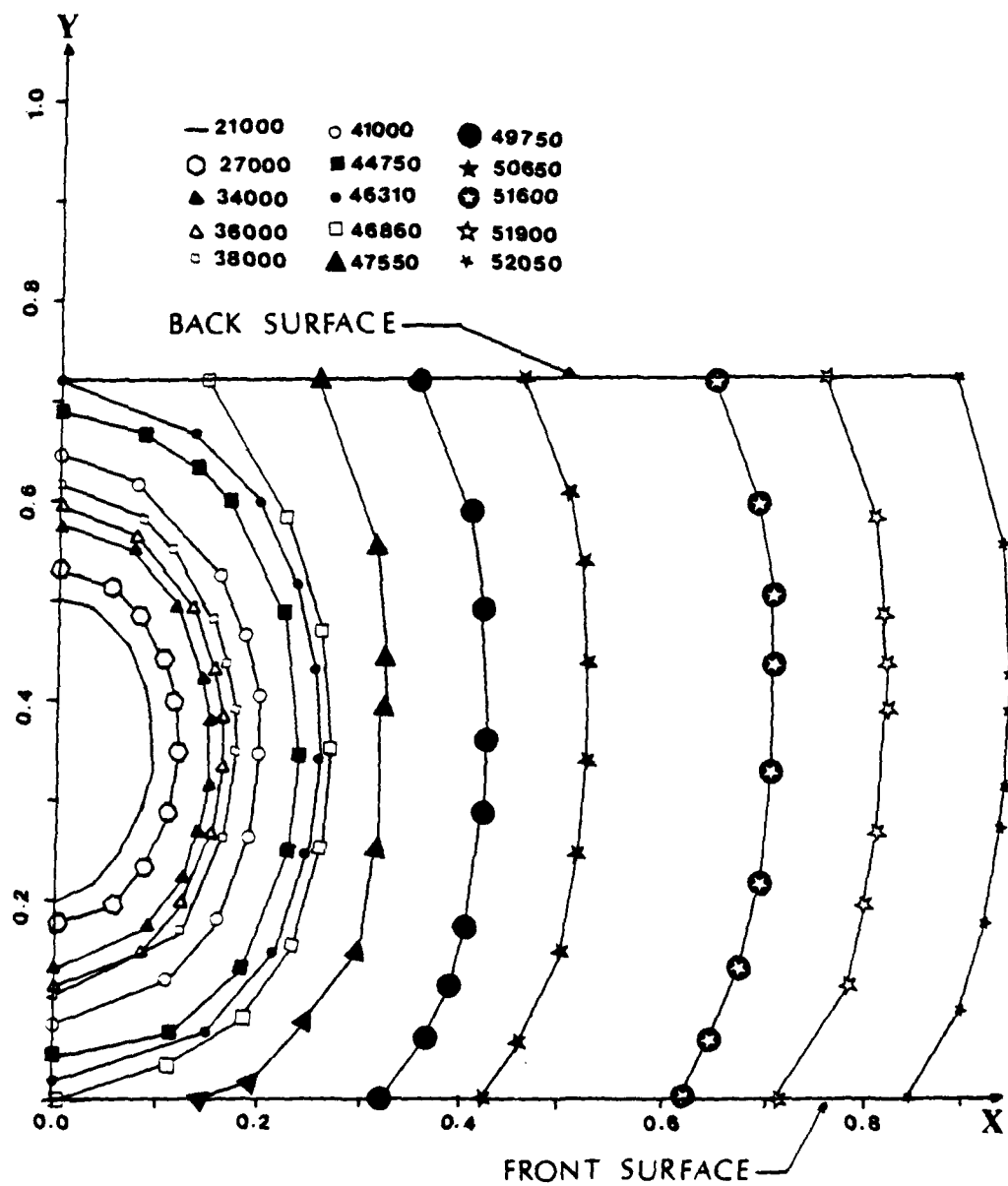
Figure 45 Digitized Fatigue Crack Profiles Showing Growth of
Embedded Surface Crack into Through-The-Thickness
Flaw (Test T2)

93

Table 4

Digitized Measurements of Crack Profiles for Embedded Surface Crack Test T2

x_i/y_i

cycles	i=1	2	3	4	5	6	7	8	9	10
21,000	.000 / .502	.036 / .491	.060 / .467	.076 / .440	.088 / .407	.095 / .349	.090 / .304	.061 / .241	.032 / .213	-.001 / .200
27,000	.000 / .532	.053 / .511	.079 / .485	.102 / .441	.113 / .399	.118 / .349	.110 / .283	.084 / .231	.053 / .191	-.007 / .171
34,000	.000 / .577	.074 / .551	.118 / .494	.142 / .424	.150 / .384	.149 / .317	.140 / .270	.123 / .226	.092 / .174	-.002 / .131
36,000	.000 / .594	.076 / .566	.134 / .493	.155 / .430	.164 / .385	.163 / .335	.154 / .270	.127 / .201	.082 / .145	-.003 / .114
38,000	.000 / .615	.083 / .563	.113 / .553	.153 / .483	.166 / .438	.175 / .393	.179 / .351	.164 / .263	.124 / .170	-.003 / .105
41,000	.000 / .645	.077 / .619	.161 / .527	.185 / .467	.199 / .407	.199 / .348	.190 / .269	.160 / .183	.110 / .120	.002 / .077
44,750	.000 / .687	.082 / .667	.137 / .634	.169 / .600	.224 / .487	.239 / .344	.228 / .251	.183 / .133	.113 / .063	.000 / .043
46,310	.000 / .720	.134 / .668	.198 / .602	.235 / .519	.254 / .433	.260 / .345	.247 / .243	.216 / .151	.152 / .071	.002 / .020

Table 4 (Continued)

x_i/y_i

cycles	i=1	2	3	4	5	6	7	8	9	10
46,860	.000 / .720	.145 / .720	.224 / .585	.260 / .472	.269 / .355	.260 / .255	.233 / .159	.187 / .084	.112 / .036	.000 / .000
47,550	.000 / .720	.201 / .720	.269 / .536	.282 / .421	.283 / .357	.261 / .198	.250 / .158	.216 / .093	.186 / .020	.143 / .000
49,750	.000 / .720	.354 / .718	.408 / .592	.419 / .494	.425 / .362	.421 / .288	.404 / .174	.390 / .117	.368 / .067	.319 / .000
50,650	.000 / .720	.464 / .723	.509 / .618	.522 / .548	.528 / .445	.526 / .347	.517 / .244	.502 / .155	.463 / .062	.423 / .000
51,600	.000 / .720	.653 / .724	.700 / .602	.711 / .508	.711 / .438	.708 / .329	.695 / .213	.675 / .122	.644 / .053	.614 / .000
51,900	.000 / .720	.772 / .721	.822 / .582	.827 / .480	.831 / .433	.828 / .384	.819 / .261	.808 / .189	.788 / .109	.722 / .000
52,050	.000 / .720	.901 / .725	.949 / .550	.952 / .418	.951 / .385	.946 / .309	.940 / .267	.925 / .175	.897 / .086	.844 / .000

SECTION VI

SUMMARY AND CONCLUSIONS

A series of fatigue tests have been conducted with initial embedded surface cracks located along the bore of a hole in a wide plate or a pin-loaded lug. The tests were conducted with transparent polymer specimens which allowed *in situ observation of the crack plane.* Crack growth was recorded by time lapse photography. Subsequent measurement of the crack photographs gave crack size and shape changes as a function of elapsed cycles.

A multidegree of freedom fracture mechanics model was developed to predict the growth of embedded surface and corner cracks located at open holes in plates loaded in remote tension. The analysis employed empirical stress intensity factor solutions reported by Newman and Raju [14] for surface and corner cracks located at open holes. Crack shape was a free parameter in the predictive model, and flaw shapes were allowed to develop naturally. Upon penetration of a free surface, the surface and corner cracks were assumed to instantly transition into uniform through-the-thickness flaws.

Predictions by the multidegree of freedom model gave excellent agreement with the actual growth of embedded surface cracks at open holes. The initial growth of the width 2a and depth c of the embedded surface cracks agreed very well with the predictions. The assumed transition into an instant through-crack gave a conservative, but good estimate of total specimen life. The predictive model was also used to analyze corner cracked hole experiments reported earlier by Snow [5]. Although the corner crack predictions generally gave shorter lives than observed experimentally, and did not show as close agreement as the embedded surface

97

cracks, the corner crack analysis still gave reasonable predictions for total specimen life. Thus, it is concluded that the Newman and Raju [14] stress intensity factor solutions for surface and corner cracked holes are quite useful for predicting the shape and size of surface and corner cracks at holes. An attempt to modify the Newman-Raju open hole solutions with a "correction factor" in order to apply them to the pin-loaded tests met with only limited success. The "correction factor" approach is not recommended for general use.

The Snow corner crack films and one of the present set of embedded surface crack photos were measured in a manner which gave a detailed record of the change in crack shape with fatigue life. The crack shapes were digitized, and coordinates of points along the crack border are presented in both graphical and tabular format. These data provide a detailed record of naturally occurring fatigue crack shapes and may be of interest to those who model surface or corner cracks by numerical techniques.

The transition of corner and surface cracks into uniform through-the-thickness flaws was examined in detail. Both three-dimensional stress intensity factor solutions and the fatigue crack growth results indicate that initial corner or embedded surface cracks try to grow into a stable through-the-thickness configuration. The stress intensity factor varies along the crack perimeter so that the maximum K occurs at the trailing, rather than the leading point of crack advance. Moreover, at the trailing point, where the crack penetrates a free surface, K varies significantly with crack advance.

The stress intensity factor reaches a large value initially after free surface penetration, but then decreases locally at that point as the free face crack length grows to a uniform through-the-thickness shape.

The stress intensity factor at the leading point of maximum crack advance usually has a smaller magnitude than at the trailing point, and is apparently unaffected by the large changes occurring at the trailing position during transition. The leading edge stress intensity factor may often be approximated during the transition period by the two-dimensional analysis for a uniform through-the-thickness crack whose length equals the distance of maximum crack advance.

The measured fatigue crack growth rates agree with the computed stress intensity factors, as the crack perimeter advances locally at rates corresponding to the K variation along the flaw perimeter. In particular, the free face crack dimension immediately grows quite rapidly after penetration, but then decreases to the rate seen by the point of maximum crack advance.

APPENDIX

DIGITIZED MEASUREMENTS OF
SNOW CORNER CRACK TESTS

This appendix presents digitized measurements of corner cracked hole experiments conducted by Snow [5]. The original filmstrips were remeasured, and the results given here in graphical and tabular form. The format is the same as that described in Section V for Test 6. Results are given for Snow's Test Numbers 1, 3, 5, 8, and 9. Specimen dimensions are given in reference [12]. In all cases, the remotely applied tension force varied between 100 and 3500 lbs. so that the applied cyclic force was 3400 lbs. At the beginning of each table, NUM refers to the total number of crack shapes digitized, 2R is the hole diameter, W is the plate width, T is the plate thickness, and LOAD is the applied cyclic force.
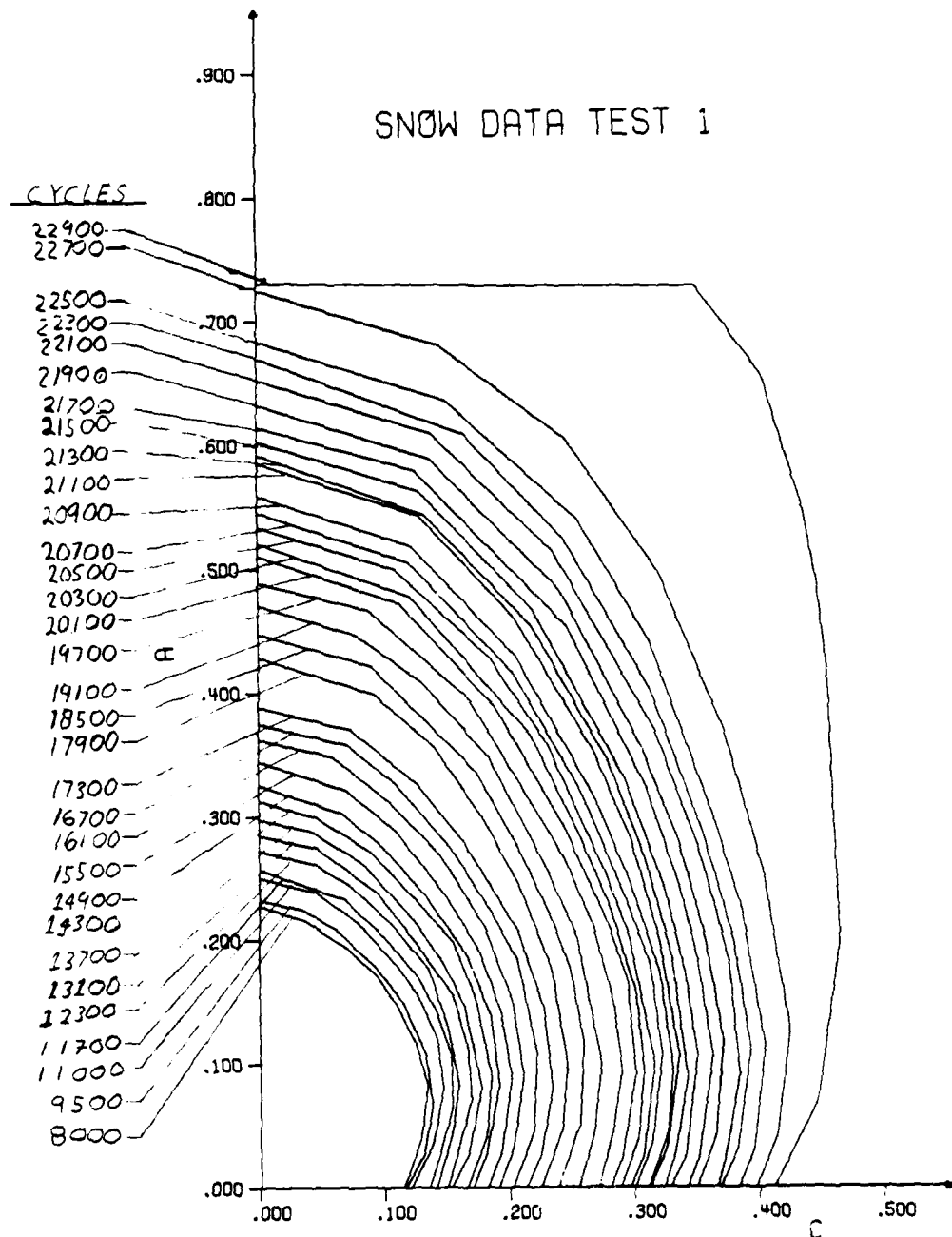
Figure 46   Digitized Crack Profiles for Snow Corner
Crack Test 1

102

Table 5   Digitized Data for Snow Test 1

```
NUM = 65      2R = .747     W = 7.980
T = .729      LOAD = 3400.
```

CYCLES =	8000.								
I =	1	2	3	4	5	6	7	8	9
X(I) =	0	.036	.072	.093	.109	.124	.134	.129	.114
Y(I) =	.227	.216	.192	.172	.148	.118	.083	.039	0

CYCLES =	8500.								
I =	1	2	3	4	5	6	7	8	9
X(I) =	0	.039	.069	.090	.112	.126	.135	.131	.114
Y(I) =	.229	.216	.196	.173	.145	.121	.083	.038	0

CYCLES =	9000.								
I =	1	2	3	4	5	6	7	8	9
X(I) =	0	.033	.061	.086	.105	.123	.135	.132	.113
Y(I) =	.228	.222	.205	.184	.160	.133	.087	.046	0

CYCLES =	9500.								
I =	1	2	3	4	5	6	7	8	9
X(I) =	0	.034	.061	.093	.115	.133	.138	.131	.116
Y(I) =	.232	.225	.209	.178	.150	.107	.066	.027	0

CYCLES =	10000.								
I =	1	2	3	4	5	6	7	8	9
X(I) =	0	.045	.078	.097	.121	.135	.140	.133	.114
Y(I) =	.238	.225	.200	.176	.143	.108	.065	.033	0

CYCLES =	10500.								
I =	1	2	3	4	5	6	7	8	9
X(I) =	0	.049	.080	.103	.123	.135	.142	.137	.120
Y(I) =	.243	.229	.211	.185	.153	.116	.073	.035	0

CYCLES =	11000.								
I =	1	2	3	4	5	6	7	8	9
X(I) =	0	.045	.079	.111	.127	.142	.147	.138	.120
Y(I) =	.250	.238	.214	.178	.155	.121	.079	.035	0

CYCLES =	11250.								
I =	1	2	3	4	5	6	7	8	9
X(I) =	0	.042	.082	.111	.129	.142	.150	.141	.124
Y(I) =	.252	.243	.218	.192	.162	.129	.071	.032	0

CYCLES =	11500.								
I =	1	2	3	4	5	6	7	8	9
X(I) =	0	.040	.070	.094	.121	.138	.152	.148	.133
Y(I) =	.259	.249	.234	.210	.178	.145	.101	.047	0

CYCLES =	11700.								
I =	1	2	3	4	5	6	7	8	9
X(I) =	0	.066	.101	.124	.141	.153	.154	.144	.135
Y(I) =	.257	.233	.201	.170	.140	.106	.063	.030	0

Table 5   continued

```
CYCLES =  11900.
   I =      1      2      3      4      5      6      7      8      9
X(I) =      0   .045   .081   .110   .136   .149   .155   .147   .137
Y(I) =   .267   .254   .229   .199   .161   .122   .067   .032      0


CYCLES =  12100.
   I =      1      2      3      4      5      6      7      8      9
X(I) =      0   .054   .083   .102   .130   .148   .158   .154   .140
Y(I) =   .273   .268   .236   .218   .181   .142   .085   .045      0


CYCLES =  12300.
   I =      1      2      3      4      5      6      7      8      9
X(I) =      0   .045   .075   .106   .135   .150   .159   .153   .140
Y(I) =   .272   .261   .242   .212   .177   .130   .083   .041      0


CYCLES =  12500.
   I =      1      2      3      4      5      6      7      8      9
X(I) =      0   .056   .091   .115   .142   .157   .162   .155   .141
Y(I) =   .278   .261   .233   .208   .172   .125   .076   .041      0


CYCLES =  12700.
   I =      1      2      3      4      5      6      7      8      9
X(I) =      0   .049   .082   .111   .135   .151   .164   .156   .143
Y(I) =   .280   .267   .243   .213   .183   .145   .085   .041      0


CYCLES =  12900.
   I =      1      2      3      4      5      6      7      8      9
X(I) =      0   .048   .084   .110   .136   .154   .166   .161   .146
Y(I) =   .284   .271   .246   .220   .185   .145   .082   .036      0


CYCLES =  13100.
   I =      1      2      3      4      5      6      7      8      9
X(I) =      0   .047   .094   .124   .155   .166   .169   .158   .149
Y(I) =   .284   .274   .238   .199   .155   .111   .072   .031      0


CYCLES =  13300.
   I =      1      2      3      4      5      6      7      8      9
X(I) =      0   .045   .080   .113   .145   .162   .171   .160   .147
Y(I) =   .290   .279   .256   .220   .176   .133   .074   .027      0


CYCLES =  13500.
   I =      1      2      3      4      5      6      7      8      9
X(I) =      0   .049   .085   .120   .164   .173   .173   .166   .152
Y(I) =   .293   .280   .255   .214   .185   .105   .065   .036      0
```

Table 5 continued

```
CYCLES =  13700.
   I  =      1       2       3       4       5       6       7       8       9
X(I) =      0    .040    .081    .121    .146    .164    .177    .166    .153
Y(I) =   .297    .288    .263    .219    .183    .146    .080    .027       0


CYCLES =  13900.
   I  =      1       2       3       4       5       6       7       8       9
X(I) =      0    .039    .078    .113    .153    .168    .179    .169    .156
Y(I) =   .299    .292    .268    .233    .181    .140    .089    .029       0


CYCLES =  14100.
   I  =      1       2       3       4       5       6       7       8       9
X(I) =      0    .058    .102    .132    .162    .176    .183    .178    .161
Y(I) =   .307    .290    .254    .222    .174    .127    .081    .039       0


CYCLES =  14300.
   I  =      1       2       3       4       5       6       7       8       9
X(I) =      0    .046    .089    .121    .155    .173    .185    .181    .165
Y(I) =   .312    .299    .271    .236    .198    .153    .089    .041       0


CYCLES =  14500.
   I  =      1       2       3       4       5       6       7       8       9
X(I) =      0    .042    .093    .128    .170    .182    .186    .178    .166
Y(I) =   .316    .305    .271    .232    .169    .118    .078    .032       0


CYCLES =  14700.
   I  =      1       2       3       4       5       6       7       8       9
X(I) =      0    .060    .097    .130    .163    .185    .191    .180    .168
Y(I) =   .320    .302    .273    .237    .169    .123    .074    .033       0


CYCLES =  14900.
   I  =      1       2       3       4       5       6       7       8       9
X(I) =      0    .066    .100    .132    .166    .185    .191    .181    .170
Y(I) =   .325    .302    .274    .236    .187    .137    .083    .028       0


CYCLES =  15100.
   I  =      1       2       3       4       5       6       7       8       9
X(I) =      0    .061    .105    .140    .168    .185    .195    .191    .181
Y(I) =   .329    .311    .274    .231    .193    .150    .088    .042       0


CYCLES =  15300.
   I  =      1       2       3       4       5       6       7       8       9
X(I) =      0    .065    .102    .135    .165    .184    .197    .191    .176
Y(I) =   .341    .319    .289    .244    .205    .164    .097    .038       0
```

Table 5   continued

```
CYCLES =   15500.
  I =       1       2       3       4       5       6       7       8       9
X(I) =       0    .070    .109    .147    .175    .193    .201    .193    .181
Y(I) =    .344    .321    .286    .238    .192    .141    .089    .030       0


CYCLES =   15700.
  I =       1       2       3       4       5       6       7       8       9
X(I) =       0    .058    .105    .138    .171    .195    .205    .199    .184
Y(I) =    .349    .334    .297    .261    .207    .148    .079    .036       0


CYCLES =   15900.
  I =       1       2       3       4       5       6       7       8       9
X(I) =       0    .065    .106    .150    .183    .199    .207    .200    .185
Y(I) =    .351    .333    .298    .245    .193    .142    .081    .033       0


CYCLES =   16100.
  I =       1       2       3       4       5       6       7       8       9
X(I) =       0    .059    .103    .144    .180    .202    .211    .203    .190
Y(I) =    .362    .348    .312    .269    .211    .151    .090    .033       0


CYCLES =   16300.
  I =       1       2       3       4       5       6       7       8       9
X(I) =       0    .066    .111    .149    .173    .197    .213    .209    .194
Y(I) =    .363    .345    .306    .260    .223    .178    .102    .033       0


CYCLES =   16500.
  I =       1       2       3       4       5       6       7       8       9
X(I) =       0    .073    .126    .163    .195    .212    .220    .212    .198
Y(I) =    .371    .349    .303    .252    .202    .145    .085    .032       0


CYCLES =   16700.
  I =       1       2       3       4       5       6       7       8       9
X(I) =       0    .071    .110    .154    .184    .207    .222    .219    .202
Y(I) =    .375    .357    .326    .272    .225    .183    .109    .044       0


CYCLES =   16900.
  I =       1       2       3       4       5       6       7       8       9
X(I) =       0    .090    .136    .170    .191    .215    .225    .223    .206
Y(I) =    .380    .349    .304    .257    .222    .174    .113    .048       0


CYCLES =   17100.
  I =       1       2       3       4       5       6       7       8       9
X(I) =       0    .075    .129    .166    .194    .222    .229    .220    .208
Y(I) =    .387    .367    .318    .271    .224    .160    .083    .028       0


CYCLES =   17300.
  I =       1       2       3       4       5       6       7       8       9
X(I) =       0    .074    .127    .166    .207    .237    .234    .225    .213
Y(I) =    .388    .369    .328    .276    .206    .145    .079    .027       0
```

106

Table 5 continued

```
CYCLES =   17500.
   I =       1       2       3       4       5       6       7       8       9
X(I) =       0    .064    .117    .164    .159    .227    .237    .234    .217
Y(I) =    .399    .387    .347    .292    .236    .182    .110    .046       0


CYCLES =   17700.
   I =       1       2       3       4       5       6       7       8       9
X(I) =       0    .085    .133    .172    .205    .228    .244    .240    .226
Y(I) =    .420    .392    .354    .302    .240    .184    .105    .044       0


CYCLES =   17900.
   I =       1       2       3       4       5       6       7       8       9
X(I) =       0    .092    .140    .179    .208    .234    .246    .242    .224
Y(I) =    .428    .399    .356    .298    .244    .176    .100    .046       0


CYCLES =   18100.
   I =       1       2       3       4       5       6       7       8       9
X(I) =       0    .086    .150    .183    .224    .245    .251    .245    .229
Y(I) =    .433    .408    .349    .298    .218    .155    .098    .037       0


CYCLES =   18300.
   I =       1       2       3       4       5       6       7       8       9
X(I) =       0    .086    .151    .190    .217    .234    .253    .251    .235
Y(I) =    .440    .412    .356    .294    .243    .202    .116    .052       0


CYCLES =   18500.
   I =       1       2       3       4       5       6       7       8       9
X(I) =       0    .090    .174    .207    .235    .249    .259    .256    .238
Y(I) =    .447    .421    .336    .274    .215    .177    .118    .052       0


CYCLES =   18700.
   I =       1       2       3       4       5       6       7       8       9
X(I) =       0    .092    .144    .190    .224    .248    .267    .262    .246
Y(I) =    .456    .430    .378    .321    .250    .195    .108    .050       0


CYCLES =   18900.
   I =       1       2       3       4       5       6       7       8       9
X(I) =       0    .083    .144    .197    .230    .250    .269    .263    .249
Y(I) =    .463    .442    .387    .315    .246    .197    .111    .052       0


CYCLES =   19100.
   I =       1       2       3       4       5       6       7       8       9
X(I) =       0    .078    .131    .184    .227    .253    .273    .267    .254
Y(I) =    .470    .446    .408    .348    .264    .201    .100    .042       0


CYCLES =   19300.
   I =       1       2       3       4       5       6       7       8       9
X(I) =       0    .080    .138    .180    .229    .254    .279    .272    .259
Y(I) =    .472    .454    .410    .357    .273    .215    .102    .033       0
```

Table 5 continued

```
CYCLES =  19500.
   I  =      1      2      3      4      5      6      7      8      9
 X(I) =      0   .063   .142   .212   .249   .276   .286   .276   .267
 Y(I) =   .483   .474   .421   .323   .246   .175   .096   .030      0


CYCLES =  19700.
   I  =      1      2      3      4      5      6      7      8      9
 X(I) =      0   .089   .169   .243   .267   .283   .290   .282   .270
 Y(I) =   .488   .466   .394   .268   .212   .151   .095   .043      0


CYCLES =  20100.
   I  =      1      2      3      4      5      6      7      8      9
 X(I) =      0   .113   .190   .243   .280   .295   .301   .290   .280
 Y(I) =   .510   .472   .388   .293   .210   .168   .092   .025      0

CYCLES =  20300.
   I  =      1      2      3      4      5      6      7      8      9
 X(I) =      0   .122   .218   .257   .282   .302   .307   .303   .288
 Y(I) =   .520   .477   .388   .282   .223   .156   .095   .039      0


CYCLES =  20500.
   I  =      1      2      3      4      5      6      7      8      9
 X(I) =      0   .109   .185   .231   .278   .297   .316   .307   .296
 Y(I) =   .534   .499   .429   .358   .252   .201   .100   .027      0


CYCLES =  20700.
   I  =      1      2      3      4      5      6      7      8      9
 X(I) =      0   .121   .204   .255   .291   .313   .322   .314   .300
 Y(I) =   .545   .505   .416   .318   .238   .180   .106   .035      0


CYCLES =  20900.
   I  =      1      2      3      4      5      6      7      8      9
 X(I) =      0   .122   .205   .299   .297   .320   .331   .325   .310
 Y(I) =   .559   .519   .430   .315   .246   .174   .096   .043      0


CYCLES =  21100.
   I  =      1      2      3      4      5      6      7      8      9
 X(I) =      0   .129   .204   .288   .297   .321   .336   .325   .312
 Y(I) =   .585   .543   .462   .353   .281   .197   .106   .032   .002


CYCLES =  21300.
   I  =      1      2      3      4      5      6      7      8      9
 X(I) =      0   .134   .219   .281   .308   .330   .342   .332   .323
 Y(I) =   .592   .544   .454   .342   .267   .186   .088   .028      0


CYCLES =  21500.
   I  =      1      2      3      4      5      6      7      8      9
 X(I) =      0   .129   .219   .293   .325   .341   .350   .341   .328
 Y(I) =   .603   .563   .468   .351   .240   .174   .106   .026      0
```

Table 5 continued

```
CYCLES =  21700.
  I =      1      2      3      4      5      6      7      8      9
X(I) =     0   .126   .247   .311   .337   .351   .363   .351   .342
Y(I) =  .614   .579   .454   .322   .242   .187   .105   .025      0


CYCLES =  21900.
  I =      1      2      3      4      5      6      7      8      9
X(I) =     0   .138   .242   .306   .336   .358   .371   .365   .349

Y(I) =  .632   .589   .483   .357   .280   .199   .118   .040      0


CYCLES =  22100.
  I =      1      2      3      4      5      6      7      8      9
X(I) =     0   .139   .236   .318   .352   .376   .384   .375   .366
Y(I) =  .652   .609   .514   .369   .274   .183   .091   .035      0


CYCLES =  22300.
  I =      1      2      3      4      5      6      7      8      9
X(I) =     0   .165   .245   .314   .354   .380   .393   .383   .369
Y(I) =  .670   .608   .525   .402   .290   .198   .111   .031      0


CYCLES =  22500.
  I =      1      2      3      4      5      6      7      8      9
X(I) =     0   .151   .256   .313   .362   .386   .405   .396   .383
Y(I) =  .663   .636   .540   .441   .304   .224   .114   .031      0


CYCLES =  22700.
  I =      1      2      3      4      5      6      7      8      9
X(I) =     0   .146   .247   .320   .374   .403   .425   .414   .397
Y(I) =  .725   .680   .605   .496   .366   .257   .127   .040      0


CYCLES =  22900.
  I =      1      2      3      4      5      6      7      8      9
X(I) =  .352   .404   .438   .449   .457   .461   .466   .447   .412
Y(I) =  .728   .657   .548   .488   .410   .306   .197   .069      0
```

SNOW DATA TEST 3
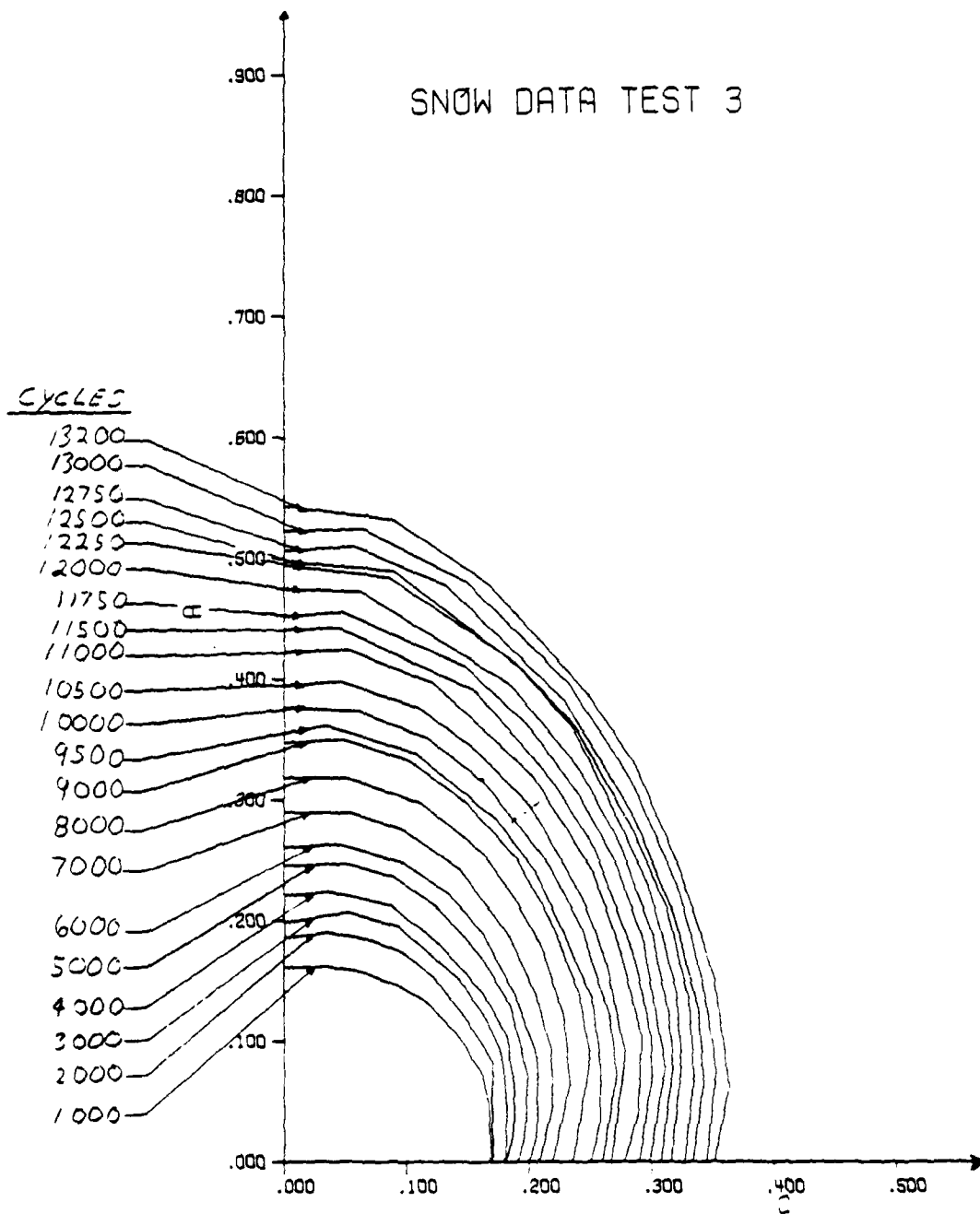
CYCLES

Figure 47 Digitized Crack Profiles for Snow Corner
Crack Test 3

110

Table 6   Digitized Data for Snow Test 3

NUM = 21   2R = .750   W = 7.980
T = .730   LOAD = 3400.

```
CYCLES =   1000.
    I =      1       2       3       4       5       6       7       8       9
  X(I) =     0    .033    .064    .097    .117    .140    .161    .167    .169
  Y(I) =   .162    .162    .157    .144    .132    .107    .075    .050      0


CYCLES =   2000.
    I =      1       2       3       4       5       6       7       8       9
  X(I) =     0    .034    .071    .099    .124    .151    .170    .170    .170
  Y(I) =   .186    .190    .184    .172    .151    .114    .082    .046      0


CYCLES =   3000.
    I =      1       2       3       4       5       6       7       8       9
  X(I) =     0    .050    .093    .122    .144    .165    .178    .182    .180
  Y(I) =   .199    .207    .195    .170    .150    .118    .087    .049      0


CYCLES =   4000.
    I =      1       2       3       4       5       6       7       8       9
  X(I) =     0    .036    .087    .126    .162    .182    .188    .187    .181
  Y(I) =   .221    .224    .213    .181    .140    .104    .060    .026      0


CYCLES =   5000.
    I =      1       2       3       4       5       6       7       8       9
  X(I) =     0    .048    .090    .125    .162    .185    .199    .197    .191
  Y(I) =   .245    .247    .236    .211    .169    .129    .071    .026      0


CYCLES =   6000.
    I =      1       2       3       4       5       6       7       8       9
  X(I) =     0    .043    .099    .135    .162    .188    .207    .206    .200
  Y(I) =   .261    .263    .247    .221    .189    .140    .084    .025      0


CYCLES =   7000.
    I =      1       2       3       4       5       6       7       8       9
  X(I) =     0    .054    .097    .144    .184    .205    .218    .219    .208
  Y(I) =   .290    .289    .275    .242    .196    .139    .091    .046      0


CYCLES =   8000.
    I =      1       2       3       4       5       6       7       8       9
  X(I) =   .000    .050    .112    .163    .187    .212    .228    .233    .219
  Y(I) =   .318    .318    .297    .255    .220    .175    .119    .063      0


CYCLES =   9000.
    I =      1       2       3       4       5       6       7       8       9
  X(I) =     0    .046    .103    .150    .195    .216    .241    .250    .235
  Y(I) =   .347    .350    .332    .296    .250    .202    .140    .085      0


CYCLES =   9900.
    I =      1       2       3       4       5       6       7       8       9
  X(I) =     0    .032    .107    .173    .206    .251    .258    .258    .250
  Y(I) =   .355    .362    .338    .284    .240    .186    .079    .032      0
```

111

Table 6 continued

```
CYCLES =  10000.
  I =       1       2       3       4       5       6       7       8       9
X(I) =      0    .061    .118    .164    .217    .243    .266    .271    .259
Y(I) =   .376    .373    .350    .314    .246    .194    .119    .072       0


CYCLES =  10500.
  I =       1       2       3       4       5       6       7       8       9
X(I) =      0    .045    .110    .158    .201    .243    .264    .278    .267
Y(I) =   .395    .398    .376    .340    .285    .219    .162    .087       0


CYCLES =  11000.
  I =       1       2       3       4       5       6       7       8       9
X(I) =      0    .051    .123    .204    .253    .276    .292    .289    .277
Y(I) =   .422    .425    .396    .318    .240    .169    .103    .040       0


CYCLES =  11500.
  I =       1       2       3       4       5       6       7       8       9
X(I) =      0    .043    .157    .219    .254    .287    .299    .300    .290
Y(I) =   .441    .443    .389    .315    .259    .165    .105    .070       0


CYCLES =  11750.
  I =       1       2       3       4       5       6       7       8       9
X(I) =      0    .047    .148    .198    .242    .272    .294    .311    .298
Y(I) =   .452    .456    .410    .363    .302    .245    .180    .073       0


CYCLES =  12000.
  I =       1       2       3       4       5       6       7       8       9
X(I) =   .003    .063    .185    .243    .275    .301    .314    .317    .307
Y(I) =   .474    .472    .395    .322    .261    .187    .123    .079       0


CYCLES =  12250.
  I =       1       2       3       4       5       6       7       8       9
X(I) =   .000    .086    .190    .235    .282    .298    .320    .324    .316
Y(I) =   .494    .484    .413    .359    .306    .228    .143    .080       0


CYCLES =  12500.
  I =       1       2       3       4       5       6       7       8       9
X(I) =      0    .090    .195    .237    .282    .312    .330    .334    .327
Y(I) =   .497    .489    .407    .361    .280    .212    .136    .069       0


CYCLES =  12750.
  I =       1       2       3       4       5       6       7       8       9
X(I) =      0    .056    .132    .229    .284    .318    .338    .342    .333
Y(I) =   .506    .510    .477    .382    .289    .205    .129    .067       0


CYCLES =  13000.
  I =       1       2       3       4       5       6       7       8       9
X(I) =      0    .063    .149    .200    .259    .322    .343    .353    .345
Y(I) =   .523    .525    .480    .395    .317    .229    .144    .075       0


CYCLES =  13200.
  I =       1       2       3       4       5       6       7       8       9
X(I) =   .001    .090    .166    .248    .288    .324    .352    .363    .351
Y(I) =   .543    .532    .479    .397    .326    .239    .150    .062       0
```

112

Figure 48   Digitized Crack Profiles for Snow Corner
Crack Test 5

113

Table 7   Digitized Data for Snow Test 5

NUM = 25   2R = .742   W = 7.950
T = .720   LOAD = 3400.

```
CYCLES =    2000.
    I =      1       2       3       4       5       6       7       8       9
  X(I) =     0    .022    .052    .084    .103    .119    .127    .132    .132
  Y(I) =  .168    .168    .162    .144    .126    .109    .090    .066       0


CYCLES =    3000.
    I =      1       2       3       4       5       6       7       8       9
  X(I) =     0    .044    .071    .095    .112    .125    .136    .142    .142
  Y(I) =  .181    .176    .165    .145    .127    .107    .077    .037       0


CYCLES =    4000.
    I =      1       2       3       4       5       6       7       8       9
  X(I) =     0    .040    .071    .100    .118    .133    .141    .147    .146
  Y(I) =  .188    .185    .172    .150    .129    .101    .075    .035       0


CYCLES =    5000.
    I =      1       2       3       4       5       6       7       8       9
  X(I) =     0    .032    .076    .109    .128    .145    .148    .148    .150
  Y(I) =  .187    .187    .169    .138    .109    .075    .049    .027       0


CYCLES =    6000.
    I =      1       2       3       4       5       6       7       8       9
  X(I) =     0    .041    .074    .104    .127    .142    .153    .155    .155
  Y(I) =  .207    .204    .193    .172    .137    .106    .069    .040       0


CYCLES =    7000.
    I =      1       2       3       4       5       6       7       8       9
  X(I) =     0    .038    .070    .099    .125    .141    .153    .160    .160
  Y(I) =  .216    .212    .203    .187    .154    .124    .091    .060       0


CYCLES =    8000.
    I =      1       2       3       4       5       6       7       8       9
  X(I) =     0    .043    .076    .104    .127    .147    .161    .168    .167
  Y(I) =  .226    .223    .216    .199    .170    .140    .099    .066       0


CYCLES =    9000.
    I =      1       2       3       4       5       6       7       8       9
  X(I) =     0    .047    .077    .114    .140    .159    .174    .179    .175
  Y(I) =  .239    .241    .231    .206    .171    .139    .083    .045       0


CYCLES =   10000.
    I =      1       2       3       4       5       6       7       8       9
  X(I) =  .000    .049    .087    .127    .150    .169    .183    .183    .181
  Y(I) =  .252    .254    .239    .209    .176    .132    .080    .043       0


CYCLES =   11000.
    I =      1       2       3       4       5       6       7       8       9
  X(I) =     0    .040    .087    .136    .160    .176    .189    .195    .190
  Y(I) =  .258    .259    .244    .214    .179    .142    .103    .055       0
```

114

Table 7 continued

```
CYCLES =  12000.
   I  =     1      2      3      4      5      6      7      8      9
X(I) =     0   .043   .103   .140   .168   .187   .205   .210   .205
Y(I) =  .279   .283   .264   .232   .195   .156   .098   .054      0


CYCLES =  13000.
   I  =     1      2      3      4      5      6      7      8      9
X(I) =     0   .041   .086   .139   .176   .202   .216   .221   .216
Y(I) =  .305   .308   .285   .263   .217   .162   .112   .067      0


CYCLES =  14000.
   I  =     1      2      3      4      5      6      7      8      9
X(I) =     0   .055   .092   .134   .168   .198   .222   .233   .226
Y(I) =  .336   .337   .322   .292   .255   .208   .145   .067      0


CYCLES =  15000.
   I  =     1      2      3      4      5      6      7      8      9
X(I) =     0   .052   .106   .149   .188   .217   .238   .255   .249
Y(I) =  .368   .368   .350   .314   .272   .222   .168   .078      0


CYCLES =  16000.
   I  =     1      2      3      4      5      6      7      8      9
X(I) =     0   .052   .104   .186   .228   .247   .262   .273   .267
Y(I) =  .404   .406   .382   .313   .244   .206   .155   .074      0


CYCLES =  17000.
   I  =     1      2      3      4      5      6      7      8      9
X(I) =     0   .066   .128   .183   .229   .252   .283   .289   .280
Y(I) =  .458   .454   .425   .367   .305   .227   .145   .063      0


CYCLES =  18000.
   I  =     1      2      3      4      5      6      7      8      9
X(I) =     0   .050   .116   .173   .220   .275   .303   .317   .308
Y(I) =  .537   .531   .514   .465   .403   .304   .204   .089      0


CYCLES =  18250.
   I  =     1      2      3      4      5      6      7      8      9
X(I) =     0   .096   .159   .201   .256   .285   .310   .324   .314
Y(I) =  .547   .534   .487   .439   .353   .290   .197   .090      0


CYCLES =  18500.
   I  =     1      2      3      4      5      6      7      8      9
X(I) =     0   .058   .119   .175   .228   .268   .303   .330   .320
Y(I) =  .573   .564   .541   .487   .425   .350   .254   .103      0


CYCLES =  18750.
   I  =     1      2      3      4      5      6      7      8      9
X(I) =  .002   .090   .152   .210   .252   .314   .332   .342   .330
Y(I) =  .589   .574   .529   .468   .389   .264   .173   .096      0
```

115

Table 7 continued

```
CYCLES =  19000.
   I  =      1        2        3        4        5        6        7        8        9
X(I) =      0    .079     .140     .192     .257     .305     .330     .350     .339
Y(I) =   .600    .593     .556     .505     .414     .311     .230     .097        0


CYCLES =  19250.
   I  =      1        2        3        4        5        6        7        8        9
X(I) =      0    .107     .176     .230     .281     .314     .341     .356     .345
Y(I) =   .649    .629     .570     .506     .421     .344     .257     .120        0


CYCLES =  19500.
   I  =      1        2        3        4        5        6        7        8        9
X(I) =      0    .093     .171     .234     .280     .332     .358     .367     .357
Y(I) =   .682    .650     .594     .518     .442     .316     .211     .116        0


CYCLES =  19750.
   I  =      1        2        3        4        5        6        7        8        9
X(I) =      0    .092     .142     .223     .277     .329     .362     .382     .373
Y(I) =   .698    .686     .653     .572     .497     .374     .270     .120        0


CYCLES =  20000.
   I  =      1        2        3        4        5        6        7        8        9
X(I) =      0    .199     .263     .306     .330     .392     .387     .398     .386
Y(I) =   .715    .715     .616     .517     .450     .348     .223     .112        0
```
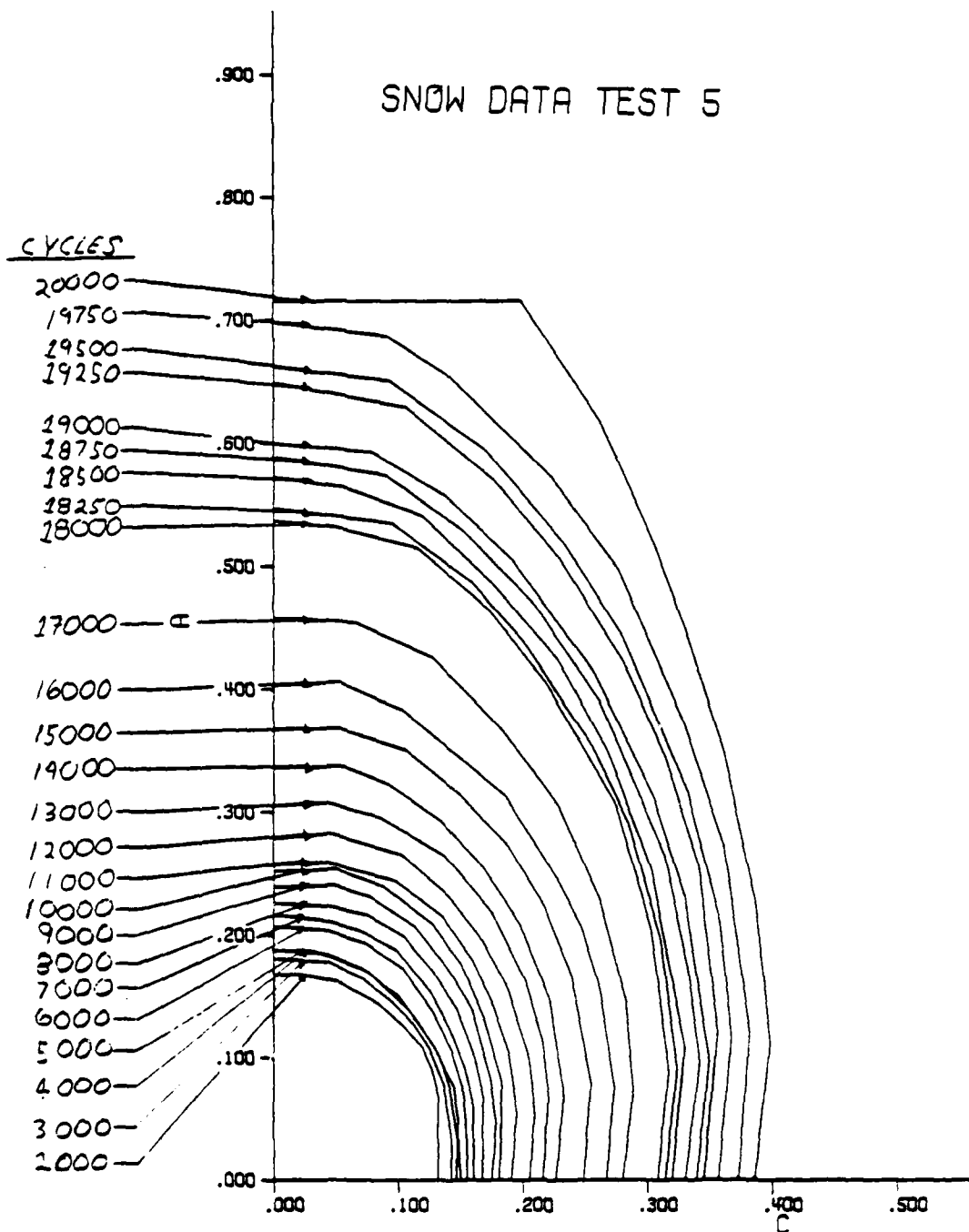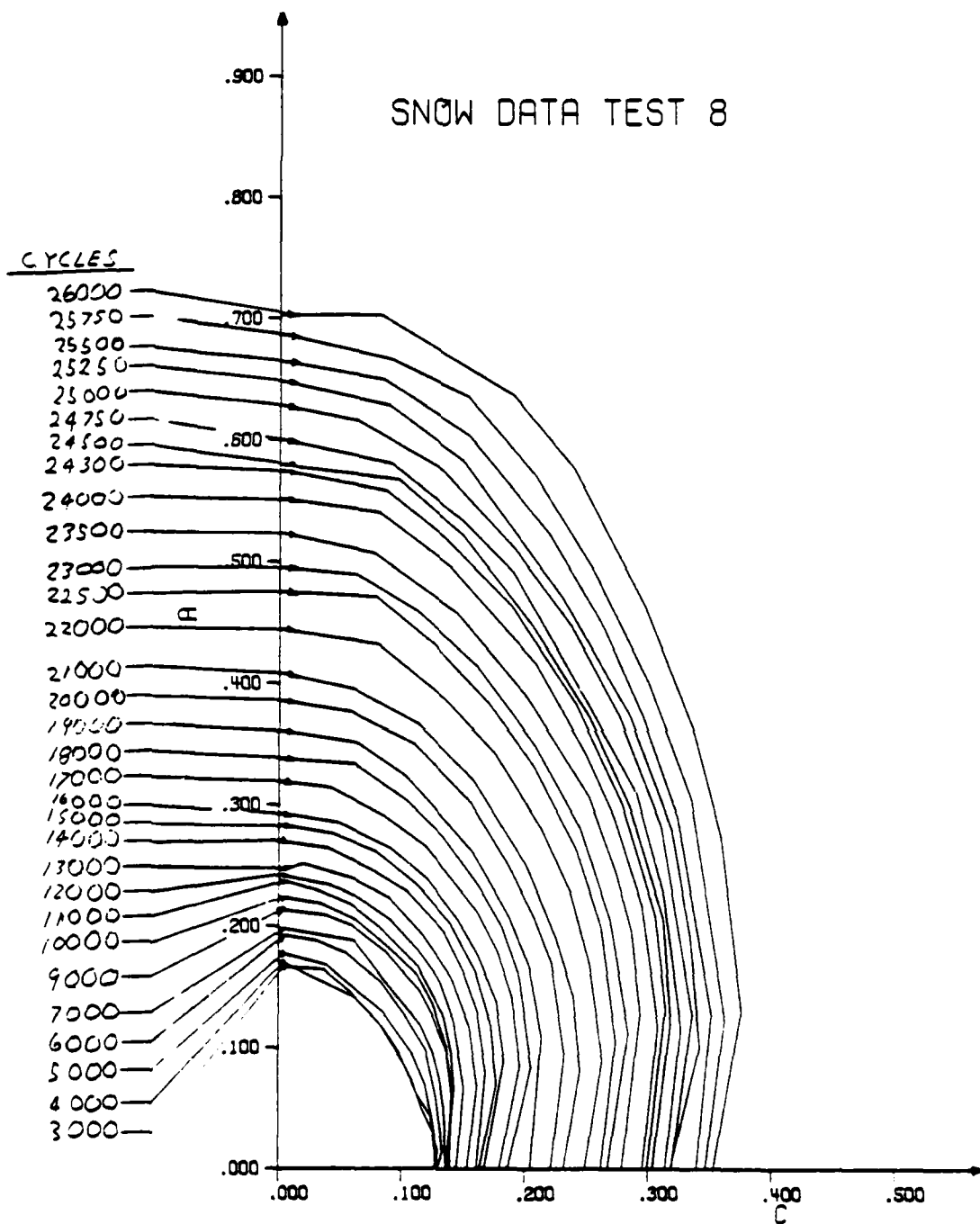
Figure 49 Digitized Crack Profiles for Snow
Corner Crack Test 8

Table 8 Digitized Data for Snow Test 8

NUM = 31   2R = .743   W = 7.920
T = .704   LOAD = 3400.

CYCLES = 3000.

I =	1	2	3	4	5	6	7	8	9
X(I) =	0	.036	.057	.082	.104	.112	.124	.127	.127
Y(I) =	.167	.164	.146	.120	.083	.062	.043	.014	0

CYCLES = 4000.

I =	1	2	3	4	5	6	7	8	9
X(I) =	0	.062	.085	.058	.109	.116	.126	.130	.128
Y(I) =	.172	.141	.116	.096	.073	.051	.028	.016	0

CYCLES = 5000.

I =	1	2	3	4	5	6	7	8	9
X(I) =	0	.039	.064	.084	.109	.119	.125	.129	.128
Y(I) =	.178	.168	.147	.130	.094	.069	.039	.011	0

CYCLES = 6000.

I =	1	2	3	4	5	6	7	8	9
X(I) =	0	.031	.055	.083	.103	.120	.128	.134	.129
Y(I) =	.193	.188	.178	.154	.126	.097	.058	.015	0

CYCLES = 7000.

I =	1	2	3	4	5	6	7	8	9
X(I) =	0	.061	.088	.115	.126	.131	.134	.135	.136
Y(I) =	.199	.168	.152	.118	.093	.076	.051	.034	0

CYCLES = 9000.

I =	1	2	3	4	5	6	7	8	9
X(I) =	0	.039	.060	.087	.115	.125	.137	.141	.139
Y(I) =	.213	.209	.200	.179	.146	.127	.095	.061	0

CYCLES = 10000.

I =	1	2	3	4	5	6	7	8	9
X(I) =	0	.035	.064	.068	.113	.125	.136	.142	.137
Y(I) =	.224	.218	.204	.183	.160	.136	.101	.065	0

CYCLES = 11000.

I =	1	2	3	4	5	6	7	8	9
X(I) =	0	.032	.060	.083	.113	.135	.141	.143	.137
Y(I) =	.238	.229	.217	.198	.167	.125	.093	.065	0

CYCLES = 12000.

I =	1	2	3	4	5	6	7	8	9
X(I) =	.001	.042	.068	.091	.113	.131	.143	.151	.145
Y(I) =	.242	.230	.223	.205	.180	.155	.121	.067	0

CYCLES = 13000.

I =	1	2	3	4	5	6	7	8	9
X(I) =	0	.019	.031	.080	.117	.140	.155	.131	.153
Y(I) =	.245	.251	.209	.220	.193	.158	.116	.068	0

Table 8   continued

```
CYCLES =   14000.
   I =      1      2      3      4      5      6      7      8      9
X(I) =      0   .041   .077   .105   .134   .150   .161   .168   .161
Y(I) =   .270   .264   .245   .228   .196   .163   .129   .079      0


CYCLES =   15000.
   I =      1      2      3      4      5      6      7      8      9
X(I) =      0   .044   .079   .112   .139   .160   .173   .177   .163
Y(I) =   .283   .276   .261   .234   .203   .162   .117   .070      0


CYCLES =   16000.
   I =      1      2      3      4      5      6      7      8      9
X(I) =      0   .049   .091   .120   .146   .161   .177   .183   .167
Y(I) =   .293   .285   .264   .239   .205   .177   .138   .088      0


CYCLES =   17000.
   I =      1      2      3      4      5      6      7      8      9
X(I) =      0   .042   .086   .120   .162   .177   .189   .196   .179
Y(I) =   .319   .314   .291   .265   .211   .180   .141   .085      0


CYCLES =   18000.
   I =      1      2      3      4      5      6      7      8      9
X(I) =      0   .062   .105   .133   .162   .181   .196   .205   .186
Y(I) =   .338   .333   .303   .274   .233   .199   .157   .084      0


CYCLES =   19000.
   I =      1      2      3      4      5      6      7      8      9
X(I) =      0   .065   .103   .127   .157   .187   .203   .214   .204
Y(I) =   .361   .350   .323   .296   .262   .208   .167   .108      0


CYCLES =   20000.
   I =      1      2      3      4      5      6      7      8      9
X(I) =      0   .058   .111   .156   .186   .207   .221   .232   .221
Y(I) =   .386   .376   .349   .302   .251   .207   .169   .092      0


CYCLES =   21000.
   I =      1      2      3      4      5      6      7      8      9
X(I) =      0   .061   .113   .156   .201   .225   .239   .245   .232
Y(I) =   .408   .395   .366   .321   .251   .190   .142   .081      0


CYCLES =   22000.
   I =      1      2      3      4      5      6      7      8      9
X(I) =      0   .080   .135   .176   .213   .237   .252   .253   .249
Y(I) =   .444   .432   .387   .342   .281   .228   .167   .089      0


CYCLES =   22500.
   I =      1      2      3      4      5      6      7      8      9
X(I) =      0   .079   .128   .170   .206   .241   .262   .274   .262
Y(I) =   .475   .471   .431   .384   .333   .284   .199   .105      0
```

Table 8 continued

```
CYCLES =  23000.
    I =     1       2       3       4       5       6       7       3       9
 X(I) =     0    .064    .113    .161    .208    .245    .269    .284    .267
 Y(I) =  .4S5    .469    .458    .414    .349    .280    .204    .112       0


CYCLES =  23500.
    I =     1       2       3       4       5       6       7       8       9
 X(I) =     0    .077    .145    .201    .252    .274    .286    .293    .279
 Y(I) =  .524    .507    .457    .389    .307    .244    .196    .126       0


CYCLES =  24000.
    I =     1       2       3       4       5       6       7       3       9
 X(I) =     0    .081    .139    .208    .249    .272    .295    .308    .295
 Y(I) =  .552    .540    .498    .416    .341    .290    .216    .117       0


CYCLES =  24300.
    I =     1       2       3       4       5       6       7       8       9
 X(I) =     0    .087    .134    .188    .241    .279    .306    .314    .299
 Y(I) =  .575    .558    .520    .464    .363    .300    .208    .131       0


CYCLES =  24500.
    I =     1       2       3       4       5       6       7       8       9
 X(I) =     0    .097    .149    .206    .251    .285    .312    .318    .304
 Y(I) =  .579    .567    .522    .447    .373    .299    .205    .119       0


CYCLES =  24750.
    I =     1       2       3       4       5       6       7       8       9
 X(I) =  .001    .091    .149    .190    .251    .290    .313    .327    .314
 Y(I) =  .600    .580    .534    .491    .382    .309    .224    .115       0


CYCLES =  25000.
    I =     1       2       3       4       5       6       7       3       9
 X(I) =     0    .065    .133    .191    .237    .276    .310    .336    .319
 Y(I) =  .628    .615    .575    .511    .447    .373    .282    .125       0


CYCLES =  25250.
    I =     1       2       3       4       5       6       7       8       9
 X(I) =     0    .089    .149    .230    .284    .319    .334    .342    .318
 Y(I) =  .646    .626    .583    .470    .374    .280    .190    .101       0


CYCLES =  25500.
    I =     1       2       3       4       5       6       7       8       9
 X(I) =     0    .085    .154    .219    .263    .295    .324    .351    .339
 Y(I) =  .665    .649    .604    .523    .447    .372    .289    .126       0


CYCLES =  25750.
    I =     1       2       3       4       5       6       7       3       9
 X(I) =     0    .090    .153    .207    .255    .300    .333    .332    .347
 Y(I) =  .627    .693    .636    .571    .493    .400    .304    .122       0


CYCLES =  26000.
    I =     1       2       3       4       5       6       7       8       9
 X(I) =     0    .082    .150    .239    .286    .338    .359    .375    .353
 Y(I) =  .703    .703    .636    .577    .465    .358    .273    .129       0
```
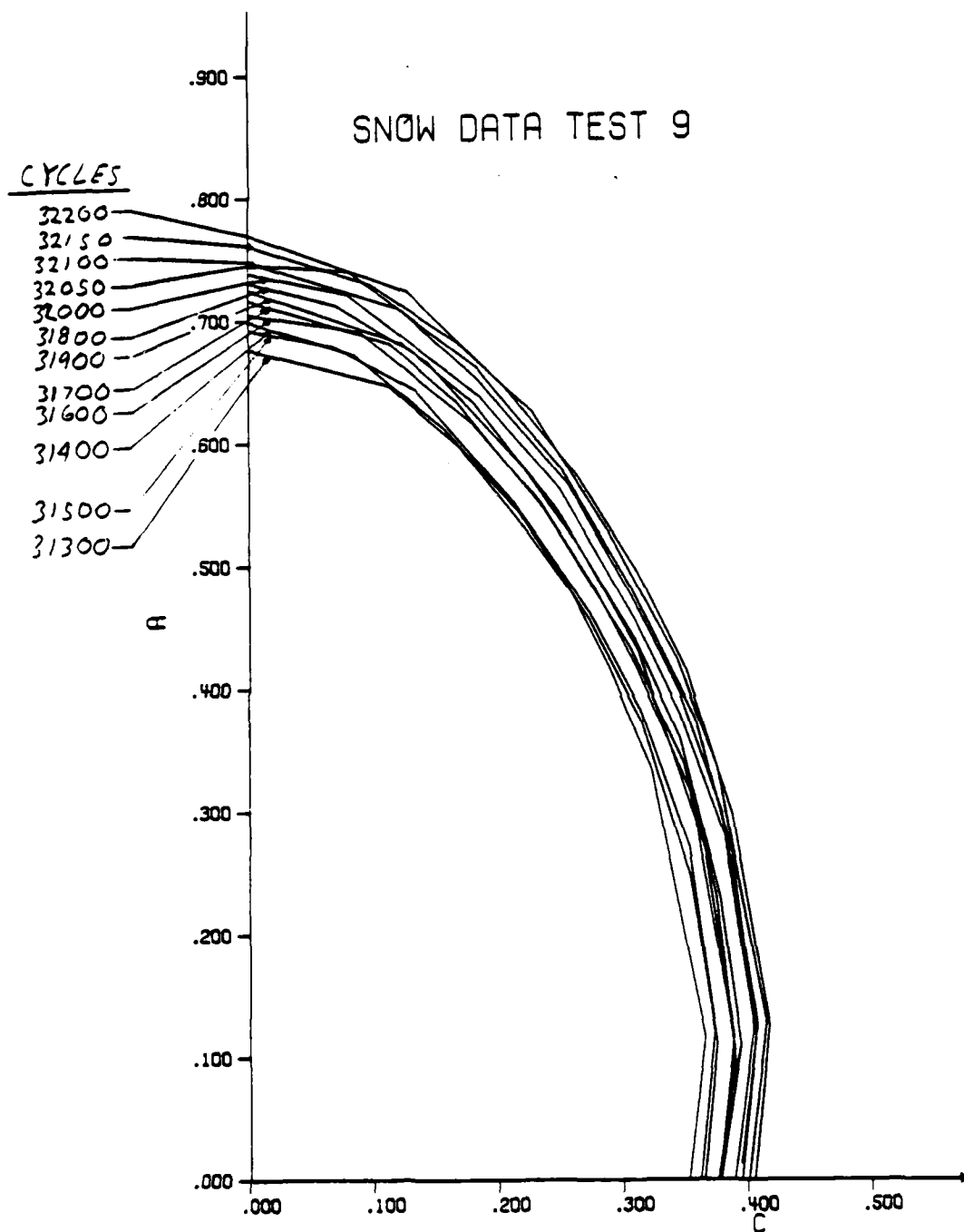
120

Figure 50 Digitized Crack Profiles for Snow Corner
Crack Test 9

121

Table 9 Digitized Data for Snow Test 9

```
NUM = 12    2R = .743    W = 7.970
T = .704    LOAD = 3400.
```

CYCLES = 31300.

I =	1	2	3	4	5	6	7	8	9
X(I) =	0	.112	.168	.215	.260	.290	.323	.366	.352
Y(I) =	.676	.647	.599	.540	.478	.415	.335	.117	0

CYCLES = 31400.

I =	1	2	3	4	5	6	7	8	9
X(I) =	0	.085	.157	.217	.272	.315	.354	.373	.361
Y(I) =	.699	.672	.613	.545	.459	.374	.246	.120	0

CYCLES = 31500.

I =	1	2	3	4	5	6	7	8	9
X(I) =	0	.069	.135	.213	.274	.315	.353	.375	.365
Y(I) =	.692	.678	.643	.553	.462	.383	.271	.111	0

CYCLES = 31600.

I =	1	2	3	4	5	6	7	8	9
X(I) =	0	.089	.179	.233	.277	.310	.355	.390	.377
Y(I) =	.705	.691	.618	.554	.484	.419	.316	.107	0

CYCLES = 31700.

I =	1	2	3	4	5	6	7	8	9
X(I) =	0	.114	.168	.237	.306	.350	.375	.390	.375
Y(I) =	.716	.681	.634	.547	.434	.339	.232	.096	0

CYCLES = 31800.

I =	1	2	3	4	5	6	7	8	9
X(I) =	.002	.070	.144	.218	.258	.312	.366	.389	.376
Y(I) =	.730	.712	.667	.584	.512	.433	.270	.117	0

CYCLES = 31900.

I =	1	2	3	4	5	6	7	8	9
X(I) =	0	.124	.181	.249	.310	.346	.378	.395	.378
Y(I) =	.725	.681	.634	.545	.441	.360	.231	.111	0

CYCLES = 32000.

I =	1	2	3	4	5	6	7	8	9
X(I) =	0	.079	.185	.249	.309	.346	.381	.403	.389
Y(I) =	.738	.722	.640	.564	.459	.380	.282	.124	0

CYCLES = 32050.

I =	1	2	3	4	5	6	7	8	9
X(I) =	0	.080	.183	.251	.307	.359	.388	.407	.395
Y(I) =	.746	.740	.663	.580	.482	.376	.266	.116	.014

CYCLES = 32100.

I =	1	2	3	4	5	6	7	8	9
X(I) =	0	.120	.184	.255	.307	.349	.330	.408	.395
Y(I) =	.748	.710	.654	.568	.477	.397	.300	.127	0

Table 9   continued

```
CYCLES =  32150.
  I  =      1       2       3       4       5       6       7       8       9
 X(I) =     0    .099    .167    .228    .289    .344    .376    .415    .400
 Y(I) =   .761    .729    .683    .627    .528    .424    .336    .128      0


CYCLES =  32200.
  I  =      1       2       3       4       5       6       7       8       9
 X(I) =     0    .128    .205    .265    .313    .351    .388    .418    .405
 Y(I) =   .770    .724    .647    .573    .495    .415    .298    .126      0
```

REFERENCES

1. R.J. Gran, F.D. Orazio, P.C. Paris, G.R. Irwin, and R. Hertzberg, *Investigation and Analysis Development of Early Life Aircraft Structural Failures*, Air Force Flight Dynamics Laboratory, Wright-Patterson Air Force Base, Ohio 45433, AFFDL-TR-70-149, March 1971.

2. J.A. Harter, *Fatigue Crack Growth of Embedded Flaws in Plate and Lug Type Fastener Holes*, Masters Thesis, School of Aeronautics and Astronautics, Purdue University, W. Lafayette, IN 47907, May 1982.

3. F.J. Pitoniak, A.F. Grandt, L.T. Montulli, and P.F. Packman, "Fatigue Crack Retardation and Closure in Polymethylmethacrylate," *Engineering Fracture Mechanics*, Vol. 6, 1974, pp. 663-670.

4. A.F. Grandt, Jr. and T.D. Hinnerichs, "Stress Intensity Factor Measurements for Flawed Fastener Holes," AMMRC MS 74-8, September 1974.

5. J.R. Snow, "A Stress Intensity Factor Calibration for Corner Flaws at an Open Hole," Technical Report AFML-TR-74-282, Air Force Materials Laboratory, Wright-Patterson AFB, Ohio, May 1975.

6. A.F. Grandt, Jr., and D.E. Macha, "Digitized Measurements of the Shape of Corner Cracks at Fastener Holes," *Engineering Fracture Mechanics*, Vol. 17, No. 1, 1983, pp. 63-73.

7. "Tentative Test Method for Constant-Load-Amplitude Fatigue Crack Growth Rates Above 10^{-8} m/cycle," ASTM Standard E647-78T, *1980 Annual Book of ASTM Standards*, Part 10, American Society for Testing and Materials, pp. 749-767.

8. C. Lanczos , *Applied Analysis*, Prentice Hall, Inc., Englewood Cliffs, N.J., 1956.

9. D.P. Rooke and D.J. Cartwright, *Stress Intensity Factors*, London, Her Majesty's Stationary Office, September 1974.

10. *Meyer Plastics Catalog*, Meyer Materials, Inc., 5101 East 65th Street, Indianapolis, Indiana, 46220, p. 130.

11. J.A. Harter, "Experimental Crack Growth Data for Embedded Flaws in Plate and Lug Fastener Holes," Technical Report 82-1, School of Aeronautics and Astronautics, Purdue University, February 1982. Single copies available on request from A.F. Grandt, School of Aeronautics and Astronautics, Purdue University, W. Lafayette, Indiana, 47907.

12. A.F. Grandt, Jr., J.A. Harter, and B.J. Heath, "The Transition of Part-Through Cracks at Holes into Through-The-Thickness Flaws," presented at ASTM 15th National Symposium on Fracture Mechanics, University of Maryland, 7 July 1982. Paper to appear in American Society for Testing and Materials Special Technical Publication devoted to symposium proceedings.

13. T.M. Hsu, "Analysis of Cracks at Attachment Lugs," _Journal of Aircraft_, Vol. 18, No. 9, September 1981, pp. 755-760.

14. J.C. Newman and I.S. Raju, "Stress Intensity Factor Equations for Cracks in Three-Dimensional Finite Bodies," NASA Technical Memorandum 83200, Langley Research Center, Hampton, Virginia, August 1981.

15. O.L. Bowie, "Analysis of an Infinite Plate Containing Radial Cracks Originating at the Boundary of an Internal Circular Hole," _Journal of Mathematics and Physics_, _Vol. 35_, 1956, pp. 60-71.